Spring 5-5-2012

# Regulation of Interferon Stimulated Genes in West Nile Virus Infected Mouse Embryofibroblasts

Joanna A. Pulit-Penaloza
*Georgia State University*

REGULATION OF INTERFERON STIMULATED GENES IN WEST NILE VIRUS INFECTED MOUSE EMBRYOFIBROBLASTS

by

JOANNA ALICJA PULIT-PENALOZA

Under the direction of Margo A. Brinton

## ABSTRACT

The induction of type I interferon (IFN) and subsequent activation of interferon stimulated genes (ISGs) represent a first line of defense against viral infection. Typically type I IFN signaling leads to the phosphorylation of the STAT1 and STAT2 transcription factors (TFs) which then form a trimetric complex with IRF-9 and translocate to the nucleus to induce ISG expression. However, the results of this study showed that IFN-mediated upregulation of the ISG Oas1b, the product of which confers resistance to flavivirus induced disease, can be induced in a STAT1-independent manner. Since numerous ISGs have antiviral functions, many viruses have evolved strategies to disrupt the type I IFN-signaling pathway. In cases when STAT1 activation is blocked by a viral infection, STAT1-independent upregulation of ISGs provides an additional strategy for the cell to mount an effective antiviral response. Infection of mouse embryofibroblasts (MEFs) with West Nile virus (WNV) induced the production of IFN beta and STAT1 and STAT2 phosphorylation but blocked nuclear translocation and binding of these TFs to the promoters of the ISGs, Oas1a, Oas1a, Irf7 and Irf1. However, each of these antiviral ISGs was efficiently upregulated in infected cells and IRF-9 was shown to be crucial for the

upregulation of Oas1a, Oas1b and Irf-7. IRF-3 or IRF-7 was needed to maintain the upregulation of these genes at later times of infection. In contrast, the upregulation of Irf1 by WNV infection did not depend on the tested IRFs but was reduced by inhibition of the p38 or NF-kappa B pathways. Although Irf1 mRNA was efficiently upregulated in WNV-infected cells IRF-1 protein synthesis was blocked. The precise mechanism of the IRF-1 translational suppression is not yet known, but the suppression was shown not to be due to increased proteasomal degradation of IRF-1 nor to alternative splicing of Irf1 mRNA. Preliminary results suggest miRNAs may play an indirect role in regulating IRF-1 translation.

The results of this study expand knowledge about the strategies evolved by viruses to evade host cell antiviral responses and also provide valuable insights about alternative mechanisms utilized by the host cell to counteract viral infections.

INDEX WORDS: West Nile virus, Type I IFN, ISG, 2'-5' Oligoadenylate synthetase, Oas1a, Oas1b, Irf1, Irf7, Translational suppression

# REGULATION OF INTERFERON STIMULATED GENES IN WEST NILE VIRUS INFECTED MOUSE EMBRYOFIBROBLASTS

by

JOANNA ALICJA PULIT-PENALOZA

A Dissertation Submitted in Partial Fulfillment of the Requirements for the Degree of Doctor of Philosophy

in the College of Arts and Sciences

Georgia State University

2012

# REGULATION OF INTERFERON STIMULATED GENES IN WEST NILE VIRUS INFECTED MOUSE EMBRYOFIBROBLASTS

by

JOANNA ALICJA PULIT-PENALOZA

Committee Chair: Margo A. Brinton

Committee: Susanna F. Greer

Casonya M. Johnson

Electronic Version Approved:

Office of Graduate Studies

College of Arts and Sciences

Georgia State University

May 2012

## DEDICATION

I would like to dedicate this dissertation to my wonderful family and friends without whom this dissertation would not be possible. To my husband, Said, who gave me the support and encouragement to pursue my educational dreams. Thank you for your unconditional love and for always helping me forget my troubles and stay positive. To my daughters, Isabella and Natalia, who came into my life during this pursuit. You brought into my life more than you will ever imagine. You filled my heart with pure love and happiness. To my parents, Monika and Marian, for always believing in me and instilling the importance of hard work and higher education. I am truly blessed with parents like you. Lastly, I would like to thank my sister Malgorzata, my brother Krzysztof, my friends and my sweet and loving mother-in-law Patricia for their help along this journey and for their love.

## ACKNOWLEDGEMENTS

My deepest gratitude goes to my advisor Dr. Margo Brinton for her years of patience and guidance of this work. I thank her for giving me the opportunity to work in her lab and receive great training and knowledge that prepared me very well for my future career as a scientist. I would also like to thank my committee members Dr. Susanna Greer and Dr. Casonya Johnson for keeping me on track and giving me valuable advice. I would like to express my sincere thanks to Dr. Svetlana Scherbik for her expert assistance, words of encouragement and great friendship. Lastly, I would like to thank all the members of the Brinton lab, past and present, for their friendship, support, advice and for keeping a great atmosphere every day.

# TABLE OF CONTENTS

# LIST OF TABLES

## LIST OF FIGURES

## LIST OF ACRONYMS

AP1- ATF2/c-Jun

ARE - AU-rich element

CARD - caspase activation and recruitment domain

ChIP – chromatin immunoprecipitation

C protein – capsid protein

dsRNA – double stranded RNA

E protein –envelope protein

GAF – IFN-alpha factor

GAS – IFN-gamma activated sequence

EBV - Epstein-Barr virus

EMSA – electrophoretic mobility shift assay

ELISA – enzyme-linked immunoabsorbent assay

ER –endoplasmic reticulum

ERK – extracellular signal-regulated kinase 2

GCN2 - general control non-derepressible-2 kinase

HIV - human immunodeficiency virus

HRI – heme-regulated inhibitor kinase

IFN – interferon

IFA – immunofluorescence assay

IPS-1 - IFN beta promoter stimulator-1

IRF – IFN regulatory factor

ISG - IFN stimulated gene

ISGF3 - IFN stimulated gene factor 3

ISRE - IFN stimulated response element

JAK – Janus kinase

JEV - Japanese encephalitis virus

JNK - c-Jun N-terminal kinase

MAPK - serine-threonine mitogen-activated kinases

MDA5 – melanoma differentiation antigen 5

MEFs – mouse embryofibroblasts

MHC – major histocompatibility complex

MOI – multiplicity of infection

miRNA - micro RNA

miRISC - miRNA-induced silencing complex

M protein –membrane protein

MVEV - Murray Valley encephalitis virus

MyD88 - myeloid differentiation factor 88

NK - natural killer cell

NS – nonstructural protein

nt - nucleotide

OAS - 2'-5'-oligoadenylate synthetase

ORF – open reading frame

PAMP - pathogen-associated molecular pattern

PABP - poly(A) binding protein

P-bodies – processing bodies

pC3H/He MEFs – primary C3H/He MEFs

PERK - PKR-like ER kinase

PI3K - phosphatidylinositol 3-kinase

PKR - double-stranded RNA-dependent protein kinase

pre-miRNA – precursor miRNA

pri-miRNA – primary miRNA

PRR - pattern recognition receptor

qPCR - quantitative polymerase chain reaction

qRT-PCR – quantitative reverse transcription polymerase chain reaction

RIG-I –retinoic acid inducible gene - I

RLR - RIG-I-like receptor

RT PCR - reverse transcription polymerase chain reaction

SLEV -St. Louis encephalitis virus

ssRNA –single stranded RNA

STAT - signal transducer and activator of transcription

TBEV - tick-borne encephalitis

tC3H/He MEFs – transformed C3H/He MEFs

TF – transcription factor

TFBS – transcription factor binding site

TLR – Toll-like receptor

TRIF - TIR domain containing adaptor-inducing IFN beta

UTR – untranslated region

VSV - vesicular stomatitis virus

WNV – West Nile virus

YFV - yellow fever virus

# CHAPTER 1

## 1 INTRODUCTION

### 1.1 Classification and medical importance of flaviviruses

The genus Flavivirus in the family *Flaviviridae* contains over 70 viruses including several human pathogens such as dengue, Japanese encephalitis virus (JEV), yellow fever virus (YFV), West Nile virus (WNV), St. Louis encephalitis virus (SLEV), Murray Valley encephalitis virus (MVEV) and tick-borne encephalitis virus (TBEV). Many flaviviruses are transmitted by arthropods and cause a variety of diseases including fever, encephalitis, meningitis and hemorrhagic fever (Lindenbach, 2007). A secondary Dengue infection with a different serotype can lead to a life threatening hemorrhagic fever with a mortality rate of about 5%. Vaccines are available for only a few flaviviruses, namely YFV, TBEV and JEV. WNV is transmitted in nature via a mosquito-bird cycle. Although WNV primarily infects birds, it occasionally infects mammals including humans and horses. The majority of WNV infections in humans are asymptomatic; however, infection induces a mild febrile illness in about 20% of infected individuals and encephalitis or poliomyelitis-like disease in less than 1% of infected individuals (Petersen et al., 2003). WNV isolates have been divided into two lineages. Lineage I strains are often associated with outbreaks of human disease, while the majority of lineage II strains are non-emerging and cause zoonotic infections in Africa (Brinton, 2002). No antiviral therapies or human vaccines have been developed so far to treat or prevent WNV infections.

### 1.2 General characteristics of WNV.

The WN virion is spherical and has a diameter of 40-60 nm. It contains a positive sense, single stranded RNA genome of about 11,000 nucleotides. Similar to cellular mRNAs, the viral genome

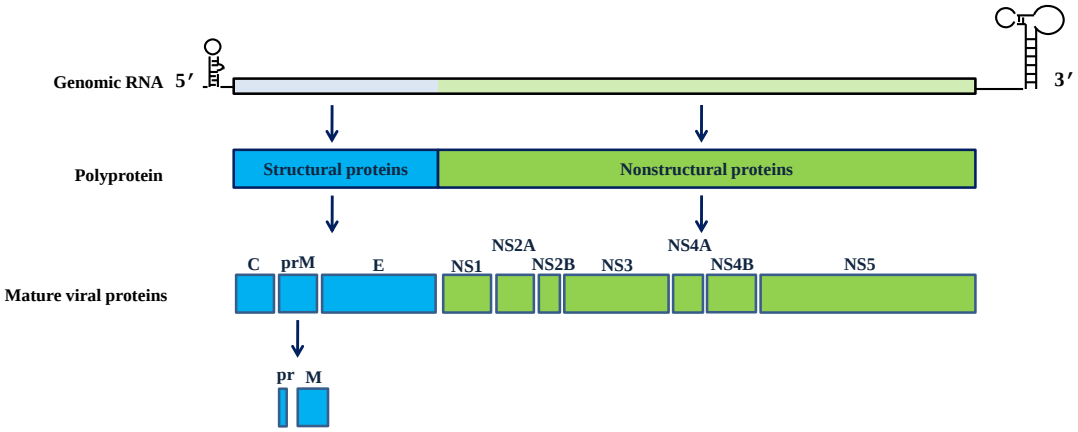


**Figure 1.1. Schematic representation of the WNV genome and polyprotein processing.** WNV genome indicated by a colored box with the 5' and 3' untranslated regions shown as black lines. The single polyprotein produced is processed by viral and cellular proteases. Mature structural proteins are shown in blue and nonstructural proteins are shown in green. Not drawn to scale. Modified from (Brinton, 2002).

is capped at the 5' end; however, it lacks a poly A at the 3' end. The single open reading frame of WNV genome encodes a polyprotein that when processed by viral and cell proteases produces ten mature viral proteins (Fig. 1.1). Viral structural proteins [capsid (C), membrane (prM/M) and the envelope (E)] are encoded by the 5' portion of the genome open reading frame (ORF) and the nonstructural proteins (NS1, NS2A, NS2B, NS3, NS4A, NS4B and NS5) are encoded by the 3' portion. The genome is surrounded by a capsid layer composed of dimers of the C protein. A host-derived lipid envelope surrounds the capsid layer and is spanned by the transmembrane regions of viral E and M proteins (Lindenbach, 2007).

### 1.3 Flavivirus replication cycle.

The flavivirus E protein binds to an unknown receptor(s) on the cell surface and this leads to clathrin-mediated endocytosis (Fig. 1.2). Upon acidification of the virion-containing endocytic vesicle, the E protein undergoes a low pH mediated conformational change that leads to the fusion of the viral envelope with the late endosome (Chu and Ng, 2004). The viral genome is released into the cytoplasm and is translated into a single polyprotein that is then processed by viral and cellular proteases to produce the mature viral proteins (Lindenbach, 2007). Viral replication occurs entirely in the cytoplasm of the infected cell. The replication of flavivirus RNA is associated with extensive membrane biogenesis and rearrangements and viral RNA replication complexes are formed in invaginations of the endoplasmic reticulum (ER). Each of these endoplasmic vesicles is connected with the cytoplasm via a narrow "neck" (Gillespie et al., 2010). Accumulation of viral nonstructural proteins including the NS5 RNA dependent RNA polymerase, results in the synthesis of negative sense RNA which in turn functions as a template for the synthesis of genomic plus strand RNA (Lindenbach, 2007). Initially the synthesis of minus and plus RNA is symmetric; however, about 6-10 h after infection, synthesis becomes

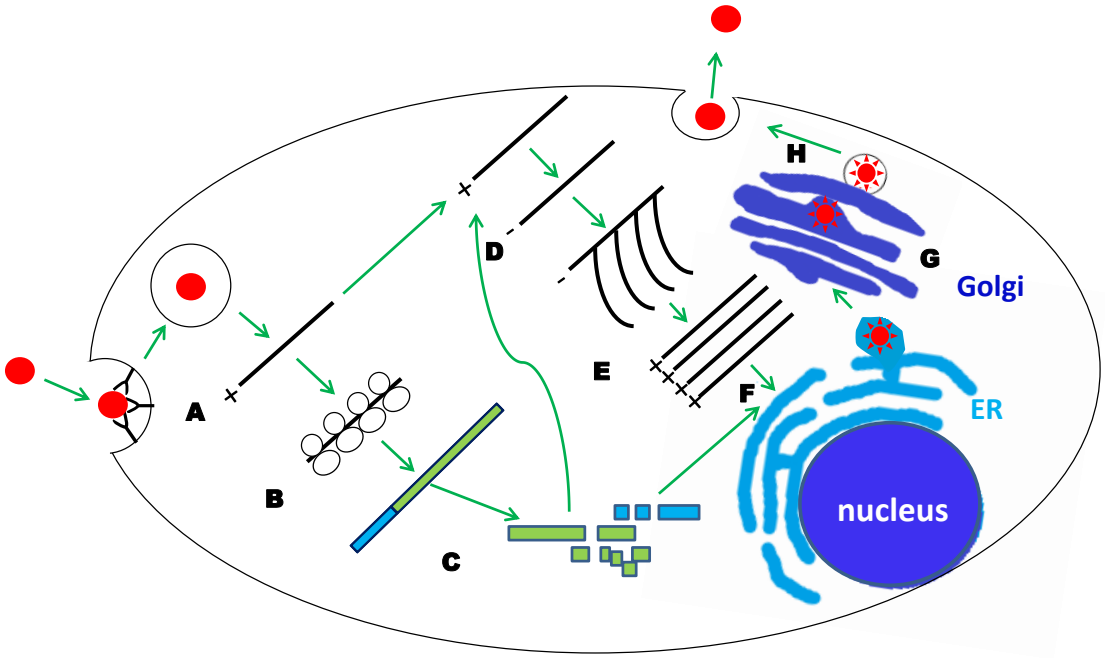


**Figure 1.2. WNV replication cycle.** **(A)** Attachment, entry and uncoating of the virion genome RNA. **(B)** Translation of the polyprotein. **(C)** Polyprotein processing. **(D)** Synthesis of minus strand RNA. **(E)** Synthesis of genomic plus strand RNA. **(F)** Encapsidation of the genome and assembly of immature virions. **(G)** Transport of the immature virions through the Golgi. **(L)** Virion maturation and release of nascent virions by exocytosis at the plasma membrane. Modified from (Brinton, 2002).

asymmetric with about 10 to 100 times more plus strand synthesis occurring (Chu and Westaway, 1985). The newly synthesized genomic RNA moves through the neck of the vesicles into the cytoplasm where it either associates with ribosomes and is translated or associates with capsid proteins associated with ER membranes that also contain E and M proteins and buds into the lumen of the ER forming immature virions (Gillespie et al., 2010). Immature virions are then transported through the *trans*-Golgi to the plasma membrane. During transport, prM is cleaved by the Golgi-resident protease furin into pr and M. As a result the prM-E complexes dissociate allowing the formation of E protein homodimers and maturation to "smooth surface" viral particles (Stadler et al., 1997). Mature virions are released from infected cells by the fusion of the virus-containing vesicle with the cell plasma membrane (Mackenzie and Westaway, 2001).

### 1.4 Host cell response to viral infection.

Viral infection is sensed through pattern recognition receptors (PRR) that recognize specific pathogen-associated molecular patterns (PAMPs) within viral structures. PRRs that recognize viral infections include Toll-like receptors (TLRs) and RIG-I-like receptors (RLRs). The TLR family includes twelve members that bind to a variety of PAMPs (Akira, 2009). Viral ribonucleic acids are recognized by three of the TLRs. TLR-3 is expressed at the cell surface or in endosomes (Matsumoto et al., 2003) and recognizes double stranded dsRNA (dsRNA) (Alexopoulou et al., 2001). Upon binding dsRNA, TLR-3 binds the TIR domain containing adaptor-inducing IFN beta (TRIF) adaptor molecule and activates the IRF-3, NF-kappa B and ATF2/c-Jun (AP1) transcription factors (TFs) which activate IFN beta expression (Akira, 2009). TLR-7 and TLR-8 recognize single stranded RNAs (ssRNAs) (Diebold et al., 2004; Heil et al., 2004; Triantafilou et al., 2005) and signal through the adaptor molecule myeloid differentiation factor 88 (MyD88) to activate IRF-7 and NF-kappa B and induce type I IFN expression (Akira,

2009). The involvement of TLR-3 in the antiviral response of mice to WNV infection is not clear. Although a previous study reported that blood-barrier permeability and WNV entry into the brain was decreased in TLR-3-/- mice, suggesting that TLR-3 promotes WNV entry into the brain (Wang et al., 2004), a second study showed that TLR-3 plays a protective role against WNV infection by restricting virus replication in neurons (Daffis et al., 2008). TLR-7 was reported to be important in promoting effective WNV clearance in mice (Town et al., 2009; Welte et al., 2009).

Viral RNA structures can also be detected by retinoic acid inducible gene-I (RIG-I) and melanoma differentiation antigen 5 (MDA5). These cytoplasmic sensors are DExD/H helicases containing two caspase activation and recruitment domains (CARDs) at their N termini. Although the RIG-I like receptors share about 25% identity within the CARD domains and about 40% identity within the helicase domains (Barral et al., 2009), they recognize different RNA species. RIG-I binds ssRNA molecules containing a 5' triphosphate, short dsRNAs, and adenosine/uridine rich RNAs while MDA5 has been shown to be activated by long dsRNAs (Hornung et al., 2006; Marques et al., 2006; Kato et al., 2008; Saito et al., 2008; Takahasi et al., 2008). Activated RIG-I and MDA5 bind the IFN beta promoter stimulator (IPS)-1 protein that serves as a downstream adaptor molecule. IPS-1 then induces downstream signaling cascades leading to the activation of TFs mediating upregulation of IFN (Barral et al., 2009). Recent studies suggest that both RIG-I and MDA5 play a role in sensing WNV infection and the induction of IFN (Fredericksen et al., 2008; Loo et al., 2008). The IFN response to WNV infection was completely abolished in cells lacking IPS-1 (Fredericksen et al., 2008) confirming the importance of the RLRs and IPS-1 signaling in the response to WNV infection.

## 1.5 IFN system

IFNs are secreted cytokines that play a pivotal role in host defense against intracellular pathogens. IFNs can directly inhibit a virus infection by the induction of IFN stimulated genes, (ISGs) many of which have antiviral functions, or indirectly through the induction of major histocompatibility complex (MHC) antigens and the activation of immune cells (Paun and Pitha, 2007). IFNs are grouped into three classes based on their amino acid sequence and recognition by specific receptors. Type I IFNs consist of IFN- alpha (α), -beta (β) and the lesser known IFNs, -omega (ω), -epsilon (ε), -kappa (κ), - delta (δ), -tau (τ) and – zeta (ζ). Only IFN alpha, beta, omega, epsilon and kappa are found in humans. IFN alpha and beta are secreted by a wide variety of cells including macrophages, lymphocytes, fibroblasts, endothelial cells, osteoblasts and others (Pestka et al., 2004) while the other type I IFNs are expressed in specific cell types (Table 1.1). IFN alpha and IFN-beta have been extensively studied and were shown to play a major role in the innate response to viral infections (Randall and Goodbourn, 2008). Since IFN-alpha and IFN-beta are secreted by fibroblasts, this dissertation will concentrate on these two subtypes of type I IFNs. The type II IFN class consists of only IFN-gamma (γ), which is critical for both the innate and adaptive immune responses to virus infection, intracellular bacterial infections as well as tumor control. IFN-gamma is produced by macrophages, natural killer cells (NK) and by CD4 and CD8 cytotoxic T-cells (Takaoka and Yanai, 2006; Schoenborn and Wilson, 2007). Type III IFNs consist of IFN-lambda 1 (λ1), -lambda 2 (λ2) and –lambda 3 (λ3) which are also referred to as IL-29, IL-28A and IL-28B, respectively. These IFNs are closely related to type I IFNs (Li et al., 2009).

**Table 1.1. Classification of IFNs, subtypes, their receptors and expression patterns.**

| Class | Subtype | Receptor subunits | Transcription factors induced | DNA binding site | Expression |
|---|---|---|---|---|---|
| I | IFN-α | IFNAR1/IFNAR2 | ISGF3* | ISRE | Ubiquitous |
| | IFN-β | IFNAR1/IFNAR2 | ISGF3 | ISRE | Ubiquitous |
| | IFN-δ | IFNAR1/IFNAR2 | ISGF3 | ISRE | Trophoblasts |
| | IFN-ε | IFNAR1/IFNAR2 | ISGF3 | ISRE | Uterus, Ovary |
| | IFN-ω | IFNAR1/IFNAR2 | ISGF3 | ISRE | Leukocytes |
| | IFN-κ | IFNAR1/IFNAR2 | ISGF3 | ISRE | Epidermal keratinocytes |
| | IFN-τ | IFNAR1/IFNAR2 | ISGF3 | ISRE | Trophoblasts |
| | IFN-ζ | IFNAR1/IFNAR2 | ISGF3 | ISRE | Spleen, thymus, lymph node |
| II | IFN-γ | IFNGR1/IFNGR2 | GAF** | GAS | Macrophage, T cell, NK cell |
| III | IFN-λ1 | IFNLR1/IL10R2 | ISGF3 | ISRE | Ubiquitous |
| | IFN-λ2 | IFNLR1/IL10R2 | ISGF3 | ISRE | Ubiquitous |
| | IFN-λ3 | IFNLR1/IL10R2 | ISGF3 | ISRE | Ubiquitous |

*ISGF3 (STAT1, STAT2 and IRF9)
**GAF (STAT1 homodimer)
Compiled from reviews (Takaoka and Yanai, 2006; de Weerd et al., 2007; Fensterl and Sen, 2009).

### 1.6 Type I IFN signaling pathway.

During a viral infection, activation of a PRR leads to the induction of signaling pathways resulting in the activation of TFs including IRF-3, NF-kappa B and AP1 which translocate to the nucleus and cooperatively activate IFN-beta gene expression (Barral et al., 2009). Secreted IFN beta binds to a cellular receptor complex composed of two subunits, IFNAR1 and IFNAR2 (Fig. 1.3), that are associated with Janus kinases (JAKs). The cytoplasmic tail of IFNAR1 is associated with the tyrosine kinase (Tyk2) while the cytoplasmic tail of IFNAR2 is associated with Jak1. The binding of IFN to the receptor complex induces cross-activation of these kinases. IFNAR1 is then phosphorylated by Tyk2 which allows recruitment of signal transducer and activator of transcription 2 (STAT2) to the receptor and its phosphorylation by Tyk2. Next STAT1 binds to STAT2 and is phopshorylated by Jak1. Phosphorylated STAT1 and STAT2 form a trimeric transcription factor complex referred to as IFN stimulated gene factor 3 (ISGF3) with IFN regulatory factor-9 (IRF-9). This complex translocates to the nucleus and binds to IFN stimulated response elements (ISREs) in the promoters of ISGs (Paun and Pitha, 2007; Randall and Goodbourn, 2008). One of the ISGs induced by IFN-beta is IRF-7. It is a transcription factor involved in the induction of the IFN-alpha genes. In addition IRF-7 forms a complex with IRF-3 that binds to the IFN-beta promoter and induces its expression (Wathelet et al., 1998). Secreted IFN-alpha utilizes the same signaling pathway as IFN beta resulting in the amplification of the type I IFN response via a positive feedback loop (Marie et al., 1998; Sato et al., 2000).

### 1.7 Type II IFN and type III IFN signaling pathways.

In the case of type II IFN signaling, IFN-gamma binds to the IFNGR1 and IFNGR2 receptor complex which leads to the formation of a STAT1 homodimer that is referred to as IFN-alpha factor (GAF). This complex translocates to the nucleus and binds to IFN-gamma activated

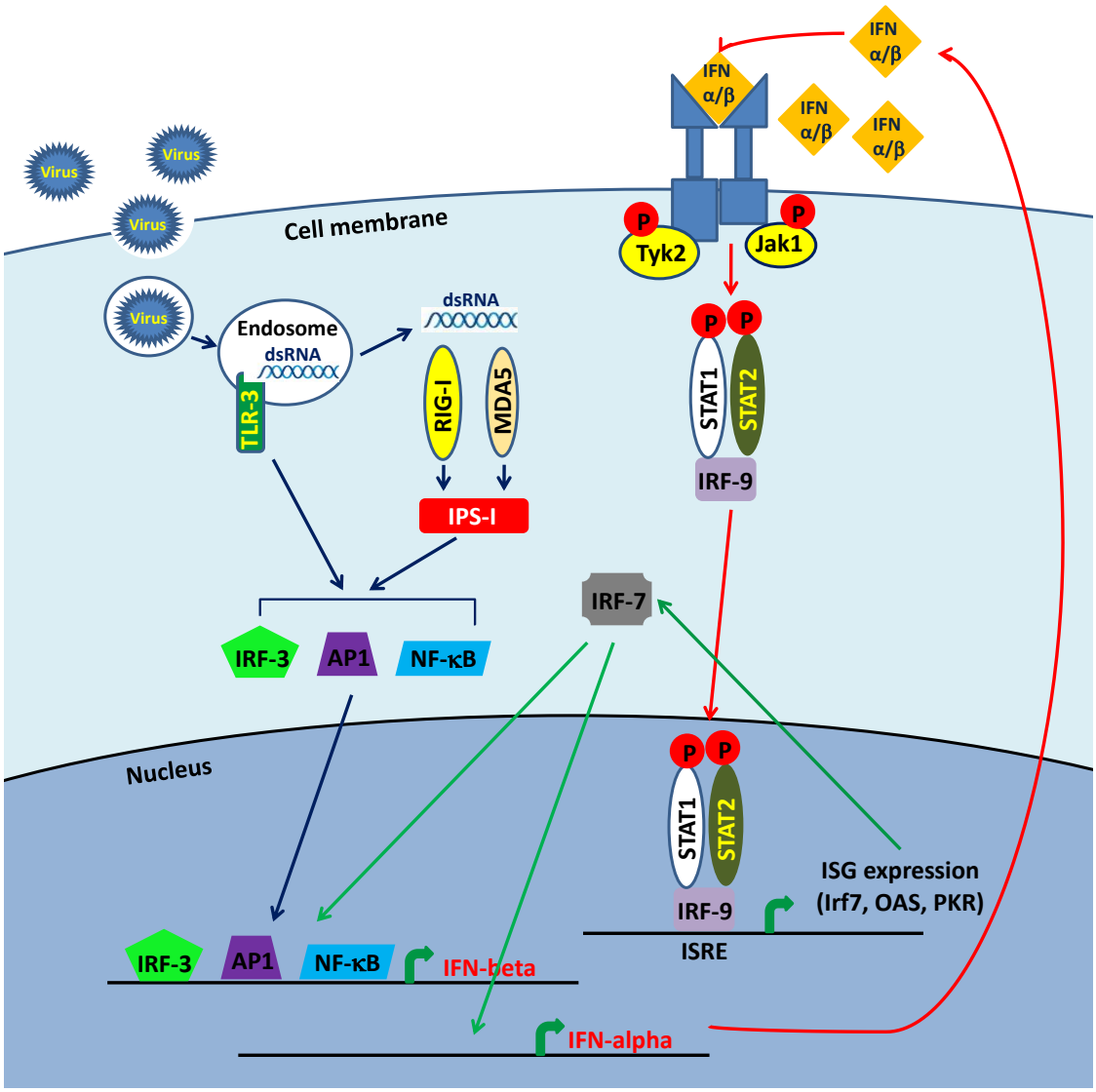


**Figure 1.3. Type I IFN induction in MEFs in response to viral dsRNA signaling in MEFs.** The binding of viral dsRNA to endoplasmic and/or cytoplasmic sensors leads to the activation of TFs required for IFN beta expression. Secreted IFN beta binds to the cellular receptor and activates the JAK-STAT signaling pathway that leads to upregulation of ISGs including Irf7. The IRF-7 TF activates the expression of IFN alpha genes and enhances upregulation of the IFN beta gene.

sequences (GAS) in the promoters of IFN-gamma responsive genes. Although IFN-gamma primarily activates the GAF complex, it can also activate the formation of the ISGF3 complex. Likewise IFN-alpha/beta signaling mainly activates the formation of ISGF3 but can also activate GAF (Kessler et al., 1990; Decker et al., 1991; Lew et al., 1991; Williams, 1991). Type III IFNs bind to a receptor complex composed of a specific receptor subunit IFNLR1and IL10R2. Similar to the type I IFN signaling pathway, the induction of IFN-lambda leads to the formation of the ISGF3 complex (Kotenko et al., 2003). However, the mechanism of IFN-lambda downstream signaling remains to be elucidated in detail.

### 1.8 Interferon regulatory factor family.

ISGs are typically induced by type I IFN through the binding of ISGF3 to ISREs with a consensus sequence 5' $^{A}/_{G}$NGAAANNGAAACT 3' located in the promoters of ISGs (Darnell et al., 1994). However, increasing evidence shows that some ISGs can be upregulated by viral infections in an IFN-independent manner. Besides ISGF3, additional complexes: ISGF1 (IRF-2) and ISGF2 (IRF-1) were identified to bind an ISRE (Kessler et al., 1988; Levy et al., 1988). The mammalian IRF family comprises of nine members, IRF-1 through IRF-9 (Table 1.2). Each of these proteins has a conserved DNA binding domain, and is a transcription factor and can bind to IRF-E binding sites in the promoters of some genes. The sequences of IRF-E sites are similar to that of the ISRE and contain tandem repeats of GAAA motifs separated by two bases (Honda and Taniguchi, 2006).

IRF-1 is a very unstable protein with a half-life of about 30 m (Watanabe et al., 1991). It is usually undetectable or expressed at low levels in a variety of cell types; however, it can be upregulated by some viral infections, type I or II IFNs or TNF$\alpha$. Activation of IRF-1 is

**Table 1.2. Comparison of IRF family members.**

| Factor | Expression pattern | Role in host defense |
|---|---|---|
| IRF-1 | Ubiquitous | Type I IFN and ISG induction |
| IRF-2 | Ubiquitous | Repression or induction of ISGs |
| IRF-3 | Ubiquitous | Type I IFN and ISG induction |
| IRF-4 | Hematopoietic cells | Immune cell differentiation and cytokine expression |
| IRF-5 | Ubiquitous | Type I IFN and cytokine induction |
| IRF-6 | High in skin cells | Unknown |
| IRF-7 | Ubiquitous | Type I IFN and ISG induction |
| IRF-8 | Hematopoietic cells | Cell differentiation and cytokine expression |
| IRF-9 | Ubiquitous | ISG induction |

Modified from (Ozato et al., 2007).

controlled by phosphorylation (Taniguchi et al., 2001). IRF-1 can also be SUMOylated, which was shown to increase its stability, or ubiquitylated, which leads to its degradation by the proteasome (Park et al., 2007). Although, IRF-1 was initially described as a transcriptional activator of IFN-beta expression (Miyamoto et al., 1988); subsequently, it was also shown to upregulate some ISGs in an IFN-independent manner (Schoggins et al., 2011). One of the IRF-1 target genes, viperin (Stirnweiss et al., 2010) was reported to inhibit both WNV and dengue infections (Jiang et al., 2010). In addition, a recent study showed that overexpression of IRF-1 leads to the inhibition of the replication of not only WNV and other flaviviruses such as dengue virus, YFV, and hepatitis C virus, but also other types of viruses including Chikungunya virus, Venezuelan encephalitis virus and human immunodeficiency virus 1 (HIV) (Schoggins et al., 2011). In addition to the induction of antiviral genes, IRF-1 also activates the expression of genes regulating innate and adaptive immune responses, the cell cycle, apoptosis, DNA damage repairs and tumor-suppression (Taniguchi et al., 2001). Because IRF-1 functions as a tumor suppressor, its expression is suppressed in many tumor cells to prevent apoptosis and cell cycle arrest from occurring (Taniguchi et al., 1997). MEFs and hepatocytes lacking IRF-1 were unable to undergo growth arrest. In addition, IRF-1 together with p53 was required for optimal induction of the cyclin-dependent kinase inhibitor p21 after treatment with ionizing radiation (Tanaka et al., 1996).

In contrast to IRF-1, IRF-2 is a relatively stable protein (half-life of about 8 h) (Watanabe et al., 1991) and it was shown to function as a transcriptional repressor of the type I IFN gene and some ISGs (Harada et al., 1989; Harada et al., 1990; Hida et al., 2000). However, additional studies

showed that IRF-2 can also act as a transcriptional activator of some genes (Vaughan et al., 1995; Jesse et al., 1998).

Similar to IRF-1, IRF-3 and IRF-7 are TFs that play distinct and nonredundant roles in the induction of type I IFN (Sato et al., 2000). IRF-3 is a constitutively expressed protein that is found in the cytoplasm of all cells in an inactive form. During a viral infection, it undergoes phosphorylation which induces dimerization followed by translocation to the nucleus in a complex with the histone acetyltransferases p300 and CREB-binding protein (CBP) (Yoneyama et al., 1998; Suhara et al., 2002; Fitzgerald et al., 2003; Sharma et al., 2003). Although IRF-3 alone is not sufficient to induce IFN beta expression, it cooperates with NF-kappa B and AP1 TFs to enhance IFN beta expression. IRF-3 was also identified as a component of the virus-inducible dsRNA-activated factor 1 complex (DRAF1) (Weaver et al., 1998) that was shown to play a role in IFN-independent upregulation of a subset of ISGs (Grandvaux et al., 2002; Andersen et al., 2008). In contrast to the constitutive expression of IRF-3, IRF-7 expression is typically induced by type I IFN signaling. IRF-7 plays a role in the later phase of the type I IFN response to viral infection through the amplification of the response via the activation of various IFN-alpha species and IFN-alpha dependent genes (Marie et al., 1998; Sato et al., 1998) as well as by enhancing IFN-beta production (Wathelet et al., 1998). Several ISGs can also be upregulated directly by IRF-7 (Barnes et al., 2004).

IRF-4 and IRF-8 expression is restricted to particular types of immune cells. These IRFs play a role in the regulation of cell differentiation, DNA repair and cytokine production (Ozato et al., 2007). IRF-5 is ubiquitously expressed and was shown to be involved in virus-mediated activation of type I IFN and inflammatory cytokines (Barnes et al., 2001; Schoenemeyer et al.,

2005; Takaoka et al., 2005; Paun et al., 2008). The role of IRF-6 in the immune response has not been studied. IRF-6 is expressed to high levels in skin cells and is important for regulation of skin cell development (Ozato et al., 2007).

IRF-9 plays a crucial role in type IFN-signaling and the activation of ISGs. It associates with STAT1 and STAT2 to form the trimeric ISGF3 transcription factor complex that binds to ISREs in the promoters of ISGs and activates their expression (Paun and Pitha, 2007) (Fig.1.3). One previous study reported that although IRF-9 translocated to the nucleus, it could not activate gene expression alone (Kraus et al., 2003). However, both a IRF-9/STAT2 complex and a IRF-9/STAT2 fusion protein were shown to efficiently activate ISRE-driven transcription of a reporter gene (Kraus et al., 2003; Lou et al., 2009) suggesting that IRF-9 may play a role in ISGF3-independent gene expression when complexed with other factor(s).

## 1.9 Strategies utilized by viruses to evade host immune antiviral responses

The establishment of an antiviral state largely depends on both the induction of IFN and the functions of antiviral ISGs and many viruses have evolved mechanisms to suppress the expression of ISGs. Three main strategies utilized by viruses to suppress the induction of ISGs are: inhibition of IFN production, inhibition of the IFN signaling pathway and blockage of the synthesis of antiviral proteins. Within each of these strategies, different viruses have evolved strain, cell type and species specific mechanisms to evade the induction of the antiviral state.

### *1.9.1 Inhibition of IFN production by viruses*

Because IFN induction is a result of the recognition of viral structures by PRRs, many viruses have developed replication strategies that minimize the production of PAMPs. For example, flaviviruses replicate their RNA in endoplasmic perinuclear membrane vesicles (Mackenzie,

2005; Welsch et al., 2009; Gillespie et al., 2010) that likely limit the detection of viral nucleic acid structures during the exponential replication phase. A recent report showed that although PKR, a dsRNA sensor, is not actively suppressed by WNV Eg101 infection, it is not activated in infected rodent cells (Elbahesh et al., 2011). However, during the initial stages of WNV infection when the replication complexes are not yet well formed the small amounts of RNA species including dsRNA produced may be detected by PRR. RIG-I and MDA5 cytoplasmic sensors were previously shown to mediate the activation of the IRF-3 (Fredericksen and Gale, 2006; Scherbik et al., 2007; Fredericksen et al., 2008) and NF-kappa B (Scherbik, Pulit-Penaloza and Brinton, unpublished data) TFs and the subsequent induction of type I IFN in WNV infected cells.

Many viruses encode proteins that were experimentally shown to antagonize IFN induction by binding dsRNA and limiting activation of host dsRNA binding sensors or by direct inhibition of RIG-I, MDA-5 or TLR-3 signaling or by blocking the activation of IRF-3 or NF-kappa B TFs [Reviewed in (Randall and Goodbourn, 2008)]. In the case of WNV, the NS2A protein of the attenuated lineage I WNV strain, Kunjin was shown to inhibit IFN beta transcription by an unknown mechanism (Liu et al., 2004; Liu et al., 2006).

### 1.9.2 *Inhibition of IFN signaling by viruses*

Numerous reports showed that viruses can block IFN signaling at virtually each step of that pathway [reviewed in (Randall and Goodbourn, 2008)]. Some of the strategies reported for different strains of WNV include downregulation of IFN alpha/beta R expression (Evans et al., 2011), suppression of type I IFN signaling through the redistribution of cholesterol (Mackenzie et al., 2007), blockage of JAK and Tyk phosphorylation (Guo et al., 2005) and blockage of

STAT1 and STAT2 phosphorylation and translocation to the nucleus (Laurent-Rolle et al.; Liu et al., 2005; Keller et al., 2006).

### *1.9.3 Mechanisms of blockage of the synthesis of antiviral proteins by viruses.*

One of the strategies utilized by viruses to antagonize the host innate response to viral infection is the inhibition of protein translation. The process of translation is divided into the initiation, elongation, termination and ribosome recycling phases. Although viruses can inhibit translation at each of these steps, most reports show that translation is mainly regulated at the level of initiation (Walsh and Mohr, 2011). Induction of global inhibition of host mRNA translation is beneficial for viruses that have evolved alternative translational mechanisms for viral protein translation. For example, both caliciviruses, which encode proteins that serve as cap-analogues, and picornaviruses, which can initiate translation from an internal ribosome entry site (IRES), can initiate translation of viral proteins when cap-dependent translation is blocked (Lopez-Lastra et al., 2010). However, many viruses including flaviviruses depend entirely on the canonical host translation machinery and so are susceptible to global translation inhibition. Hence, inhibition of host translation is not observed in flavivirus infected cells (Lindenbach, 2007).

An alternative means of inhibiting protein translation by viruses is blocking the export of cellular mRNAs from the nucleus as has been observed for adenovirus, influenza virus and vesicular stomatitis virus (VSV) infections (Faria et al., 2005; Satterly et al., 2007; Yatherajam et al., 2011). Some herpesviruses have also been shown to suppress host protein translation through the induction of increased cell mRNA turnover (Glaunsinger and Ganem, 2004; Feng et al., 2005; Lee and Glaunsinger, 2009; Clyde and Glaunsinger, 2010).

Several known mechanisms of transcript specific suppression of translation have been reported. One of these involves the binding of host RNA binding proteins to *cis*-acting elements in the 3'UTRs of target mRNAs which inhibits translation initiation (Abaza and Gebauer, 2008). For example, translational repression by trans-acting proteins binding to the 3'UTR was reported for the 15-lipoxygenase (Ostareck et al., 1997), MEF-2A (Black et al., 1997) and p53 (Fu and Benchimol, 1997) mRNAs. Proteins binding to AU-rich elements (AREs) in the 3'UTRs of target mRNAs can cause either destabilization or stabilization mRNA or suppress translation (Zhang et al., 2002). In rare instances, translation initiation can be blocked by the binding of a RNA binding protein to a *cis*-element in the 5'UTR (Gray and Hentze, 1994). It is possible that a viral infection may induce this type of transcript regulation of protein translation but no examples have yet been reported.

Transcript specific protein synthesis can also be suppressed by specific micro RNAs (miRNAs). RNA interference was first described as an antiviral mechanism in plants (Lindbo et al., 1993; Ratcliff et al., 1997; Anandalakshmi et al., 1998; Brigneti et al., 1998; Kasschau and Carrington, 1998; Hamilton and Baulcombe, 1999). Hundreds of miRNAs have been identified in humans with each of the miRNAs having the potential to regulate multiple genes (Bentwich, 2005). Many miRNA genes are transcribed under strict developmental-stage and tissue-specific control. Primary miRNA transcripts (pri-miRNAs) form stem-loop structures which are cleaved by the RNase III enzyme drosha to precursor miRNAs (pre-miRNAs) that are transported from the nucleus into the cytoplasm by exportin 5. In the cytoplasm, pre-miRNAs are cleaved by the RNase III enzyme dicer into mature miRNAs (Murchison and Hannon, 2004). The guide strand of a mature ~22 nucleotide miRNA associates with argonaute proteins and other components to form miRNA-induced silencing complexes (miRISC). The miRNAs guide these complexes to

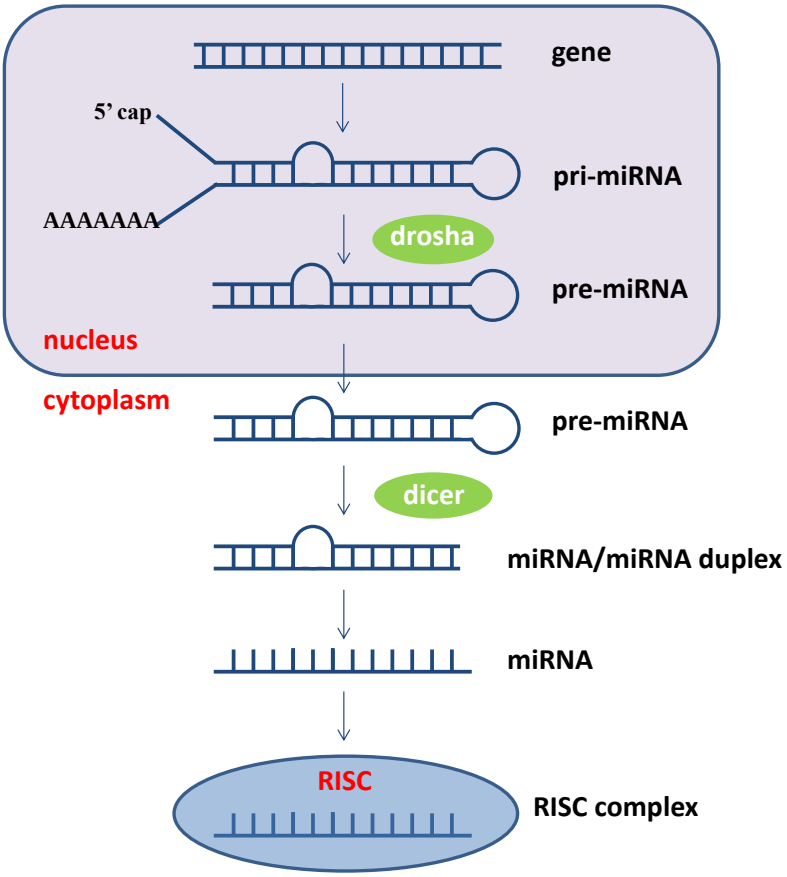


**Figure 1.4. miRNA maturation.** Primary pri-miRNA is cleaved by Drosha in the nucleus. The pre-miRNA is then transported into the cytoplasm where is cleaved into mature miRNA by dicer. The miRNA guide strand then associates with argonaute proteins and other components of the miRISC complex and targets a specific mRNA.

the target mRNAs and the interaction of usually multiple miRNAs with a target RNAs leads to translation suppression or inhibition or alteration of target mRNA stability (Eulalio et al., 2008; Hutvagner and Simard, 2008). miRNAs most often bind to the 3'UTR of a target message. Occasionally, miRNAs bind to 5'UTR or ORF regions but they are usually less effective in silencing translation at these sites (Lytle et al., 2007). Additionally, it has been shown that the binding of miRNAs can lead to sequestering target mRNAs in processing bodies (P-bodies) (Parker and Sheth, 2007).

Some viruses including herpesviruses, adenoviruses and polyomaviruses encode miRNAs which regulate viral and/or host cell gene translation (Gottwein and Cullen, 2008; Grundhoff and Sullivan, 2011). Other viruses such as Epstein-Barr virus (Motsch et al., 2007; Cameron et al., 2008; Ho et al., 2011) and enteroviruses (Ho et al., 2011) induce the expression of cellular miRNAs that benefit the virus, while HIV infections downregulate cellular miRNAs that inhibit viral replication (Triboulet et al., 2007). The majority of known viral miRNAs are encoded by DNA viruses due to the fact that the maturation of miRNAs involves cleavage by drosha in the nucleus (Rouha et al., 2010). However, a recent study showed that TBEV containing a EBV pre-miRNA in its genome can express mature miRNA in the cytoplasm without the involvement of drosha processing (Rouha et al., 2010). Although none of the so far identified viral miRNAs are encoded by RNA viruses which replicate in the cytoplasm this study indicates that the generation of miRNAs by cytoplasmic viruses is mechanistically feasible. Interestingly, several flaviviruses produce a highly structured, nuclease resistant, noncoding RNA derived from the 3' UTR of the viral genome that was shown to be crucial for virus-induced cytopathicity and pathogenicity (Pijlman et al., 2008). More recently the 3'UTR of the WNV strain Kunjin was reported to

encode a miRNA-like small RNA that is important for efficient replication of this virus in mosquito cells (Hussain et al., 2011).

## GOALS OF THE DISSERATION

WNV-host cell interactions are not fully understood and the overall goal of this study is to investigate mechanisms by which WNV modulates the expression of host antiviral genes. Although WNV strains have the ability to inhibit IFN signaling, efficient upregulation of many ISGs including Oas1a, Oas1b and Irf7 was still observed in cells infected with these viruses (Fredericksen et al., 2004; Scherbik et al., 2006; Daffis et al., 2007; Scherbik et al., 2007; Daffis et al., 2008; Fredericksen et al., 2008). Although it was previously reported that the expression of some ISGs can be upregulated in an IFN-independent manner, many ISGs including Irf7, Oas1a were thought to be activated only in a type I IFN-dependent-manner. In addition, our previous results showed that the upregulation of a subset of ISGs including Irf1 is delayed in WNV-infected cells. Also protein expression of the delayed subset of ISGs was suppressed in WNV Eg101-infected MEFs (Scherbik et al., 2007). The mechanisms of ISG transcription regulation in IFN beta-treated and WNV Eg101-infected MEFs will be investigated under Aims 1 and 2, while the mechanism of WNV Eg101 induced suppression of ISG protein levels will be analyzed under Aim 3.

**AIM 1. Functional analysis of the induction of Oas1a and Oas1b promoters by type I IFN.**

**AIM 2. Investigation of the activation of ISGs in MEFs infected with WNV Eg101.**

**AIM 3. Investigation of transcriptional and translational regulation of IRF-1 expression in WNV Eg101-infected MEFs.**

# CHAPTER 2

## 2 AIM 1: Functional analysis of the induction of Oas1a and Oas1b promoters by type I IFN.

*The data from this aim has been accepted for publication in Virology, 2012.*

### INTRODUCTION

The recognition of viral dsRNA by cellular sensors in infected cells leads to activation of the NF-kappa B, IRF-3 and ATF2/c-Jun transcription factors that bind cooperatively to the interferon (IFN) beta promoter and activate its transcription (Merika and Thanos, 2001). IFN beta secreted by infected cells binds to IFN alpha/beta receptors on the surfaces of both infected and uninfected cells resulting in activation of JAK1 and Tyk2 kinases that phosphorylate STAT1 and STAT2 transcription factors. Phosphorylated STAT1 and STAT2 and IFN regulatory factor 9 (IRF-9) form the IFN stimulated gene factor 3 complex (ISGF3) that translocates to the nucleus where it binds to IFN stimulated response elements (ISREs) in the promoters of IFN stimulated genes (ISGs) and upregulates their expression (Stark et al., 1998).

Three oligoadenylate synthetase genes (OAS1, OAS2 and OAS3) and one OAS-like (OASL) gene have been identified in the human genome (Hovnanian et al., 1998; Rebouillat et al., 1998). The transcripts of three of these genes are alternatively spliced and polymorphisms have been identified that alter splicing sites. Five isoforms have been reported for OAS1 (p42, p44, p46/p48 and p52), two for OAS2 (p69 and p71), one for OAS3 (p100) and two for OASL (p30 and p59) (Hartmann et al., 1998; Rebouillat et al., 1998; Hovnanian et al., 1999; Justesen et al., 2000; Bonnevie-Nielsen et al., 2005). In contrast, the mouse genome contains eight OAS1 (Oas1a-

Oas1h), two OASL (Oasl1 and Oasl2), one OAS2 (Oas2) and one OAS3 (Oas3) gene orthologs (Rutherford et al., 1991; Justesen et al., 2000; Shibata et al., 2001; Kakuta et al., 2002). Gene duplication, rather than alternative splicing, is responsible for the multiple murine Oas1 isoforms (Perelygin et al., 2006). Enzymatically active OAS proteins play an important antiviral role. When activated by viral dsRNA, they catalyze the synthesis of short 2'-5'-oligoadenylates (2-5A) from ATP. 2-5A activates latent endonuclease RNase L which degrades both cellular and viral single-stranded RNAs (Samuel, 2001). Among the eight murine Oas1 proteins, only Oas1a and Oas1g have been reported to be active 2'-5'-oligoadenylate synthetases (Kakuta et al., 2002; Elbahesh et al., 2011). However, the inactive synthetase Oas1b mediates resistance to flavivirus-induced disease through an unknown mechanism that is independent of RNase L (Scherbik et al., 2006). The flavivirus-induced disease resistant mouse strain C3H/RV is homozygous for the dominant $Oas1b^{r}$ allele encoding a full length Oas1b protein, while the congenic susceptible mouse strain C3H/He is homozygous for the recessive $Oas1b^{s}$ allele that encodes a C-terminally truncated $Oas1b^{tr}$ protein (Perelygin et al., 2002). A previous study showed that the full length Oas1b protein, which is an inactive synthetase, can inhibit *in vitro* Oas1a synthetase activity in a dose-dependent manner and reduce 2-5A production *in vivo* in response to poly(I:C) (Elbahesh et al., 2011). A similar function was reported for Oas1d, another of the inactive Oas1 proteins (Yan et al., 2005).

Each of the human OAS genes contains an ISRE in its promoter and is induced by type I IFN (Wang and Floyd-Smith, 1997; Hartmann et al., 1998; Floyd-Smith et al., 1999; Yu et al., 1999; Rebouillat et al., 2000). Similarly, murine Oas gene expression with the exception of Oas1f was reported to be activated by type I IFN (Eskildsen et al., 2002; Eskildsen et al., 2003). A previous

TFSEARCH analysis predicted transcription factor binding sites (TFBSs) in 500 bp promoter fragments of the murine Oas1a-h, Oas2 and Oas3 genes and identified an ISRE in only the promoters of the Oas1a, Oas1b, Oas1g and Oas2 genes (Mashimo et al., 2003). Only the ISRE in the Oas1b promoter was predicted to overlap GAS and NF-kappa B sites. These results suggested the possibility of differential regulation of Oas1a and Oas1b expression by IFN and/or viral infection but this prediction was not functionally tested.

In the present study, the Oas1a and Oas1b promoters from both C3H/RV and C3H/He mouse embryofibroblasts (MEFs) were cloned and sequenced. A GENOMATIX search of the Oas1a and Oas1b promoter sequences predicted that neither had a TATA box but that both had a canonical initiator element (INR). An inverted CCAAT element (ICE) was predicted and functional analysis showed that it may be important for the basal activities of the C3H/He and C3H/RV Oas1b promoters and the C3H/RV Oas1a promoter. The C3H/He Oas1a promoter contained a mutation in this site that was predicted to make it nonfunctional. A single ISRE as well as overlapping STAT and IRF sites were predicted in both promoters. Functional mapping of the Oas1a and Oas1b promoters by sequential 5' deletion and TFBS mutagenesis indicated that the ISRE as well as the overlapping STAT site are required for Oas1a promoter induction by IFN beta while Oas1b expression requires only the ISRE. Also, both STAT1 and STAT2 are required for Oas1a upregulation by IFN beta, while only STAT2 is required for Oas1b upregulation. A single nucleotide difference between the STAT sites of the Oas1b and Oas1a promoters appeared to be responsible for the differential STAT1-dependence of Oas1a and Oas1b expression.

# RESULTS

## 2.1 Mapping the Oas1a and Oas1b gene promoter regions required for basal promoter expression and induction by IFN beta.

The Oas1a and Oas1b genes are ISGs and after treatment of C3H/He MEFs with 1000 U/ml of murine IFN beta for 3 h, Oas1a mRNA was upregulated by about 9 fold while the Oas1b mRNA was upregulated by about 7 fold (Fig. 2.1A). The time and the dose of IFN treatment was selected based on a previous study showing that the highest level of ISG induction was at 3h after IFN treatment of MEFs and that the levels of ISG mRNA upregulation were similar with 10, 100 and 1000 U/ml of IFN beta (Scherbik et al., 2007). The regions of the Oas1a and Oas1b proximal promoters required for basal gene expression and activation by IFN beta were then mapped using luciferase reporter assays. Two firefly luciferase reporter gene constructs, one containing a C3H/RV Oas1a gene promoter fragment [Oas1a (-1768, +28)] and the other containing a C3H/RV Oas1b gene promoter fragment [Oas1b (-1398, +51)], were first generated and then a set of 5' sequentially deleted constructs was made for each promoter. C3H/RV MEFs were transfected with construct DNA, and 24 h later cell lysates were harvested and used to analyze basal promoter activity. To analyze the effect of IFN on Oas1 promoter activity, cells transfected with a luciferase reporter for 24 h were incubated with murine IFN beta. Initial pilot experiments showed that although luciferase activity was the highest at both 3 and 6 h after treatment, the 3h peak level was the most reproducible. At 24 and 48 h, luciferase activity was significantly decreased. Based on these preliminary results and the maximum half-life of the firefly luciferase protein of 4 h (Thompson et al., 1991; Brandes et al., 1996), assays were done in all subsequent luciferase reporter experiments after 3 h of IFN beta treatment. Low basal luciferase activities were detected for both the longest Oas1a (-1768, +28) construct (Fig. 2.1B)

**Table 2.1. Primers used to generate the Oas1a and Oas1b promoter deletion reporter constructs.**

| Construct | Forward primer | Reverse primer |
|---|---|---|
| Oas1a (-854 to +28) | AGCTAGCTAGGCTCGGGGACCAGTAGTAG[1] | AAGATCTGCTAAGTCTGGAGCTTCCTGG[1] |
| Oas1a (-722 to +28) | AGCTAGCGCCCATGAGTGATCCTCCA | AAGATCTGCTAAGTCTGGAGCTTCCTGG |
| Oas1a (-641 to +28) | AGCTAGCTCAACCTTGGGAATGTCCTGG | AAGATCTGCTAAGTCTGGAGCTTCCTGG |
| Oas1a (-468to +28) | AGCTAGCGATGTGAGTAAGAGAGGGGGC | AAGATCTGCTAAGTCTGGAGCTTCCTGG |
| Oas1a (-396 to +28) | AGCTAGCAAAGAAAGAAAGAAAGGAAGAAAG | AAGATCTGCTAAGTCTGGAGCTTCCTGG |
| Oas1a (-289 to +28) | AGCTAGCTGGAAGCCACAGCCACCTTCTGCAG | AAGATCTGCTAAGTCTGGAGCTTCCTGG |
| Oas1a (-176 to +28) | AGCTAGCAGAAGAAACCCCAAGAAAGCCAG | AAGATCTGCTAAGTCTGGAGCTTCCTGG |
| Oas1a (-87 to +28) | AGCTAGCTGGTCAGAAGCTCTGAAGCC | AAGATCTGCTAAGTCTGGAGCTTCCTGG |
| Oas1b (-1398 to +51) | AGCTAGCTTTTTCCCCCTCACACTCTG | AAGATCTCCTCTGCAGCCAGCAGGTCCT |
| Oas1b (-991 to +51) | AGCTAGCCCAATCCTGCTCTTGCAGAAGGC | AAGATCTCCTCTGCAGCCAGCAGGTCCT |
| Oas1b (-814 to +51) | AGCTAGCGTGTGTGTGTGTGTGTGTTTGGGAC | AAGATCTCCTCTGCAGCCAGCAGGTCCT |
| Oas1b (-742 to +51) | AGCTAGCACAGCCCGAGCTCTTAAACTCTGAG | AAGATCTCCTCTGCAGCCAGCAGGTCCT |
| Oas1b (-507 to +51) | AGCTAGCAGACCCCACCCTCACCCAGAC | AAGATCTCCTCTGCAGCCAGCAGGTCCT |
| Oas1b (-394 to +51) | AGCTAGCACCTGCAAGTCCAGAGGTAAAGG | AAGATCTCCTCTGCAGCCAGCAGGTCCT |
| Oas1b (-181 to +51) | AGCTAGCCAGAAGAAATCCCGAGAAAG | AAGATCTCCTCTGCAGCCAGCAGGTCCT |
| Oas1b (-116 to +51) | AGCTAGCGTACCTGTTCAGAAGCCCTAACGCC | AAGATCTCCTCTGCAGCCAGCAGGTCCT |

[1]Underlined sequences indicate an NheI restriction site included in all forward primers and a BglII restriction site included in the reverse primers.

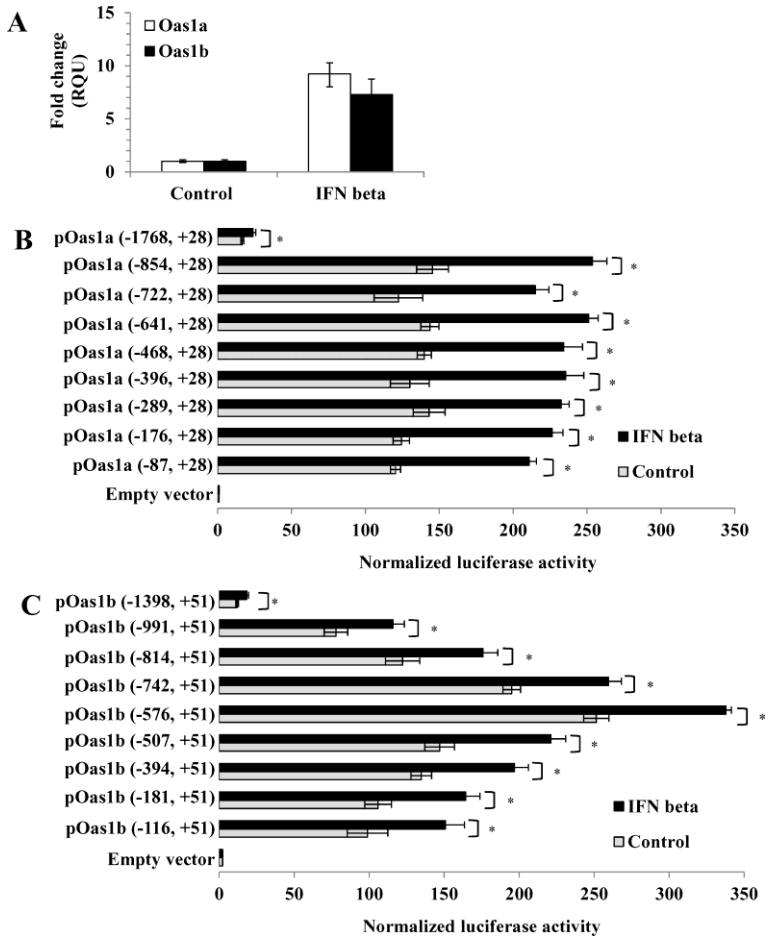


**Figure 2.1. IFN beta-induced upregulation f Oas1a and Oas1b *in vivo* and of promoter reporter constructs *in vitro.*** **(A)** C3H/He MEFs were treated with 1000 U/ml of murine IFN beta for 3h or left untreated (control). Total RNA was extracted and Oas1a and Oas1b mRNA levels were measured by real time qRT-PCR. The mRNA level for each gene was normalized to the level of GAPDH mRNA in the same sample and is shown as the fold change over the amount of mRNA in mock samples expressed in relative quantification units (RQU). Each experiment was performed in triplicate. Luciferase reporter assays were done with **(B)** Oas1a and **(C)** Oas1b promoter fragments of different lengths. C3H/RV MEFs were co-transfected with either a luciferase reporter construct DNA or a control empty vector DNA and *Renilla* luciferase reporter vector DNA (transfection efficiency control). At 24 h after transfection, MEFs were either treated with 1000 U/ml of murine IFN beta for 3 h or left untreated (control). Cell lysates were prepared and firefly luciferase activity was measured in triplicate. Firefly luciferase activity was normalized to *Renilla* luciferase activity for each sample. Error bars represent standard error of the mean (SEM) (n=3). Significant differences were determined with a Student's *t* test (∗, $P < 0.05$).

and the longest Oas1b (-1398, +51) construct (Fig. 2.1C). These constructs showed a modest but significant increase in promoter activity after IFN treatment. The observation that the longest Oas1a and Oas1b promoter fragments tested produced the lowest reporter activities suggested the presence of upstream transcriptional repressor elements that negatively affected the basal and IFN-induced expression levels of both promoters.

Promoter constructs with sequential 5' deletions were used to determine the shortest Oas1a and Oas1b promoter fragments able to produce increased luciferase activity upon stimulation with IFN beta. Each of the 5' deleted Oas1a promoter constructs tested produced similar significantly increased basal luciferase activities compared to the Oas1a (1768, +28) construct and the activities for each of these constructs increased upon stimulation with IFN beta (Fig. 2.1B). For instance, the Oas1a (-87, +28) and Oas1a (-854, +28) constructs had basal activities that were 7.1 and 8.6 fold higher, respectively, than that of the Oas1a (-1768, +28) construct and both showed a 1.75 fold increase in luciferase activity after stimulation with IFN beta. These results indicated that the TFBSs required for IFN induction of the Oas1a are located between -87 and +28.

In contrast to what was observed with the truncated Oas1a constructs, the activities of each of the 5' deleted Oas1b constructs varied. The Oas1b (-576, +51) construct showed a 21 fold increase over the activity produced by the Oas1b (-1398, +51) construct (Fig. 2.1C). Constructs that were either shorter or longer than Oas1b (-576, +51) produced lower basal activities. The observation that the basal activity of the Oas1b (-116 to +51) construct was 2.5 fold lower than that of Oas1b (-576, +51) suggested that the region between -576 and -116 contains elements that enhance basal Oas1b expression. As the length of the Oas1b constructs increased beyond -576 bp, the

basal activity decreased suggesting the presence of repressor elements in this region. The activity of each of the truncated Oas1b promoter constructs was induced to a similar extent above its basal level by IFN beta treatment (Fig. 2.1C) indicating that the elements required for the induction of the Oas1b promoter by IFN beta are located between -116 and +51 bp.

Although the results obtained were reproducible and statistically significant, basal levels were high and the maximal induction observed with IFN beta was about 2 fold. The low levels of induction by IFN are likely to be due to the use of promoter fragments with only a single ISRE in the context of a natural promoter sequence which also contains multiple additional TF binding sites that modulate both basal and IFN-induced luciferase activity. Previous studies using natural TLR9 (Guo et al., 2005) and RIG-I (Su et al., 2007) promoter sequences with single copies of an ISRE also reported a 2 fold or lower activation of the reporter gene after stimulation with IFN beta.

### 2.2 Analysis of the core promoter elements in the Oas1a and Oas1b promoters.

Elements in the -87 to +28 C3H/RV Oas1a promoter fragment and in the -116 to +51 C3H/RV Oas1b promoter fragment were predicted with GENOMATIX and TFSEARCH programs. Neither promoter contained a TATA box but each contained an INR (Fig. 2.2), an element commonly found in TATA-less promoters and known to be able to direct transcriptional initiation (Smale and Baltimore, 1989; Smale, 1997). Within the INR consensus $^{C}/_{T}{}^{C}/_{T}A_{+1}N^{A}/_{T}{}^{C}/_{T}{}^{C}/_{T,}$ the adenine is the transcription start site (TSS) and this nucleotide was used to predict the location of the Oas1a and Oas1b TSSs. The GENOMATIX program also predicted an inverted CCAAT element (ICE) at -63 to -68 in the Oas1a promoter and at -62 to -67 in the Oas1b promoter. CCAAT boxes in either the forward (CCAAT) or reverse (ICE; ATTGG)

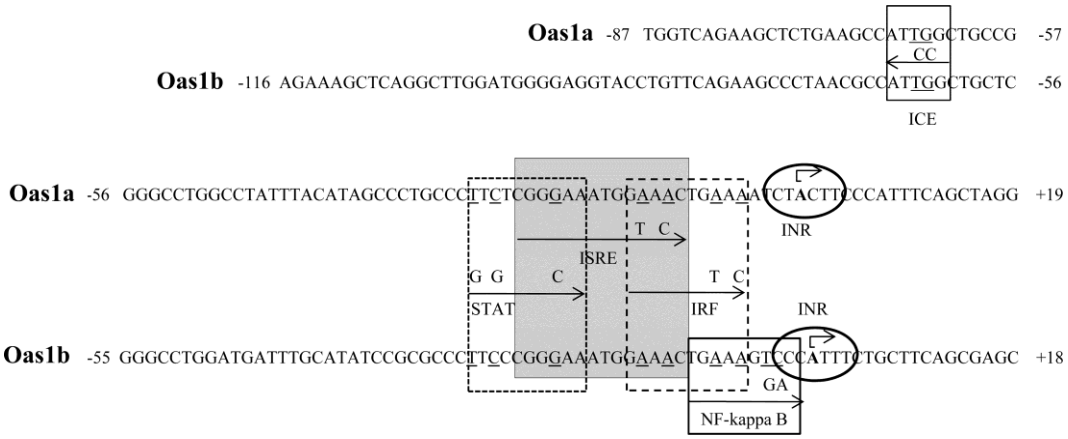


**Figure 2.2. Predicted TFBSs in the Oas1a and Oas1b promoters.** TFBSs predicted by the GENOMATIX search program. The locations of the DNA fragments with respect to the predicted TSS in an INR are indicated with an arrow. Substituted nucleotides in both promoters are underlined and substitutions made in promoter fragments are shown above arrows indicating the boundaries of individual TFBSs.

orientation are typically located about 60 to 100 nucleotides upstream of the TSS (Mantovani, 1999; Dolfini et al., 2009). To determine whether the predicted ICE plays a functional role in the Oas1a and Oas1b promoters, two nucleotides (ATTGG → ATCCG) were substituted in this element in the Oas1a (-854, +28) and Oas1b (-576, +51) constructs. A GENOMATIX search confirmed that the introduced mutations eliminated the targeted binding site and did not create a new TFBS. Mutation of ICE reduced the basal luciferase activity of the Oas1a and Oas1b promoters by 43% and 40%, respectively, but did not negatively affect induction of either promoter by IFN beta (Fig.2.3A). IFN beta induced the wild type and ICE-mutated Oas1a promoters by 1.7- and 1.9 fold, respectively, and the wild type and ICE-mutated Oas1b promoter by 1.4 and 1.5 fold, respectively.

DNA probes consisting of the -88 to -49 bp for Oas1a or -82 to -48 bp for Oas1b (Table 2.3) were next used in an electrophoretic mobility shift assay (EMSA) to determine whether TFs bind to the ICE sequence. Oas1a and Oas1b probes with a wild type ICE bound to two complexes in nuclear extracts from untreated C3H/RV MEFs **(**Fig. 2.3B). With both probes, the upper band was much darker than the lower band. These bands were either not detected or were much fainter when a specific unlabeled competitor DNA was included in the reaction suggesting that the binding detected was specific. Neither of the shift bands was observed when an Oas1a probe containing a mutated ICE was tested. An Oas1b probe with a mutated ICE detected a faint lower complex band but did not detect an upper complex band. The results suggest that nuclear extracts from untreated control cells contain TFs that bind to the ICE. Although the TFs binding to the ICE in the Oas1a and Oas1b promoters were not identified, both the reporter assay (Fig. 2.3A) and the EMSA (Fig. 3B) results suggest that the ICE element plays a role in the regulation of basal transcription from both genes.

## Table 2.2. Primers used for site directed mutagenesis.

| Construct | Primer | Primer sequence |
|---|---|---|
| Oas1a (-854, +28) mIRF | F[1] | GCCCTTCTCGGGAAATGGAAACTGTACATCTACTTCCC[2] |
| | R | GGGAAGTAGATGTACAGTTTCCATTTCCCGAGAAGGGC |
| Oas1a (-854, +28) mISRE | F | GCCCTTCTCGGGAAATGGTACCTGAAAATCTACTTCCC |
| | R | GGGAAGTAGATTTTCAGGTACCATTTCCCGAGAAGGGC |
| Oas1a (-854, +28) mSTAT | F | CATAGCCCTGCCCGTGTCGGCAAATGGAAACTG |
| | R | CAGTTTCCATTTGCCGACACGGGCAGGGCTATG |
| Oas1a (-854, +28) mICE | F | CAGAAGCTCTGAAGCCATCCGCTGCCGGGGCCTGG |
| | R | CCAGGCCCCGGCAGCGGATGGCTTCAGAGCTTCTG |
| Oas1b (-576, +51) mNF-kappa B | F | CCCGGGAAATGGAAACTGAAAGGACCATTTCTGCTTCAGCG |
| | R | CGCTGAAGCAGAAATGGTCCTTTCAGTTTCCATTTCCCGGG |
| Oas1b (-576, +51) mIRF | F | CCCGGGAAATGGAAACTGTACGTCCCATTTCTGCTTCAGCG |
| | R | CGCTGAAGCAGAAATGGGACGTACAGTTTCCATTTCCCGGG |
| Oas1b (-576, +51) mISRE | F | GCCCTTCCCGGGAAATGGTACCTGAAAGTCCC |
| | R | GGGACTTTCAGGTACCATTTCCCGGGAAGGGC |
| Oas1b (-576, +51) mSTAT | F | GCATATCCGCGCCCGTGCCGGCAAATGGAAACTGAAAGTCCC |
| | R | GGGACTTTCAGTTTCCATTTGCCGGCACGGGCGCGGATATGC |
| Oas1b (-576, +51) mICE | F | CAGAAGCCCTAACGCCATCCGCTGCTCGGGCCTGG |
| | R | CCAGGCCCGAGCAGCGGATGGCGTTAGGGCTTCTG |

[1] F, forward primer; R, reverse primer
[2] Underlined letters indicate mutated nts.

## Table 2.3. Sequences of DNA probes used in EMSA.

| Gene | TFBS | Location | Sequence |
|---|---|---|---|
| Oas1a | ISRE | -31 to +7 | GCCCTTCTCGGGAAATGGAAACTGAAAATCTACTTCCC |
| Oas1a | ICE | -83 to -49 | CAGAAGCTCTGAAGCCATTGGCTGCCGGGGCCTGG |
| Oas1a | mutICE | -83 to -49 | CAGAAGCTCTGAAGCCATCCGCTGCCGGGGCCTGG |
| Oas1b | ISRE | -33 to +8 | CGCCCTTCCCGGGAAATGGAAACTGAAAGTCCCATTTCTGC |
| Oas1b | ICE | -82 to -48 | CAGAAGCCCTAACGCCATTGGCTGCTCGGGCCTGG |
| Oas1b | mutICE | -82 to -48 | CAGAAGCCCTAACGCCATCCGCTGCTCGGGCCTGG |

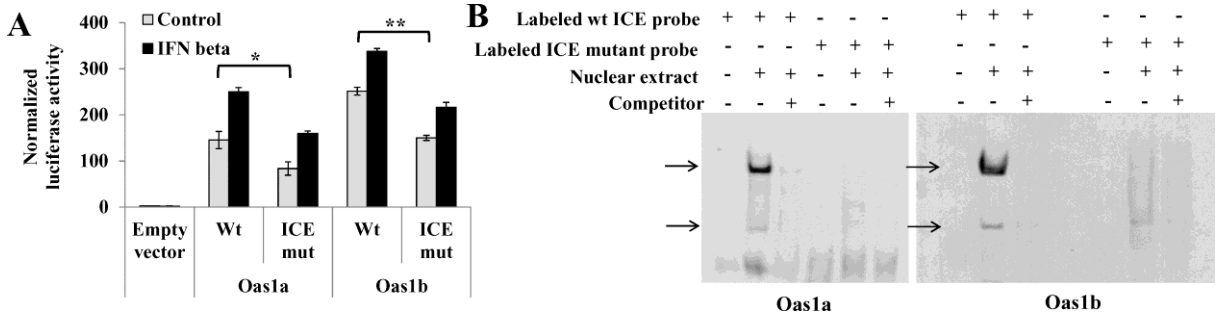


**Figure 2.3. Functional analysis of the predicted Oas1a and Oas1b ICEs. (A)** Luciferase reporter assays were done with control and mutated ICE constructs. Two nts in the ICE of the Oas1a (-854, +28) and Oas1b (-576, +51) constructs were substituted as indicated in Fig. 2. At 24 h after transfection of a wild type or mutant construct, C3H/RV MEFs were either treated with murine IFN beta (1000 U/ml) for 3 h or untreated and then luciferase activities were analyzed. Firefly luciferase activity measured in triplicate was normalized to *Renilla* luciferase activity. Error bars represent SEM (n=3). Statistical significance was determined with a Student ‘s *t* test (∗, $P < 0.05$; ∗∗, $P < 0.005$). **(B)** EMSA. DIG-labeled Oas1b and Oas1a DNA probes containing either a wild type or mutated ICE and nuclear extracts from C3H/RV MEFs were used for the binding reactions. A 200 fold excess of unlabeled specific competitor DNA was added prior to addition of the probe in the indicated reactions. DNA-protein complexes were resolved on 6% native gels and the bound labeled probe was detected using anti-DIG antibody. The results shown are representative of at least two independent experiments.

## 2.3 Comparison of the sequences of the Oas1a and Oas1b promoters in resistant C3H/RV and susceptible C3H/He MEFs.

To determine whether the sequences of the Oas1a or Oas1b promoters differ between congenic flavivirus disease susceptible C3H/He and flavivirus disease resistant C3H/RV mice, Oas1a (-1768, +28) and Oas1b (-1398, +51) DNA fragments were amplified by PCR from MEFs from each mouse strain, cloned and sequenced. Although complete identity was observed between the C3H/RV and C57BL/6J (NT_078458.6) Oas1a and Oas1b promoter sequences, the C3H/He Oas1a promoter sequence differed by T to C substitutions at positions -66 and -298 and the C3H/He Oas1b promoter sequence differed by a G to C substitution at position +15 and a 4 nt deletion between -327 and -323. GENOMATIX and TFSEARCH TFBS searches of the C3H/He promoter sequences predicted that only the T to C substitution at -66 in the Oas1a promoter was located in a TFBS. This substitution changed the ICE from ATTGG to ATCGG. Based on the observation that mutation of the ICE from ATTGG to ATCCG significantly decreased the basal activities of both the C3H/RV Oas1a and Oas1b promoters, the single nucleotide substitution in the C3H/He Oas1a promoter producing a ATCGG ICE sequence would be expected to reduce the basal expression level of the Oas1a gene in C3H/He MEFs.

## 2.4 Analysis of transcription factors binding to the Oas1a and Oas1b promoters.

Both the previously published search (Mashimo et al., 2003) and the TFSEARCH and GENOMATX TFBS searches done in this study predicted canonical ISREs with identical sequences (5' GGGAAATGGAAACT 3') between -22 to -9 bp in the Oas1a promoter and between -23 to -10 bp in the Oas1b promoter (Fig. 2B). To determine whether the components of

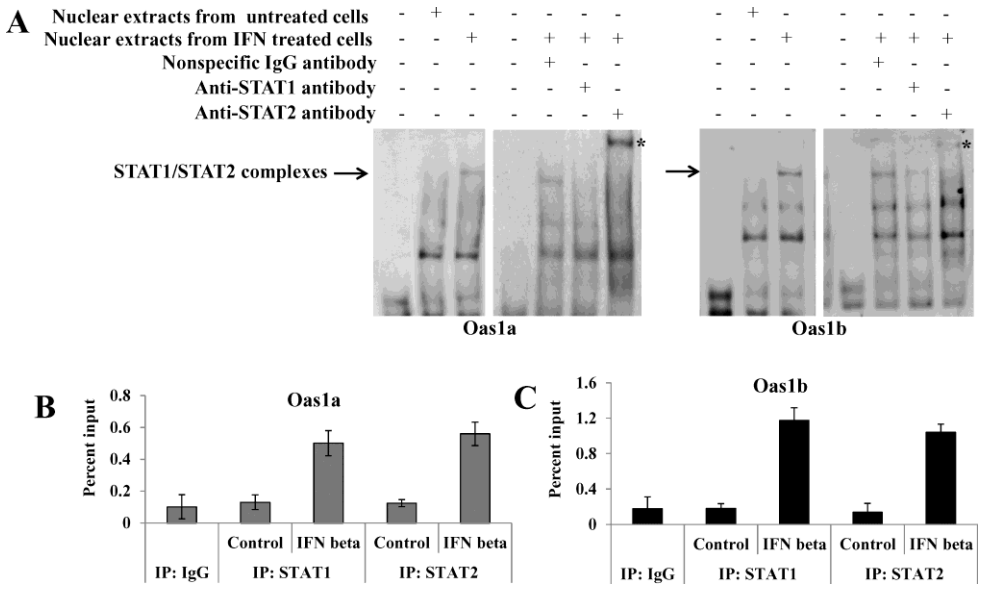


**Figure 2.4. Binding of STAT1 and STAT2 to the Oas1a and Oas1b promoters in *in viro* and *in vivo*.** DIG-labeled Oas1b and Oas1a DNA probes and nuclear extracts from untreated or murine IFN beta (1000 U/ml) treated C3H/RV MEFs were used for EMSA. Anti-STAT1, anti-STAT2 or a nonspecific IgG antibody was added to the nuclear extract prior to addition of the probe. DNA-protein complexes were resolved on 6% native gels and the labeled probe was detected with anti-DIG antibody. The results shown are representative of at least two independent experiments. ChIP analysis of the binding of STAT1 or STAT2 to the **(B)** Oas1a or **(C)** Oas1b promoter in control or 30 min IFN beta-treated C3H/He cells. The amounts of precipitated Oas1a and Oas1b promoter DNA were quantified by real-time qPCR using promoter-specific primers and fluorogenic TaqMan FAM/MGB probes. Nonspecific IgG antibody was used as a negative control and averaged values are shown. The error bars represent standard deviation of the mean (SDM) (n=3).

the ISGF3 complex bind to the predicted Oas1a and Oas1b ISREs, -31 to +6 bp Oas1a and -32 to +5 bp Oas1b DNA fragments were used as probes in EMSAs with nuclear extracts from untreated or murine IFN beta-treated MEFs. Two bands were detected with the Oas1a probe and three with the Oas1b probe using nuclear extracts from IFN-treated cells (Fig. 4A). However, the upper complex band was not observed with either probe when the reaction was done with nuclear extracts from untreated cells. To determine whether the STAT1 and STAT2 transcription factors were present in one or more of these bands, nuclear extracts were incubated with either anti-STAT1 or anti-STAT2 antibody prior to addition of the probe. With the Oas1a probe, the upper band was not detected when STAT1 antibody was present, and a supershift band (indicated by an arrow) was observed when STAT2 antibody was present. With the Oas1b probe, a decrease in the intensity of the upper band was observed when STAT1 antibody was added and a supershift band was detected when the STAT2 antibody was added. The addition of a nonspecific rabbit IgG did not alter the band patterns of either probe. The results suggested that both STAT1 and STAT2 were present in the upper complex band detected by both probes. In order to confirm the validity of the supershift data the binding of STAT1 and STAT2 to the ISREs in the Oas1a and Oas1b promoters in cells stimulated with IFN beta was analyzed by ChIP (Fig. 2.4B and C). Pilot ChIP experiments showed that the levels of STAT1 and STAT2 bound to these ISG promoters was higher at 30 m than at 3 h after treatment with IFN beta. C3H/He cells were left untreated or treated with 1000 U/ml of IFN beta for 30 m and then treated with formaldehyde. Crosslinked DNA- protein complexes were immunoprecipitated using anti-STAT1, anti-STAT2 or a nonspecific IgG antibody. The crosslinks were reversed and the immunoprecipitated DNA was purified and quantified by real time qPCR. The results showed that both STAT1 and STAT2 are present on the Oas1a and Oas1b promoters after stimulation of

the C3H/He cells by IFN beta. Although one of the two anti-IRF-9 antibodies (Santa Cruz Biotechnology) tested detected IRF-9 in Western blots, neither of these antibodies was found to be suitable for EMSA nor ChIP, therefore the interaction of IRF-9 with the ISREs of these promoters could not be directly tested.

### 2.5 Functional analysis of TFBSs predicted in the Oas1a and Oas1b promoters.

The GENOMATIX search done in the present study predicted a STAT site overlapping the 5' end and an IRF site overlapping the 3' end of both the Oas1a and Oas1b ISREs (Fig. 2.2). These predictions suggested that the sequences located immediately upstream and downstream of the ISRE might be important for stabilizing the binding of STAT1 and IRF-9 to the core ISRE and/or for facilitating the binding of additional STAT and IRF factors. To functionally test these predictions, the ISRE and overlapping STAT and IRF TFBSs were individually mutated in the Oas1a (-854, +28) and Oas1b (-576, +51) constructs as indicated in Fig. 2. The luciferase activity of each mutated reporter construct after stimulation with murine IFN beta was compared to that of the wild type construct. A GENOMATIX search confirmed that the introduced mutations eliminated the targeted binding site but did not create a new TFBS. Mutation of the ISRE (3' GAAA to 3' GTAC) in the Oas1a (Fig. 5A) and Oas1b (Fig. 2.5B) constructs reduced the basal activities of both promoters by more than 80% suggesting that the ISRE plays a role in modulating the basal expression of Oas1a and Oas1b. Low levels of IFN were previously reported to be secreted by unstimulated, cultured MEFs (Takaoka and Yanai, 2006) and this could explain the negative effect of the ISRE mutation on basal expression. No increase in activity above basal levels was observed for either the Oas1a or Oas1b promoter with a mutated ISRE after stimulation with IFN beta confirming that the ISRE is required for IFN beta-induction of both genes.

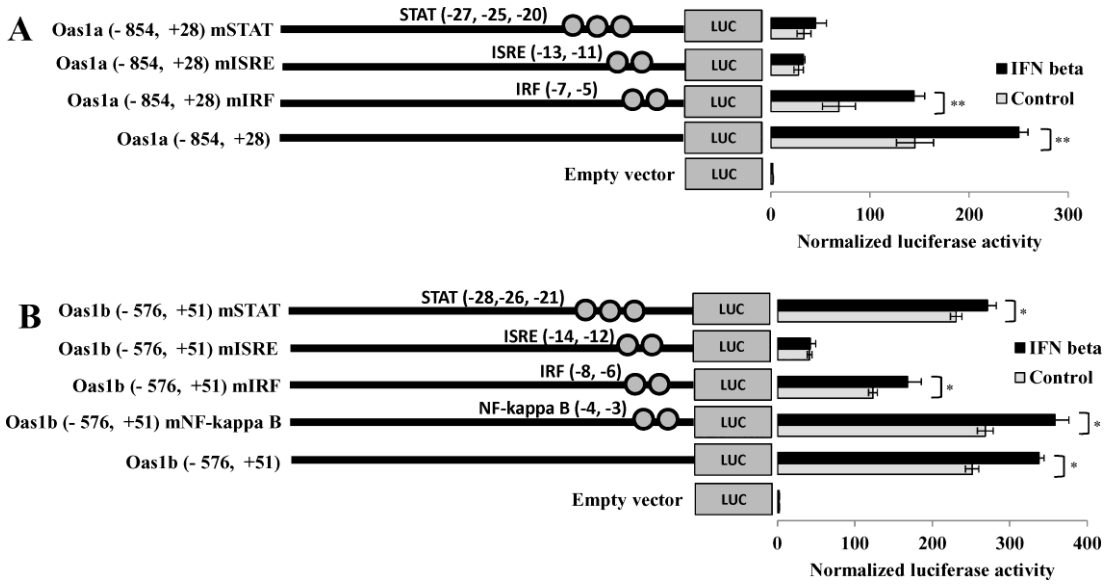


**Figure 2.5. Effect of mutation of the ISRE or overlapping/adjacent TFBSs on Oas1a and Oas1b promoter activity.** Individual TFBSs were mutated in reporter constructs as indicated in Fig. 2. The luciferase activities of control and mutated **(A)** Oas1a and **(B)** Oas1b reporter constructs were assayed. Each construct was transfected into C3H/RV cells and 24 h after transfection, cells were treated with 1000 U/ml of murine IFN beta for 3 h or left untreated. Firefly luciferase activity was measured in triplicate and normalized to *Renilla* luciferase activity. The values shown are the average of three independent experiments. Error bars represent SEM (n=3). Statistical significance was determined with a Student's *t* test (∗, $P < 0.05$; ∗∗, $P < 0.005$)

The predicted IRF site overlapping the 3' end of the ISRE was mutated at the -5 and -7 positions in the Oas1a promoter and at the -6 and -8 positions in the Oas1b promoter (Fig. 2.2). Although mutation of the IRF site resulted in about a 50% reduction in basal Oas1a and Oas1b promoter activity, both mutated promoters were efficiently upregulated by IFN (Fig. 2.5). IFN beta induced the wild type Oas1a construct activity by 1.7 fold and that of the Oas1a IRF mutant construct by 2.1 fold. Both the wild type and mutant IRF Oas1b constructs showed a 1.3 fold induction after IFN treatment. These results indicate that the IRF binding site overlapping the ISRE in both promoters positively regulates basal promoter activity, but does not contribute to the induction of these promoters by IFN beta.

Mutations were next introduced into the STAT site overlapping the 5' end of the Oas1a and Oas1b ISREs. Substitutions were introduced at positions -20, -25 and -27 in the Oas1a promoter and at positions -21, -26 and -28 in the Oas1b promoter (Fig. 2.2). Similar to what was observed for the Oas1a construct with a mutated ISRE, the Oas1a mutant STAT construct showed a more than an 80% reduction in basal activity but was not upregulated by IFN beta. In contrast, mutation of the STAT site in the Oas1b promoter only minimally affected basal or IFN beta-induced activities. These results suggest that the STAT site overlapping the Oas1a ISRE is required for the induction of this promoter by IFN beta, while the STAT site overlapping the Oas1b ISRE is not.

The TFBS searches done by Mashimo et al. (2003) and those done in the present study predicted an NF-kappa B site immediately downstream of the Oas1b ISRE but not of the Oas1a ISRE. The sequence of this site differs from the NF-kappa B consensus $\underline{G}G\underline{G}^{A}/_{G}NN^{C}/_{T}{}^{C}/_{T}CC$ (Grilli et al., 1993) at the two underlined positions (Fig. 2). Type 1 IFN binding to the IFN alpha/beta receptor

has been reported to also activate the phosphatidylinositol 3 kinase (PI3K) pathway (Kaur et al., 2005) which was shown to play a role in activating NF-kappa B (Chang et al., 2006). The Oas1b NF-kappa B site was mutated as indicated in Fig. 2. The luciferase activity observed for this mutant construct was the same as that for the wild type construct with and without IFN treatment (Fig. 2.5B). These results indicate that the NF-kappa B site does not modulate the induction of the Oas1b promoter by IFN beta and does not affect basal activity.

## 2.6 IFN beta-induction of the Oas1a and Oas1b genes in the absence of STAT1 or STAT2.

As one means of determining whether STAT1 is required for the activation of the Oas1a and Oas1b genes by IFN beta, the expression of these genes was analyzed by real time qRT-PCR in wild type, STAT1-/- and STAT2-/- MEFs. In wild type MEFs, Oas1a and Oas1b gene expression was efficiently induced by IFN beta (Fig. 2.6A). Basal levels of Oas1a mRNA were not detectable in either untreated STAT1-/- or STAT2-/- MEFs and minimal upregulation of Oas1a expression was observed after incubation of these cells with IFN beta. Basal levels of Oas1b were detected in both STAT1-/- and STAT2-/- MEFs. Although IFN beta did not upregulate Oas1b expression in STAT2-/- MEFs, it efficiently upregulated Oas1b expression in STAT1-/- MEFs. To confirm these observations, the binding of STAT1 and STAT2 to the Oas1a and Oas1b promoters in control, STAT-/- and STAT2-/- MEFs was analyzed by ChIP. Both STAT1 and STAT2 bound the Oas1a and Oas1b promoters in IFN beta-treated control 129 MEFs but neither bound to either promoter in the STAT2-/- MEFs (Fig.2.6B and C). In contrast, STAT2 bound to the Oas1b promoter but not to the Oas1a promoter in STAT1-/- MEFs confirming that Oas1a promoter induction by IFN beta occurs in a STAT1- and STAT2-

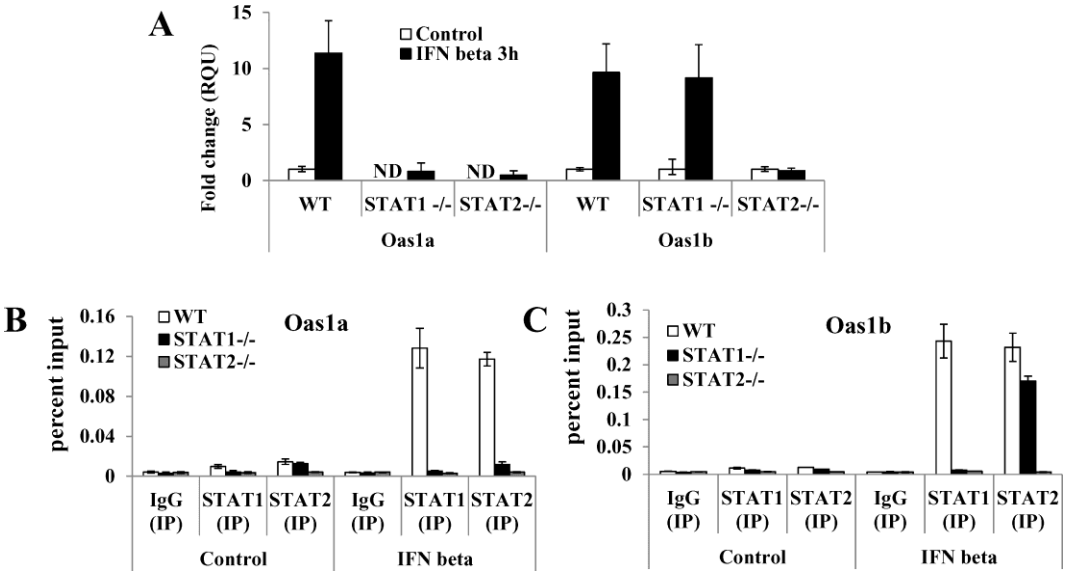


**Figure 2.6. Analysis of the inductionof Oas1a and Oas1b by IFN beta in wild type, STAT1-/- and STAT2-/- MEFs.** MEFs were treated with 1000 U/ml of murine IFN beta for 3 h or left untreated. Total RNA was collected and fold induction of Oas1a and Oas1b mRNA expression levels was measured by real-time qRT-PCR. The mRNA level of each gene was normalized to the level of GAPDH mRNA in the same sample. The fold change over the amount of mRNA in mock samples is expressed in RQU. Each experiment was performed in triplicate. ND - not detected. ChIP analysis of the binding of STAT1 or STAT2 to the **(B)** Oas1a or **(C)** Oas1b promoter in control 129, STAT1-/- and STAT2-/- MEFs mock-treated or treated with 1000 U/ml of IFN beta for 30 min. The amounts of precipitated Oas1a and Oas1b promoter DNA were quantified by real-time qPCR using promoter specific primers and fluorogenic TaqMan FAM/MGB probes. Nonspecific IgG antibody was used as a negative control and averaged values are shown. The error bars represent SDM (n=3).

dependent manner, while the induction of Oas1b by IFN beta is STAT2-dependent but can be STAT1-independent.

## DISCUSSION

The mouse genome contains 8 duplications of the Oas1 gene. As an active 2-5 A synthetase murine Oas1a functions as a broad spectrum antiviral protein through its ability to activate RNase L (Kakuta et al., 2002). Oas1b is an inactive synthetase that can function in a dominant negative manner to suppress Oas1a synthetase activity (Elbahesh et al., 2011). Oas1b also provides flavivirus-specific antiviral activity through an as yet uncharacterized mechanism that does not involve the RNase L pathway (Scherbik et al., 2006). Based on TFBS differences identified in the Oas1a and Oas1b promoters, a previous study predicted that these two genes may be differentially activated by IFN and/or virus infection but this hypothesis was not functionally tested (Mashimo et al., 2003). In the present study, a firefly luciferase reporter assay and truncated and mutated promoter constructs were used to map the Oas1a and Oas1b promoter regions required for basal activity and IFN beta induction. For both genes, the lowest basal promoter activity was observed with the longest promoter fragment tested but activity increased significantly with 5' truncation suggesting the presence of binding sites for transcriptional repressors in the upstream region. Deletion of the 5' upstream region was previously reported a prerequisite for mapping the activation sites in the proximal promoters of the interleukin 19 and fucosyltransferase VI genes (Chen et al., 2006; Higai et al., 2008). Upstream sites that repress the transcriptional activation by TFs binding to TFBSs in the proximal promoter region were also previously identified in the promoters of genes for which transcription is known to be tightly regulated (Garban and Bonavida, 2001; Lindas and Tomkinson, 2007). Since activation of the

RNase L pathway by 2-5A leads to degradation of not only viral but also cellular ssRNAs, it would be expected that the expression of the Oas1 genes would be tightly regulated.

The core promoters of the Oas1a and Oas1b genes contain an INR element and an inverted ICE. Mutation of the ICE element reduced the basal activities of the Oas1a and Oas1b promoters by about 40% but did not affect the induction of either promoter by IFN beta suggesting that ICE plays a role in basal promoter activity but not in IFN-mediated induction. The EMSA results showed that TFs in control cell nuclear extracts bound to a probe with a wild type but not a mutated ICE sequence. Although the identities of the TFs were not determined, NF-Y, also termed CBF (CCAAT binding factor), was previously shown to be the primary TF binding to the CCAAT element in either orientation (Mantovani, 1999). NF-Y is a ubiquitous transcription factor composed of three subunits that can increase the DNA binding affinity of factors bound to neighboring TFBSs (Reith et al., 1994; Wright et al., 1995; Jackson et al., 1998) and interact with p300/CBP, GCN5 and PCAF complexes that mediate promoter acetylation (Currie, 1998; Jin and Scotto, 1998; Li et al., 1998; Salsi et al., 2003). NF-Y has also been reported to recruit RNA polymerase II to a promoter (Kabe et al., 2005). The mutation identified in the ICE of the C3H/He Oas1a promoter suggests that the basal levels of Oas1a expression would be reduced in the cells of these mice.

Deletion analysis of the Oas1b promoter showed that the regulation of this gene is more complex than that of the Oas1a gene. The mapping data indicated that the region of the Oas1b promoter between -576 and -116 contains elements that enhance basal Oas1b expression. TFBSs predicted by TFSEARCH and GENOMATIX in this region of the Oas1b promoter that were not found in

the Oas1a promoter include C/EBPb, GATA-1, AML-1, CdxA, HSF2, IK-2, Lyf-1, and MZF-1. C/EBPb (also known as CCAAT/enhancer-binding protein beta) was previously shown to positively regulate gene induction by recruiting transcriptional coactivators as well as basal transcription factors (Kowenz-Leutz and Leutz, 1999).

Upon type I IFN stimulation, the transcription factor complex ISGF3, composed of STAT1, STAT2 and IRF-9, binds to ISREs in ISG promoters with the consensus sequence 5' $^{A}/_{G}$NGAAANNGAAACT 3' (Darnell et al., 1994). The Oas1a and Oas1b promoters were each predicted to have a single canonical ISRE by a previous TFSEARCH (Mashimo et al., 2003) and also by both the GENOMATIX and TFSEARCH database searches done in the present study. Since the structure of ISGF3/DNA complex has not yet been solved is not clear exactly how the ISGF3 complex components bind to the ISRE. It was previously reported that STAT1 recognizes the 5' GAAA sequence and IRF-9 recognizes the 3' GAAA sequence in the ISRE. STAT2 does not stably bind to DNA but interacts with both STAT1 and IRF-9 and is essential for the transcriptional activity of the ISGF3 complex (Bluyssen et al., 1995; Qureshi et al., 1995). The substitutions introduced into the ISRE 3' GAAA in both the Oas1a and Oas1b promoters abolished IFN beta induction indicating that this region is required for IFN beta induction of these ISGs. A GAS site was previously predicted to overlap the 5' end of the Oas1b ISRE but not that of the Oas1a (Mashimo et al., 2003). GAS elements were originally identified in the promoters of IFN-gamma responsive genes. Upon IFN-gamma stimulation, a STAT1 homodimer, also referred to as the gamma interferon activation factor (GAF), was shown to bind to GAS elements with the consensus sequence TTCN$_{2-4}$GAA (Decker et al., 1997). Although other STATs can bind to this consensus sequence, the DNA binding specificities of different

STAT proteins depends on the length of the spacer sequence and specific nucleotides in both the binding site and immediately adjacent to it (Darnell, 1997; Decker et al., 1997; Ehret et al., 2001). The GENOMATIX search done in this study predicted a STAT binding site overlapping the 5'GAAA motif of the ISRE in both the Oas1a and Oas1b promoters. Substitution of the G in this ISRE motif was reported to prevent the binding of STAT1 but not of the IRF-9/STAT2 complex (Bluyssen and Levy, 1997). Mutation of the Oas1a STAT site including the G mentioned above abolished IFN beta-induced promoter activity suggesting that the binding of STAT1 is crucial for the induction of this promoter by IFN beta. In contrast, mutation of the same nucleotides in the Oas1b STAT site did not significantly reduce upregulation by IFN beta. Consistent with these observations, the Oas1b gene but not the Oas1a gene was efficiently upregulated in IFN-treated STAT1-/- MEFs confirming that the induction of Oas1b by IFN beta does not require STAT1.

Although the sequences of the Oas1a and Oas1b ISREs are identical, the STAT sites overlapping the 5' ISRE GAAA motif differ by one nt, Oas1a (TTCTCGGGAA) and Oas1b (TTCCCGGGAA). A previous report proposed that the presence of an A, G or T at this position promotes STAT2 binding (Tenoever et al., 2007). However, the finding in the present study that IFN beta activation of the Oas1a promoter with a T in this position is STAT1-dependent while activation of the Oas1b promoter with a C in this position is STAT1-independent suggests that this site is important for stabilizing STAT1 binding and that the substitution at this site is responsible for the differential STAT1 dependence between these two promoters. Although other ISGs, such as Adar1, APOBEC3G and Irf7, were previously reported to be upregulated by type I IFN in a STAT1-independent manner, the TF complexes involved in the STAT1-independent

activation of ISGs by type I IFN have not yet been well characterized (Ousman et al., 2005; Sarkis et al., 2006; George et al., 2008). Expression of a IRF-9/STAT2 fusion protein efficiently activated the transcription of an ISRE-dependent luciferase reporter in the absence of type I IFN stimulation (Kraus et al., 2003). Also, an IRF-9/STAT2 complex was sufficient to induce the expression of a reporter construct containing the RIG-G gene promoter upon stimulation with IFN alpha (Lou et al., 2009). However, it is currently not known whether additional factors are also involved in STAT1-independent upregulation of ISGs by type I IFN.

The GENOMATIX search predicted an IRF binding site overlapping the 3'GAAA motif of the ISRE in both the Oas1a and Oas1b promoters and an NF-kappa B binding site immediately downstream of the Oas1b ISRE. Although these sites were not found to be involved in gene activation by IFN, they may be involved in the upregulation of these genes in virus-infected cells. It was previously reported that IRF-3, IRF-7 and NF-kappa B transcription factors are activated during viral infections and mediate induction of type I IFN as well as upregulate a subset of ISGs independently of IFN (Nakaya et al., 2001; Grandvaux et al., 2002; Peters et al., 2002; Barnes et al., 2004; Elco et al., 2005; Andersen et al., 2008; Basagoudanavar et al., 2011).

Low levels of IFN produced by uninfected cells are required for maintaining basal levels of ISGs (Taniguchi and Takaoka, 2001). Low level constitutive expression of ISGs in uninfected cells is thought to be crucial for mounting an effective antiviral response in the initial stages of a virus infection (Basagoudanavar et al., 2011). However, the data obtained in this study indicated that basal expression of neither Oas1a nor Oas1b is solely dependent on type I IFN. Many viruses antagonize type I IFN signaling and the induction of antiviral ISGs by blocking the activation of

the Jak-STAT signaling pathway (Randall and Goodbourn, 2008; Diamond, 2009). The observation made in this study that Oas1b and in previous studies, showing some other ISGs can be induced by type I IFN in a STAT1-independent manner indicates that an effective antiviral response can still be mounted in infected cells when STAT1 activation/translocation is blocked. The importance of an alternative STAT1-independent response in providing host protection was reported for dengue virus (another flavivirus) in a mouse model (Perry et al., 2011). However, other types of viruses, such as measles virus and lymphocytic choriomeningitis virus, have been reported to enhance their survival by suppressing dendritic cell development and expansion through a STAT2-dependent but STAT-1-independent pathway (Hahm et al., 2005).

## MATERIALS AND METHODS

### 2.7 Cells.

SV40-T antigen transformed C3H/He and C3H/RV MEFs were grown in minimal essential medium (MEM) supplemented with 5% fetal bovine serum (FBS) and 10 µg/ml gentamicin. Transformed 129/SvEv, STAT1-/- and STAT2-/- MEF lines (provided by Christian Schindler, Columbia University, New York, NY) were grown in MEM supplemented with 10% FBS and 1% PenStrep (Gibco).

### 2.8 Quantification of mRNA levels.

Real time quantitative reverse transcription-PCR (qRT-PCR) analyses of mouse Oas1a and Oas1b gene expression were performed using 50 µl reaction mixture containing 500 ng of total cellular RNA, the primer pair (1 µM), and the probe (0.2 µM) in an Applied Biosystems 7500 Sequence Detection System. Applied Biosystems Assays-on-Demand 20x primer and fluorogenic TaqMan FAM/MGB probe mixes (Mn00836412_m1 for Oas1a and Mn00449297_m1 for Oas1b) were used. Glyceraldehyde-3-phosphate dehydrogenase (GAPDH) mRNA was used as

an endogenous control for each sample and was detected using TaqMan mouse GAPDH primers and probe (Applied Biosystems). One-step RT-PCR was performed for each target gene and for the endogenous control in a singleplex format using 200 ng of RNA and the TaqMan One-Step RT-PCR Master Mix Reagent Kit (Applied Biosystems). The cycling parameters were as follows: reverse transcription at 48°C for 30 m, AmpliTaq activation at 95°C for 10 m, denaturation at 95°C for 15 s, and annealing/extension at 60°C for 1 m (cycle repeated 40 times). The values were normalized to those for GAPDH and presented as the relative fold change compared to the uninfected calibrator sample in relative quantification (RQ) units.

### 2.9 Cloning the Oas1a and Oas1b gene promoter regions.

A DNA fragment consisting of 1768 bp upstream and 28 bp downstream of the Oas1a gene TSS and a fragment consisting of 1398 bp upstream and 51 bp downstream of the Oas1b TSS were amplified from C3H/He and C3H/RV genomic DNA using primers designed from the GenBank C57BL/6J mouse genomic sequence [(NCBI) Genbank ID: NT_078458.6]. The amplified PCR products were cloned into a TopoXL vector (Invitrogen) and sequenced. The C3H/RV DNA fragments were then subcloned into the pGL4.17 firefly luciferase reporter vector (Promega) using NheI and BgLII cloning sites to generate the Oas1a (-1768, +28) and Oas1b (-1398, +51) reporter constructs. These two constructs were subsequently used as templates in additional PCR reactions to amplify DNA fragments containing sequential 5' deletions. Each of the deleted PCR products was then cloned into the pGL4.17 firefly luciferase reporter vector to generate eight additional Oas1a reporter constructs [Oas1a (-854, +28), Oas1a (-722, +28), Oas1a (-641, +28), Oas1a (-468, +28), Oas1a (-396, +28), Oas1a (-289, +28), Oas1a (-176, +28) and Oas1a (-87, +28)] and eight additional Oas1b reporter constructs [Oas1b (-991, +51), Oas1b (-814, +51),

Oas1b (-742, +51), Oas1b (-576, +51) Oas1b (-507, +51), Oas1b (-394, +51), Oas1b (-181, +51), and Oas1b (-116, +51)]. The primers used for these PCR reactions are listed in Table 2.1.

### 2.10 Prediction and mutation of TFBSs.

The TFSEARCH (version 1.3) and GENONATIX programs were used to predict TFBSs in the Oas1a and Oas1b promoter fragment sequences. Specific mutations in predicted IRF, ISRE, STAT and ICE binding sites (Fig. 2.2) were introduced into the promoter sequence in the Oas1a (-854, +28) construct to generate the Oas1a (-854, +28) mIRF, Oas1a (-854, +28) mISRE, Oas1a (-854, +28) mSTAT and Oas1a (-854, +28) mICE reporter constructs, respectively. Specific mutations in the predicted NF-kappa B, IRF, ISRE, STAT and ICE binding sites (Fig 2.2) were introduced into the Oas1b (-576, +51) construct to generate the Oas1b (-576, +51) mNF-kappa B, Oas1b (-576, +51) mIRF, Oas1b (-576, +51) mISRE, Oas1b (-576, +51) mSTAT Oas1b (-576, +51) mICE constructs, respectively. The mutations were introduced using the primers shown in Table 2.2 and a QuikChange II Site-Directed Mutagenesis Kit (Stratagene) according to the manufacturer's protocol. The mutant promoter sequences were analyzed using GENOMATIX software to ensure that the substitutions introduced eliminated the targeted binding site but did not create a new TFBS. The sequences of all the constructs generated were verified by DNA sequencing.

### 2.11 Luciferase reporter assay.

The pGL4.17 firefly luciferase reporter plasmid DNA (1 μg) containing either an Oas1a or Oas1b promoter fragment and 20 ng of a pGL4.74 *Renilla* luciferase reporter construct DNA (Promega) in a solution consisting of 3 μl of FuGENE 6 (Roche Applied Science) and 97 μl of serum free media were added to C3H/RV MEF cultures (50-70% confluency) and the cells were incubated at 37°C for 24 h. Murine recombinant IFN beta (1000 U/ml) (PBL Interferon Source)

was added to the cell cultures 21 h after transfection. After a 3 h incubation, cells were harvested using the lysis buffer supplied with the Dual Luciferase Reporter Assay System (Promega). Firefly and *Renilla* luciferase activities were separately measured according to the manufacturer's protocol using a luminometer (LMax II$^{384}$, Molecular Devices). The firefly luciferase activity was normalized to the *Renilla* luciferase activity in each sample.

### 2.12 EMSA

The Oas1a and Oas1b DNA probes (Table 2.3) were labeled using a DIG gel shift 2$^{nd}$ generation kit (Roche Applied Science) according to the manufacturer's instructions. Nuclear extracts (2 μg) prepared from C3H/RV MEFs that were either untreated or treated with 1000 U/ml of murine IFN beta for 1 h were used for EMSA. The specificity of the binding detected was analyzed by addition of a 200 fold excess of unlabeled probe to one of the reactions. For supershift assays, nuclear extracts were incubated with anti-STAT1 (Santa Cruz Biotechnology Inc.), anti-STAT2 (provided by Christian Schindler, Colombia University, New York, NY) or a nonspecific IgG antibody (Zymed) for 30 m at room temperature. Binding reactions were prepared according to the DIG gel shift 2$^{nd}$ generation kit protocol. DNA-protein complexes were resolved on a 6% native polyacrylamide gel and labeled probe was detected using the anti-DIG antibody supplied with the kit.

### 2.13 ChIP.

Confluent C3H/He monolayers were incubated with 1000 U/ml of murine IFN beta for 30 min or left untreated. Chromatin was crosslinked *in situ* with 1% formaldehyde for 10 min at ~25°C. After washing with ice cold phosphate-buffered saline (PBS), cells were incubated with 1 ml of cell lysis buffer [5 mM PIPES pH 8.0, 85 mM KCl, 0.5% NP40 and Complete EDTA-free Protease Inhibitors (Roche Applied Sciences)] for 10 m and the nuclei were pelleted at 2000 rpm

at 4°C. Nuclei were then incubated with SDS lysis buffer (1% SDS, 10 mM EDTA, 50 mM Tris pH 8.0, and Complete EDTA-free Protease Inhibitors) for 20 m on ice. The crosslinked chromatin was sonicated to an average size of 500−1,000 base pairs. Sonicated chromatin obtained from 1 x $10^6$ cells was used for each immunoprecipitation reaction. Samples were first precleared with 60 μl of salmon sperm DNA-coated agarose beads (Millipore) and then incubated with 5 μg of anti-STAT1 (Santa Cruz Biotechnology), anti-STAT2 (provided by Christian Schindler, Columbia University, New York, NY) or rabbit nonspecific IgG antibody overnight at 4°C. After incubation with 60 μl salmon sperm-coated agarose beads, the samples were washed sequentially for 5 m at 4°C with each of the following buffers: low salt buffer (0.1% SDS, 1% Triton X-100, 2 mM EDTA, 20 mM Tris, pH 8.0 and 150 mM NaCl), high salt buffer (0.1% SDS, 1% Triton X-100, 2 mM EDTA, 20 mM Tris, pH 8.0 and 500 mM NaCl) and LiCl buffer (0.25 M LiCl, 1% NP40, 1% DOC, 1 mM EDTA and 10 mM Tris, pH 8.0). Finally, the samples were washed twice with TE buffer (1 mM EDTA and 10 mM Tris, pH 8.0), and then eluted with 500 μl of SDS elution buffer (1% SDS, 0.1 M $NaHCO_3$). Samples were incubated with 20 μl of 5 M NaCl at 65°C overnight to reverse the crosslinks, then 10 μl of 500 mM EDTA, 20 μl of Tris pH 6.5, and 2 μl of Proteinase K (10 mg/mL) were added and the samples were incubated for 1 h at 45°C. Input and immunoprecipitated DNA were isolated using a phenol:chloroform:isoamyl alcohol mixture (USB Biochemicals) according to the manufacturer's protocol and analyzed by real time quantitative PCR (qPCR) using probes and primers designed to span the proximal Oas1a and Oas1b promoters. The sequences of the primers were: Oas1a forward primer 5'-GGATCCTAAGAAAGCTCAGACTTCA-3', Oas1a reverse primer 5'-CCCGGCAGCCAATGG-3', Oas1b forward primer 5'- GAAGCCCTAACGCCATTGG-3', Oas1b reverse primer 5'-AGGGCGCGGATATGCA-3'. The sequence of the FAM-MGB Oas1a

probe was 5'-TGGAAGTGTGGGAAAGGTCTTT-3' and that of the Oas1b probe was 5'-CGGGCCTGGATGAT-3'. To generate standard curves, known amounts of Oas1a, Oas1b and Irf7 promoter DNA in a TOPO-XL vector (Invitrogen) were titrated and assayed by real time qPCR using a FastStart Universal Probe Master (ROX) kit (Roche Applied Science) according to the manufacturer's protocol. The standard curves were independently generated at the same time as the immunoprecipitated DNA samples were assayed by qPCR and used to quantify the immunoprecipitated DNA.

# CHAPTER 3

## 3 AIM 2: Investigation of the activation of ISGs in MEFs infected with WNV Eg101.

### INTRODUCTION

The family *Flaviviridae*, genus *Flavivirus*, contains several human pathogens including West Nile virus (WNV), dengue virus, yellow fever virus (YFV), Japanese encephalitis virus (JEV) and tick borne encephalitis virus (TBEV). WNV is a mosquito-borne virus that is transmitted in a bird-mosquito cycle but occasionally mammals including humans and horses are infected. WNV infections in humans are usually asymptomatic but can induce a mild febrile illness; however, some patients develop encephalitis or a poliomyelitis-like disease. WNV particles contain a single-stranded, positive-sense RNA genome encoding a single polyprotein that is cleaved by viral and cellular proteases into three structural and seven nonstructural proteins (Brinton, 2002). WNV isolates have been divided into two main lineages. Lineage I strains are often associated with outbreaks of human disease, while the majority of lineage II strains are non-emerging and cause zoonotic infections in Africa (Brinton, 2002).

IFNs were first discovered as cytokines that inhibit viral replication (Isaacs and Lindenmann, 1957). Induction of type I IFNs is primarily triggered by pattern recognition receptors (PRRs) that recognize viral nucleic acids. Viral double stranded RNA (dsRNAs) or single stranded RNAs (ssRNAs) are recognized by cytoplasmic PRRs, such as retinoic acid inducible gene-I (RIG-I) and melanoma differentiation antigen 5 (MDA5), or by cell surface and endosomal PRRs, such as Toll-like receptor 3 (TLR-3), TLR7 and TLR-8 (Saito and Gale, 2007). Recognition of viral nucleic acids by these PRRs leads to activation of the TFs, IRF-3, NF-kappa B and ATF2/c-Jun (AP1), that assemble on the IFN-beta promoter and activate IFN-beta gene

expression (Merika and Thanos, 2001). Secreted IFN beta binds to cell surface IFN alpha/beta receptor (IFN alpha/beta R) complexes inducing activation of receptor-associated Jak kinases followed by recruitment and phosphorylation of the TFs, STAT1 and STAT2. STAT1, STAT2 and IFN regulatory factor-9 (IRF-9) form a trimeric transcription factor complex referred to as IFN stimulated gene factor 3 (ISGF3) that translocates to the nucleus and binds to IFN-stimulated response elements (ISREs) in the promoters of IFN-stimulated genes (ISGs) (Stark et al., 1998). The induction of IFN-beta is biphasic due to the induction of ISGs, such as IRF-7, which enhance IFN beta gene expression and sustain ISG production. IRF-7 also induces the expression of IFN-alpha which amplifies the type I IFN response via a positive feedback loop (Marie et al., 1998; Sato et al., 2000).

The expression of IFN-beta and multiple interferon stimulated genes (ISGs), many of which have antiviral functions, represents the first line of defense against a viral infection. Many viruses suppress this innate immune response by blocking the Jak-STAT signaling pathway. Different flaviviruses were reported to block this pathway by either inhibiting Jak phosphorylation (Lin et al., 2004; Best et al., 2005; Guo et al., 2005; Ho et al., 2005), reducing the expression of STAT2 (Jones et al., 2005; Mazzon et al., 2009) or blocking STAT1 and STAT2 phosphorylation (Munoz-Jordan et al., 2003; Best et al., 2005; Liu et al., 2005; Munoz-Jordan et al., 2005). The lineage I WNV strains TX02 and NY99 were previously shown to effectively block STAT1 phosphorylation in primate cells (Laurent-Rolle et al.; Liu et al., 2005; Keller et al., 2006). In contrast, WNV Eg101, a lineage I stain closely related to NY99 but less neurounvasive (Beasley et al., 2002) was previously reported not to inhibit STAT1 phosphorylation in mouse cells . (Scherbik et al., 2006; Scherbik et al., 2007). However, the effects of WNV Eg101 infection on STAT2 phosphorylation and ISGF3 nuclear translocation in these cells were not investigated.

Inhibition of the Jak-STAT signaling pathway by a viral infection would be expected to suppress ISG expression which is required for the establishment of an effective cellular antiviral response. However, even though ISGs were first described as IFN-induced genes, some were subsequently shown to be upregulated by viral infections in an IFN-independent manner though recognition of viral components by PRRs and activation of constitutively expressed TFs such as IRF-3 and NF-kappa B (Nakaya et al., 2001; Grandvaux et al., 2002; Peters et al., 2002; Elco et al., 2005; Andersen et al., 2008; Basagoudanavar et al., 2011). Subsequent upregulation of additional TFs, such as IRF-7, was also shown to play a role in the expression of some ISGs in infected cells (Barnes et al., 2004). A previous report showed that IRF-7 and IRF-3 were important for IFN production and protection against WNV (Fredericksen et al., 2004; Daffis et al., 2007; Daffis et al., 2008).

Due to the high degree of homology between the ISRE and IRF binding element (IRF-E) consensus sequences, the ISREs of some ISGs can be directly induced by either IRF-3 or IRF-7 (Lin et al., 2000; Morin et al., 2002; Schmid et al., 2010). In MEFs, Irf7 gene expression must first be induced and then IRF-7 has to be activated before this TF can directly upregulate a subset of ISGs (Barnes et al., 2004). In contrast, IRF-3 is a constitutively expressed protein that is found in the cytoplasm of all cells in an inactive form. IRF-3 activation is mediated by phosphorylation at multiple C terminal serine and threonine residues**.** Phosphorylation-induced dimerization leads to nuclear translocation of IRF-3 in a complex with histone acetyltransferases p300 and CREB-binding protein (CBP) (Yoneyama et al., 1998; Suhara et al., 2002; Fitzgerald et al., 2003; Sharma et al., 2003). The results of an analysis of murine ISG expression during a Newcastle disease virus (NDV) infection in IRF-3-/- MEFs led to the classification of ISGs such as ISG15, ISG54, IP-10 and GBP as genes activated in an IRF-3-dependent manner and ISGs

such as Oas1a and Irf7 as genes upregulated in an IRF-3-independent but IFN-dependent manner through activation of the ISGF3 transcription factor complex (Nakaya et al., 2001). A more recent analysis of ISG expression in IRF-3-/- MEFs infected with NDV confirmed that the expression of the Oas1a and Irf7 did not depend on IRF-3 and showed that this was also the case for the Oas1b and Irf1 genes (Andersen et al., 2008).

NF-kappa B exists in the cytoplasm in an inactive form in a complex with an inhibitory I kappa B protein (Whiteside and Israel, 1997). Activation of the NF-kappa B pathway by viral infection upregulates the expression of a specific subset of ISGs encoding cytokines and chemokines, such as RANTES, TNF alpha and others, regulators of apoptosis and TFs, including A20, Irf1 and Irf2 and others (Pahl, 1999; Elco et al., 2005).

The murine 2'-5' oligoadenylate synthetase 1a (Oas1a) and Oas1b genes are ISGs that have antiviral functions. Oas1a is an enzymatically active synthetase that upon binding to viral dsRNA synthetizes 2'-5'-oligoadenylates (2-5A) from ATP which activate the latent endonuclease RNase L. Activated RNaseL degrades both cellular and viral single-stranded RNAs (Samuel, 2001). Oas1b is an inactive synthetase that mediates resistance to flavivirus-induced disease through an unknown RNase L independent mechanism (Scherbik et al., 2006). Oas1b was also reported to inhibit *in vitro* Oas1a synthetase activity in a dose-dependent manner (Elbahesh et al., 2011). IFN beta activation of Oas1a expression was shown to be STAT1- and STAT2-dependent while that of Oas1b was STAT1-independent and STAT2-dependent indicating that these two duplicated genes are differentially regulated by IFN beta (Pulit-Penaloza et al., 2012). WNV Eg101 infection in MEFs was previously reported to activate IFN-beta expression, induce STAT1 Tyr701 phosphorylation and upregulate the expression of Oas1a, Oas1b as well as other ISGs including Irf7 and Irf1(Scherbik et al., 2006; Scherbik et al., 2007).

However, whether the upregulation of these IRF-3-independent ISGs in WNV-infected cells is mediated by IFN or by an alternative virus-activated pathway was not previously analyzed.

Although IFN beta expression is upregulated and STAT1 and STAT2 are phosphorylated in WNV Eg101 infected cells, the present study showed that nuclear translocation of these TFs was blocked. Consistent with this observation, no increase in the binding of either STAT1 or STAT2 to the Oas1a, Oas1b or Irf7 promoters or of STAT1 to the Irf1 promoter was observed. Each of these genes was also upregulated by WNV Eg101 infection in control, STAT1-/-, STAT2-/- and IFN alpha/beta R-/- MEFs indicating that these ISGs were not upregulated by the canonical type 1 IFN-mediated Jak-STAT pathway or by an alternative IFN alpha/beta R-mediated signaling pathway. Oas1a, Oas1b and Irf7 were also upregulated in infected IRF-3-/-, IRF-7-/- MEFs and initially in IRF-3/7-/- MEFs but not in infected IRF-3/9-/- MEFs suggesting the involvement of IRF-9. Either IRF-3 or IRF-7 could enhance Oas1a and Oas1b upregulation at later times after infection. Activation of Irf1 in infected MEFs did not depend on any of these IRFs. The IPS-1 signaling pathway was shown to be involved in the expression of all four ISGs. The data support the existence of alternative mechanisms of ISG upregulation when the canonical type I IFN pathway is blocked by a WNV infection.

## RESULTS

### 3.1 The kinetics of IFN beta expression, secretion and signaling in WNV Eg101-infected MEFs.

Previous studies reported increased STAT1 phosphorylation as well as increased expression of many ISGs, including Oas1a, Oas1b, Irf1 and Irf7 in WNV Eg101-infected MEFs (Scherbik et al., 2006; Scherbik et al., 2007). To determine whether ISG expression in WNV Eg101-infected MEFs is temporally related to the induction of IFN beta, the kinetics of IFN beta expression in

WNV Eg101 infected [multiplicity of infection (MOI) of 5], transformed C3H/He (tC3H/He) MEFs were analyzed by real time qRT-PCR. IFN beta mRNA levels in tC3H/He MEFs were elevated by 10 fold at 6 h, by 100 fold at 12 h and by more than 5000 fold at 24 and 48 h after WNV Eg101 infection (Fig. 3.1A). The results obtained were similar to those previously reported for infected primary C3H/He (pC3H/He) MEFs (Scherbik et al., 2006). Analysis of extracellular IFN beta protein levels with an enzyme-linked immunosorbent assay (ELISA) detected low levels of IFN beta at 16 h after WNV Eg101 infection of tC3H/He MEFs that continued to increase through 48 h (Fig. 3.1B). At 48 h, 860 pg/ml of IFN beta were detected which corresponds to about 730 International units/ml based on ELISA data obtained with standard curves done on dilutions of an IFN beta sample of known unit concentration. Similar IFN levels were previously reported for primary MEFs (Daffis et al., 2009).

The binding of IFN beta to its cell surface receptor results in activation of the Jak-STAT signaling pathway and phosphorylation of STAT1 and STAT2. A previous study showed that robust phosphorylation of STAT1 occurred in primary C3H/He MEFs after infection with WNV Eg101 (Scherbik et al., 2007). To determine whether this was also the case in transformed MEFs, activation of the Jak-STAT signaling pathway in tC3H/He MEFs by either IFN beta treatment or WNV Eg101-infection were analyzed by Western blotting. Increased levels of both total and phospho-STAT1 as well as of total and phospho-STAT2 were observed after a 3 h incubation of cells with murine IFN beta (Fig. 3.1C). Upregulation of both total STAT1 and STAT2 levels was also observed from 12 h through 48 h after WNV Eg101 infection. Low levels of phopshorylated STAT1 (Tyr 701) were detected at 2, 6 and 12 h after infection, while robust phosphorylation was seen at 24 and 48 h. Low levels of STAT2 phosphorylation (Tyr 690) were detected at 2 through 6 h and high levels were seen at 12 and 24 h after infection but not at 48 h. IRF-9

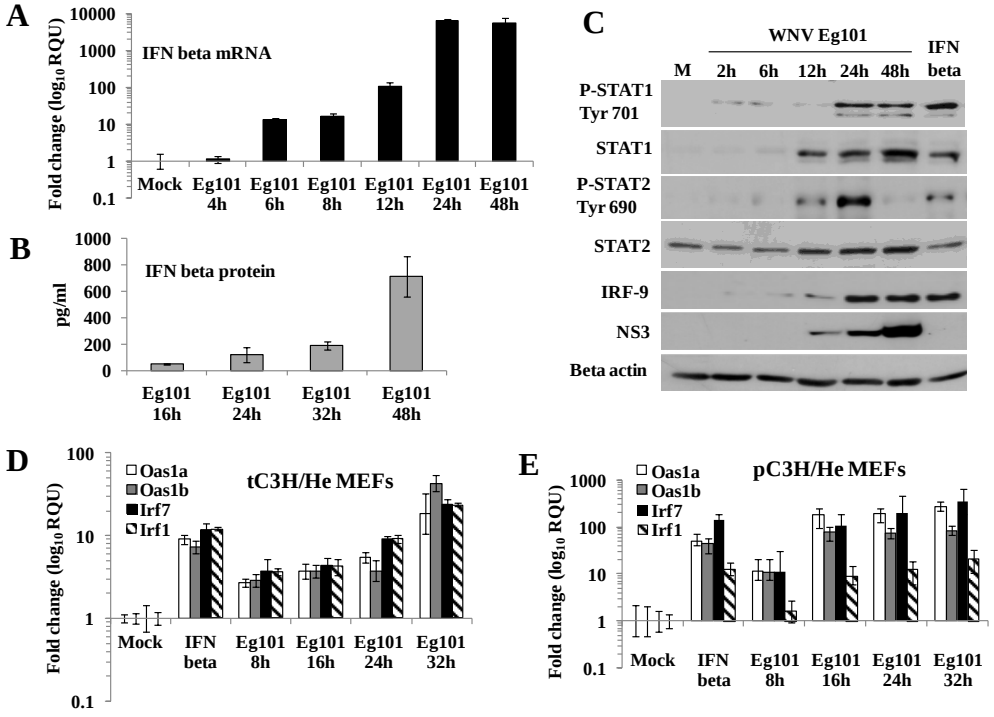


**Figure 3.1. IFN beta is produced by WNV Eg101-infected MEFs and induces phosphorylation of STAT1 and STAT2.** MEFs were mock-infected or infected with WNV Eg101 at a MOI of 5 for the indicated times or treated with 1000 U/ml of murine IFN beta for 3h. **(A)** Total RNA from tC3H/He MEFs was extracted and IFN beta mRNA levels were measured by real-time qRT-PCR. **(B)** Extracellular IFN beta protein levels in tC3H/He MEF culture fluid was measured by ELISA. The values shown are averages from at least two independent experiments performed in triplicate. The error bars represent SDM. **(C)** tC3H/He cell lysates were analyzed by Western blotting using antibodies specific for the indicated proteins. Actin was used as the loading control. The blots shown are representative of results obtained from three independent experiments. **(D)** and **(E)** Comparison of ISG activation by IFN beta in primary and transformed MEFs. Total RNA was extracted from **(D)** tC3H/He or **(E)** pC3H/He MEFs infected with WNV Eg101 (MOI 5) for the indicated times, mock-infected or treated with murine IFN beta (1000 U/ml) for 3h. The changes in the levels of Oas1a and Oas1b mRNA were assessed by real-time qRT-PCR. Each experiment was repeated at least two times in triplicate. The mRNA level of each gene was normalized to the level of GAPDH mRNA in that sample and is shown as the fold change over the amount of mRNA in mock samples expressed in relative quantification units (RQU). The error bars represent the calculated SEM (n = 3) and are based on an $RQ_{Min/Max}$ of the 95% confidence level.

upregulation was detected as early as 6 h and was robust by 24 h after infection and also after a 3 h incubation with IFN beta. Viral NS3 protein levels were analyzed to estimate the efficiency of viral infection. NS3 was detected by 12 h after infection and the levels increased at both 24 and 48 h (Fig 3.1C). The results indicated that upregulation of IFN beta production and its activation of the Jak-STAT signaling pathway began early in WNV Eg101-infected MEFs and continued throughout the infection. Although WNV Eg101 infection induced STAT1 and STAT2 phosphorylation in murine cells, infection of A549 (human) or MA104 (African green monkey) cells with the this virus did not result in STAT phosphorylation (data not shown) similar to what was previously reported for other lineage I WNV strain infections in primate cells (Laurent-Rolle et al.; Liu et al., 2005; Keller et al., 2006).

### 3.2 Comparison of Oas1a, Oas1b, Irf7 and Irf1 expression levels in primary and transformed C3H/He MEFs infected with WNV Eg101.

It was previously reported that transformed cells respond to IFN beta treatment but that the levels of ISG upregulation are lower in these cells compared to those in primary cells (Bartee and McFadden, 2009). Since both primary and transformed MEFs were used in this study, IFN-induced ISG upregulation in tC3H/He (Fig. 3.1D) and pC3H/He (Fig. 3.1E) MEFs was compared. The four ISGs analyzed, Oas1a, Oas1b, Irf7 and Irf1, were upregulated in both types of cells by IFN beta-treatment and WNV Eg101-infection. However, consistent with the previous report, higher levels of ISG induction by both IFN and virus were observed in infected primary MEFs than in transformed MEFs.

### 3.3 Association of STAT1 and STAT2 with ISG promoters in WNV Eg101-infected MEFs.

The observation that STAT1 and STAT2 were phosphorylated in WNV Eg101-infected MEFs suggested that upregulation of the Oas1a, Oas1b, Irf7 and Irf1 genes might be mediated by the canonical type I IFN pathway. The Oas1a and Oas1b promoters each contain a canonical ISRE (Pulit-Penaloza et al., 2012), Irf7 contains an inverted ISRE (Ning et al., 2005; Schmid et al., 2010) and the Irf1 promoter has a GAS element instead of an ISRE which is upregulated in IFN-stimulated cells by a STAT1 dimer (Pine et al., 1994). STAT1 and STAT2 occupancy on the Oas1a, Oas1b and Irf7 promoters and STAT1 occupancy on the Irf1 promoter *in vivo* was analyzed with a chromatin immunoprecipitation (ChIP) assay done as described in Materials and Methods using tC3H/He MEFs that were mock-infected, infected with WNV Eg101 (MOI of 5) for 7, 16 or 24 h or treated with 1000 U/ml of murine IFN beta for 30 m. Briefly, *in vivo* crosslinked DNA-protein complexes were immunoprecipitated using anti-STAT1, anti-STAT2 or a nonspecific IgG antibody. After reversing the crosslinks, immunoprecipitated DNA was purified and quantified by real-time qPCR. An increase in STAT1 (Fig. 3.2A) and STAT2 (Fig. 3.2B) promoter binding compared to that in untreated cells was detected for Oas1a, Oas1b and Irf7 in cells treated with IFN beta. In contrast, no significant increase in either STAT1 or STAT2 promoter binding compared to mock infected cells was detected in cells infected with WNV Eg101 for 7, 16 or 24 h. An increase in STAT1 binding to the Irf1 promoter was observed in cells treated with IFN but not in cells infected with WNV Eg101. These results suggested that the nuclear translocation of phosphorylated STAT1 and STAT2 was blocked in the WNV Eg101-infected cells. To test this hypothesis, the kinetics of STAT1 and STAT2 nuclear translocation in tC3H/He MEFs infected with WNV Eg101 (MOI of 5) were analyzed by

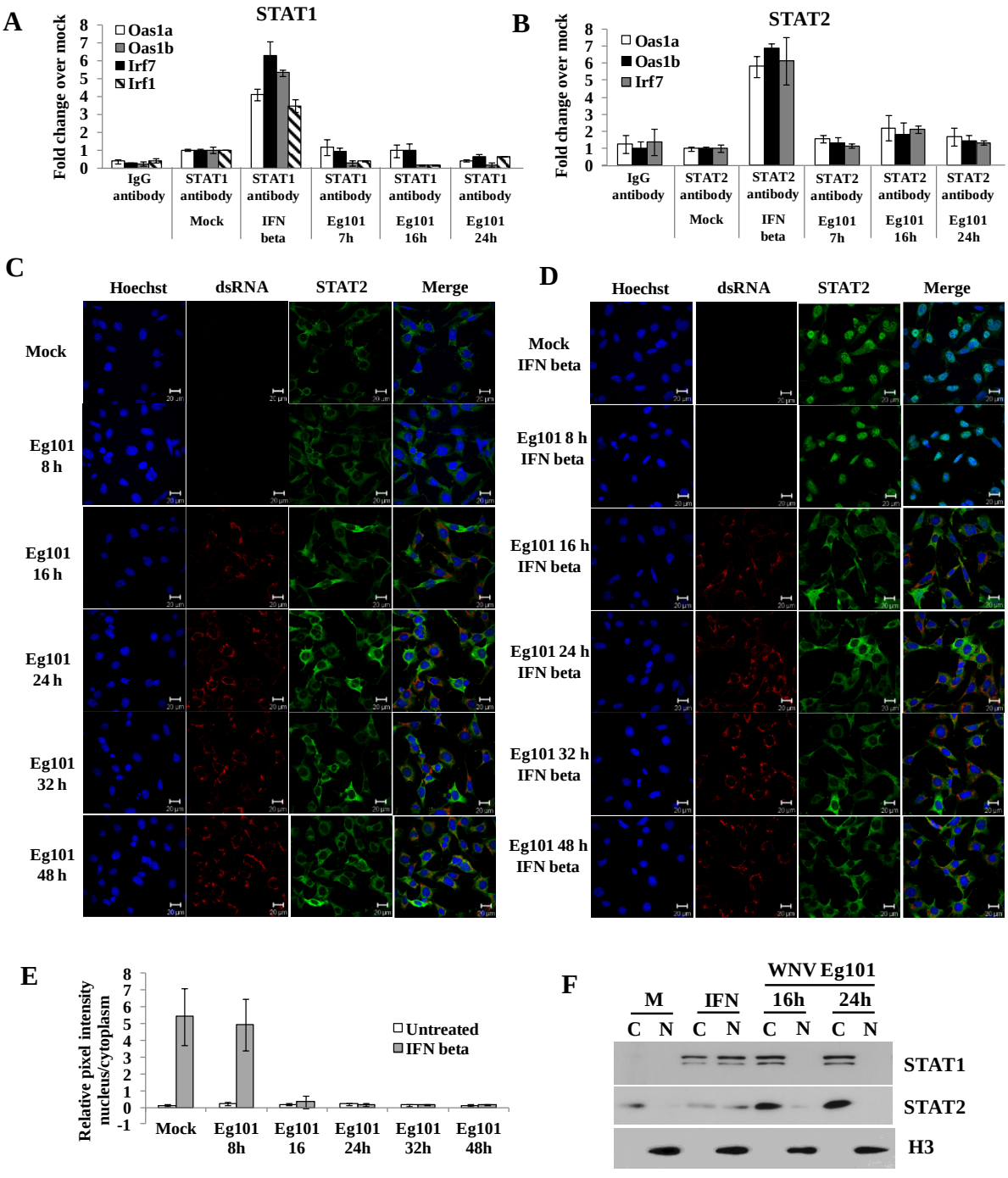
A
STAT1
Fold change over mock
Oas1a
Oas1b
Irf7
Irf1
IgG antibody
STAT1 antibody
Mock
IFN beta
Eg101 7h
Eg101 16h
Eg101 24h
B
STAT2
Oas1a
Oas1b
Irf7
STAT2 antibody
C
Hoechst
dsRNA
STAT2
Merge
Mock
Eg101 8 h
Eg101 16 h
Eg101 24 h
Eg101 32 h
Eg101 48 h
D
Mock IFN beta
Eg101 8 h IFN beta
Eg101 16 h IFN beta
Eg101 24 h IFN beta
Eg101 32 h IFN beta
Eg101 48 h IFN beta
E
Relative pixel intensity nucleus/cytoplasm
Untreated
IFN beta
Mock
Eg101 8h
Eg101 16
Eg101 24h
Eg101 32h
Eg101 48h
F
WNV Eg101
M
IFN
16h
24h
C N C N C N C N
STAT1
STAT2
H3

**Figure 3.2. STAT1 and STAT2 translocation to the nucleus is inhibited in WNV Eg101-infected MEFs.** A chromatin immunoprecipitation assay (ChIP) assessed binding **(A)** of STAT1 to the Oas1a, Oas1b, Irf7 and Irf1 promoters and **(B)** of STAT2 to the Oas1a, Oas1b and Irf7 promoters *in vivo*. The amount of precipitated Oas1a and Oas1b promoter DNA was quantified by real-time qPCR with promoter specific primers and fluorogenic TaqMan FAM/MGB probes. Nonspecific IgG antibody was used as a negative control and averaged values are shown. The averages from at least two independent experiments performed in triplicate were plotted and the error bars show SDM. **(C)** tC3H/He MEFs were infected with WNV at a MOI of 5 for the indicated times. **(D)** tC3H/He MEFs were incubated with 1000 U/ml of IFN beta for 30 m at different times after WNV Eg101 infection. Cellular localization was analyzed by laser scanning confocal microscopy. Nuclei were stained with Hoescht dye (blue), STAT2 was detected using anti-STAT2 antibody (green) and infected cells were detected with anti-dsRNA antibody (red). The results are representative of two independent experiments. **(E)** Quantification of the results in panels A and B. The pixel intensity in the representative area in nucleus was measured and divided by the pixel intensity of the same size area in the cytoplasm. The measurement was done for 20 cells at each time after infection and each treatment. The mean values were plotted and error bars indicate SDM (n = 20). **(F)** t129 MEFs were mock treated, treated with IFN beta (500 U/ml) for 30 m or infected with WNV Eg101 at a MOI of 5 for 16 or 24 h. Whole cell lysates were separated into cytoplasmic and nuclear fractions and analyzed by Western blotting using antibodies specific for STAT1, STAT2 or histone 3 (H3). H3 was used as a control nuclear protein. The blots shown are representative of the results obtained from two independent experiments.

confocal microscopy. Robust STAT2 nuclear translocation, as indicated by STAT2 accumulation in the nucleus, was detected in IFN beta-treated cells (Fig. 3.2D top row) but not in mock-treated cells or cells infected with WNV Eg101 for 8, 16, 24, 32 and 48 h (Fig. 3.2C and E). Similar confocal microscopy results were also observed for STAT1 (data not shown). Western blotting of cytoplasmic and nuclear cell fractions from infected and IFN-treated t129 MEFs cells confirmed the lack of STAT1 and STAT2 nuclear accumulation in infected MEFs of a different genetic background (Fig. 3.2F). Similar Western results were obtained with tC3H/He MEFs (data not shown). To test whether a WNV Eg101 infection could block STAT2 nuclear translocation mediated by the addition of exogenous IFN beta, tC3H/He MEFs infected with WNV Eg101 for 8, 16, 24, 32 or 48 h were incubated with murine IFN beta (1000 U/ml) for 30 m before fixing the cells. In mock-infected cells and cells infected for 8 h (a time when viral dsRNA is not yet detectable by immunofluorescence; Fig. 3.2C second row), the addition of IFN beta resulted in detectable STAT2 nuclear translocation (Fig. 3.2D second row). In contrast, nuclear translocation of STAT2 was not observed when IFN beta was added to cells infected for 16, 24, 32 or 48 h (Fig. 3.2D). The results indicate that similar to other lineage I WNV strains studied (Keller et al., 2006; Laurent-Rolle et al., 2010), a WNV Eg101 infection can block STAT1 and STAT2 nuclear translocation.

### 3.4 Expression of ISGs in WNV Eg101-infected tSTAT1-/- and tSTAT2-/- MEFs.

The ChIP and nuclear translocation assay results indicated that upregulation of Oas1a, Oas1b, Irf7 and Irf1 gene expression in WNV Eg101-infected MEFs was mediated in a STAT1- and STAT2-independent manner. As an additional means of confirming this, the expression of these four ISGs genes was analyzed by real time qRT-PCR in tSTAT1-/- and tSTAT2-/- MEFs and

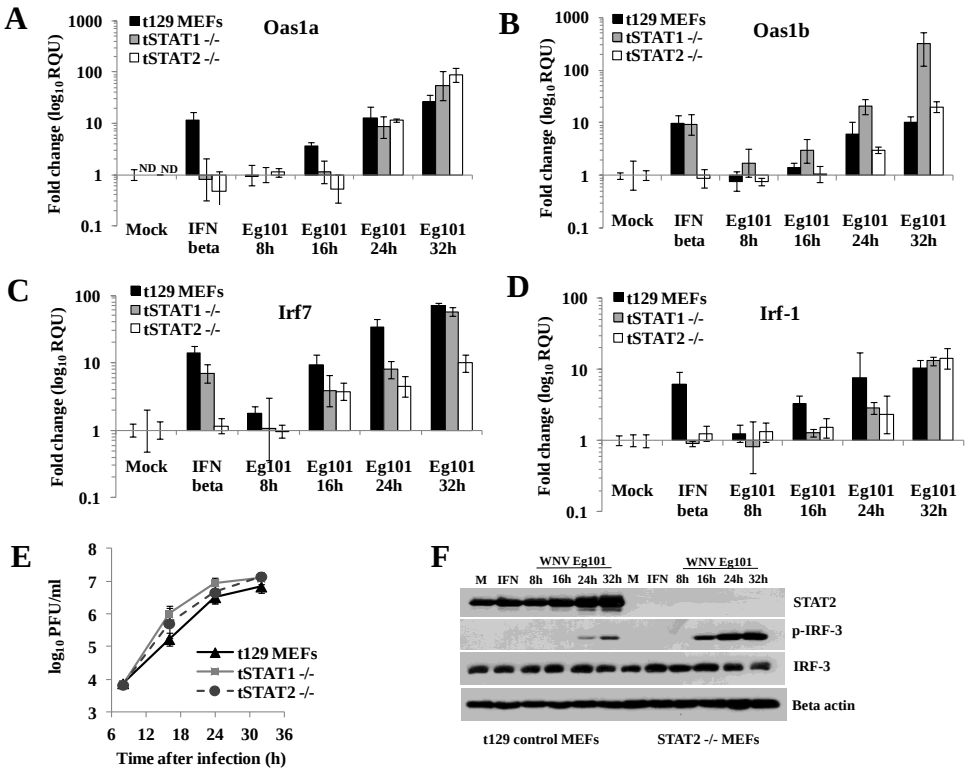


**Figure 3.3. Oas1a, Oas1b, Irf7 and Irf1 gene expression is induced in WNV Eg101-infcted tSTAT1-/- and tSTAT2-/- MEFs.** Fold induction of **(A)** Oas1a, **(B)** Oas1b, **(C)** Irf7 and **(D)** Irf1 mRNA mRNA expression levels in t129, tSTAT1-/- and tSTAT2-/- MEF cell lines was measured by real-time qRT-PCR. Because the expression of Oas1a was not detected (ND) in the mock-treated tSTAT1-/- and tSTAT2-/- MEFs, the expression of Oas1a was normalized to the 8 h WNV Eg101 sample. Each experiment was repeated at least two times in triplicate. The mRNA level of each gene was normalized to the level of GAPDH mRNA in that sample and is shown as the fold change over the amount of mRNA in mock samples expressed in RQU. The error bars represent the calculated SEM (n = 3) and are based on an $RQ_{Min/Max}$ of the 95% confidence level. **(E)** Culture fluid samples harvested at the indicated times after infection were titered for infectivity by plaque assay. Each data point is the average of duplicate titrations from at least two experiments. Error bars indicate SDM. **(F)** t129 and tSTAT2-/- MEF cell lysates were analyzed by Western blotting using antibodies specific for the indicated proteins. Actin was used as the loading control. The blots shown are representative of results obtained from two independent experiments.

matched control wild type t129 MEFs that were mock-infected, infected with WNV Eg101 (MOI of 5) or treated with murine IFN beta (1000 U/ml) for 3 h. A 10-fold or greater increase in Oas1a, Oas1b and Irf7 mRNA levels was observed in wild type t129 MEFs stimulated with IFN beta for 3 h or infected with WNV Eg101 for 32 h (Fig. 3.3A, B and C). Consistent with previous observations (Ousman et al., 2005; Pulit-Penaloza et al., 2012), no upregulation of Oas1a after stimulation with IFN beta was observed in either tSTAT1-/- or tSTAT2-/- MEFs (Fig. 3.3A), while Oas1b (Fig. 3.3B) and Irf7 (Fig.3.3C) upregulation was observed in tSTAT1-/- but not in tSTAT2-/- MEFs. In contrast to the tSTAT1- and tSTAT2-dependence of Oas1a upregulation by IFN beta, Oas1a mRNA was detected at 8 h and increased by more than 50 fold by 32 h after WNV infection in both tSTAT1-/- and tSTAT2-/- MEFs (Fig. 3.3A). Oas1b mRNA levels increased by about 3-fold at 24 h and by about 300-fold at 32 h after infection in tSTAT1-/- MEFs and by about 3-fold at 24 h and by about 20-fold at 32 h after infection in tSTAT2-/- MEFs. Although the fold increase observed for Oas1b expression in infected tSTAT2-/- MEFs was lower than that in tSTAT1-/- MEFs, it was still higher than the 10-fold increase observed in infected control t129 MEFs. In both tSTAT1-/- and tSTAT2-/- MEFs, Irf7 mRNA levels increased by about 2-fold by 16 h after infection. Although a 60-fold increase in Irf7 expression was observed in both wild type t129 and tSTAT1-/- MEFs by 32 h after infection, only a 7-fold increase in Irf7 mRNA levels was observed in infected tSTAT2-/- MEFs by this time. No upregulation of Irf-1 after stimulation with IFN beta was observed in either tSTAT1-/- or tSTAT2-/- MEFs similar to what was observed with Oas1a. A significant increase in Irf1 mRNA levels was observed in both tSTAT1-/- and tSTAT2-/- MEFs at 24 h after infection but these levels were lower compared to those in the control t129 MEFs. However, by 32 h, the levels of Irf1 mRNA were the same in the control and both types of knockout cells (Fig. 3.3D). Virus

yields from tSTAT1-/- and tSTAT2-/- MEFs were initially higher than those from t129 control cells but all of these cell types produced a peak titer of about $10^7$ PFU/ml by 32 h after infection (Fig. 3.3E).

IRF-3 was previously reported to be activated by 16 h after a WNV Eg101 infection in pC3H/He MEFs indicating virus activation of cytoplasmic PRRs (Scherbik et al., 2007). The activation of IRF-3 was compared in t129 and tSTAT2-/- MEFs by Western blotting using antibodies against total IRF-3 and IRF-3 phosphorylated on Ser396. Phosphorylated IRF-3 was detected at 24 and 32 h after WNV Eg101 infection in control t129 MEFs and at 16, 24 and 32 h in tSTAT2 -/- MEFs (Fig. 3.3F). Although earlier and more robust activation of IRF-3 was observed in tSTAT2-/- MEFs compared to wild type MEFs the level of ISG upregulation was lower in these cells.

## 3.5 Analysis of the dependence of Oas1a, Oas1b, Irf7 and Irf1 expression in WNV Eg101-infected MEFs on alternative signaling pathways activated by the IFN alpha/beta receptor.

In addition to activation of the Jak-STAT pathway, type I IFN binding to the IFN alpha/beta R has also been reported to activate the PI3K (Kaur et al., 2005) and p38 mitogen-activated protein kinase (MAPK) signaling pathways (Katsoulidis et al., 2005). Although the results described above indicate that the Jak-STAT pathway is not involved in the upregulation of the ISGs analyzed in WNV Eg101-infected MEFs, the involvement of an alternative signaling cascade induced by type I IFN had not been ruled out. To determine whether the upregulation of the Oas1a, Oas1b, Irf7 and Irf1 genes in WNV Eg101-infected MEFs was mediated by type 1 IFN alpha/beta R signaling through an alternative pathway, the expression of these genes was

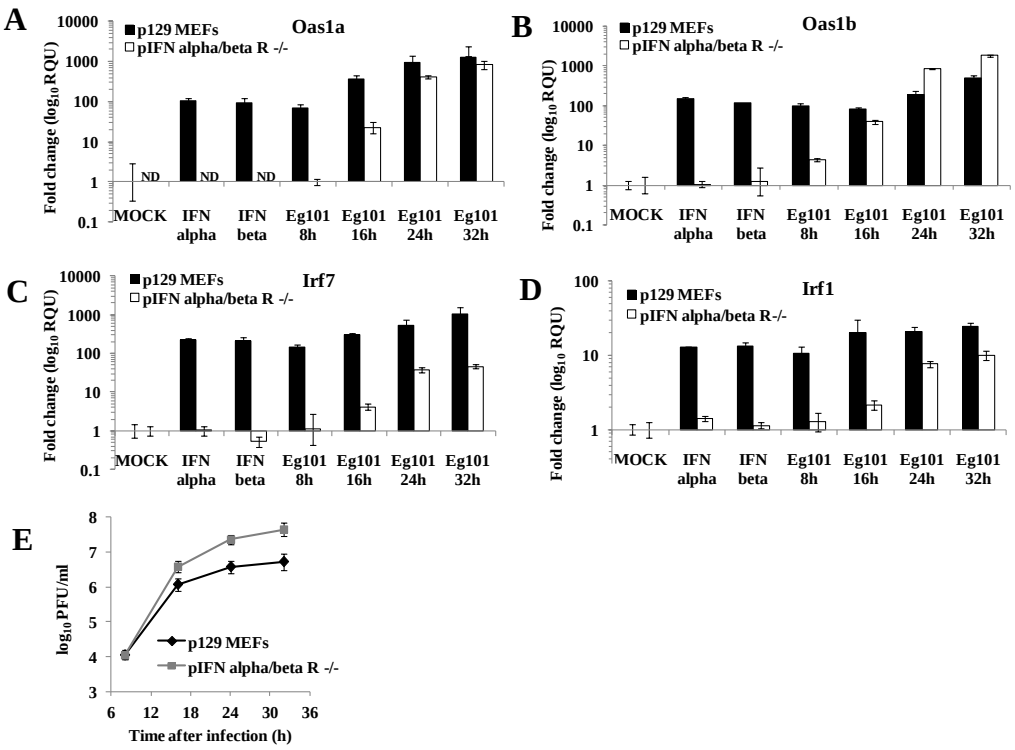


**Figure 3.4. Oas1a, Oas1b, Irf7 and Irf1 are induced in a type I IFN-independent manner in MEFs infected with WNV Eg101.** Fold increase in **(A)** Oas1a, **(B)** Oas1b, **(C)** Irf7 and **(D)** Irf1 mRNA mRNA expression levels in p129 and pIFN alpha/beta R -/- MEFs was measured by real-time qRT-PCR. The mRNA level of each gene was normalized to the level of GAPDH mRNA in that sample and is shown as the fold change over the amount of mRNA in mock samples expressed in RQU. Because the expression of Oas1a was not detected (ND) in the mock-, IFN alpha- or IFN beta-treated pIFN alpha/beta R-/- cells, Oas1a expression in these cells was normalized to the 8 h WNV Eg101 sample. Each experiment was repeated at least two times in triplicate. The error bars represent the calculated SEM (n = 3) and are based on an $RQ_{Min/Max}$ of the 95% confidence level. **(E)** Culture fluid harvested at the indicated times after infection was titered for infectivity by plaque assay. Each data point is the average of duplicate titrations from at least two experiments. Error bars indicate SDM.

analyzed in pIFN alpha/beta R -/- MEFs infected with WNV Eg101 (MOI of 5) by real time qRT-PCR. All four of the ISGs were upregulated in control p129 MEFs treated with either universal type I IFN (human IFN alpha) or murine IFN beta as well as in control MEFs infected with WNV Eg101 (Fig. 3.4A, B, C and D). Because primary 129 MEFs were used for these experiments, the level of gene upregulation was higher compared to that in the transformed 129 MEFs used for the experiments shown in Fig. 3.3. As expected, no increase in Oas1a, Oas1b, Irf7 or Irf1 expression was observed in pIFN alpha/beta R -/- MEFs after IFN alpha or IFN beta treatment. Consistent with the results obtained with tSTAT1-/- and tSTAT2-/- MEFs, basal Oas1a expression was also not detected in mock-infected pIFN alpha/beta R -/- MEFs. In contrast to the lack of upregulation by IFN beta, a significant increase in Oas1a, Oas1b, Irf7 and Irf1 gene expression was observed in pIFN alpha/beta R -/- MEFs infected with WNV Eg101 for 16, 24 or 32 h. The upregulation of the Oas1a and Oas1b genes in the infected pIFN alpha/beta R -/- MEFs was delayed compared to that in the control MEFs; however, by 24 h after infection the mRNA levels for both these genes were comparable to those in wild type MEFs. The activation of Irf7 was delayed and although Irf7 mRNA levels increased by about 50-fold by 32 h after infection in pIFN alpha/beta R -/- MEFs, the maximal upregulation was 20 times less efficient compared to that in the wild type cells (Fig. 3.4C). Irf1 expression in the IFN receptor knockout cells was also delayed and less efficient as compared to that observed in the wild type cells (Fig. 3.4D). Similar to what was previously reported for WNV NY 2000 (Daffis et al., 2009), WNV Eg101 replicated more efficiently in IFN alpha/beta R-/- MEFs than in the control MEFs (Fig. 3.4E).

### 3.6 Analysis of the transcription factors regulating ISG expression during WNV Eg101 infection.

To further investigate the role of IRF-3 in upregulating the four ISGs analyzed in WNV Eg101-infected MEFs, pIRF-3-/- and matched wild type pC57/BL6 MEFs were infected with WNV Eg101 (MOI 5) and the Oas1a, Oas1b, Irf7 and Irf1 mRNA levels were measured by real time qRT-PCR. The Oas1a, Oas1b and Irf7 genes were efficiently upregulated in IRF-3-/- and control cells by both IFN beta and WNV infection (Fig. 3.5A, B and C). Similarly, the Oas1a and Oas1b genes were efficiently upregulated by IFN beta and WNV infection in pIRF-7-/- MEFs. These data suggest that neither IRF-3 nor IRF-7 alone is critical for the upregulation these ISGs in WNV Eg101-infected MEFs**.** The more efficient upregulation of the tested ISG observed in cells deficient in IRF-3 or IRF-7 compared to the wild type control cells suggested the possibility that these two transcription factors may be involved in a negative feedback mechanism of ISG expression. Since the combination of IRF-3 and IRF-7 was previously reported to be required for robust production of type I IFN as well as for the induction of ISGs such as ISG54, ISG49 and RIG-I in MEFs infected with WNV NY 2000 (Daffis et al., 2009), the induction of Oas1a and Oas1b expression was also analyzed in pIRF-3/7-/- MEFs. Although Oas1a and Oas1b expression was upregulated to similar levels in control and pIRF-3/7-/- MEFs at 8 and 16 h after WNV Eg101 infection, a decrease in Oas1a and Oas1b mRNA levels compared to the control cells was observed at 24 and 32 h after infection suggesting that at least one of these TFs is needed to enhance the upregulation of these ISGs in infected cells at later times of infection. Irf1 upregulation by WNV Eg101 infection was similar in pIRF-3/7-/- and control MEFs (Fig. 3.5D). Irf9 mRNA levels were also assessed in pIRF-3/7-/- MEFs. Irf9 was upregulated to similar levels in WNV Eg101-infected control and pIRF-3/7-/- MEFs (Fig. 3.5E). WNV Eg101 replicated as

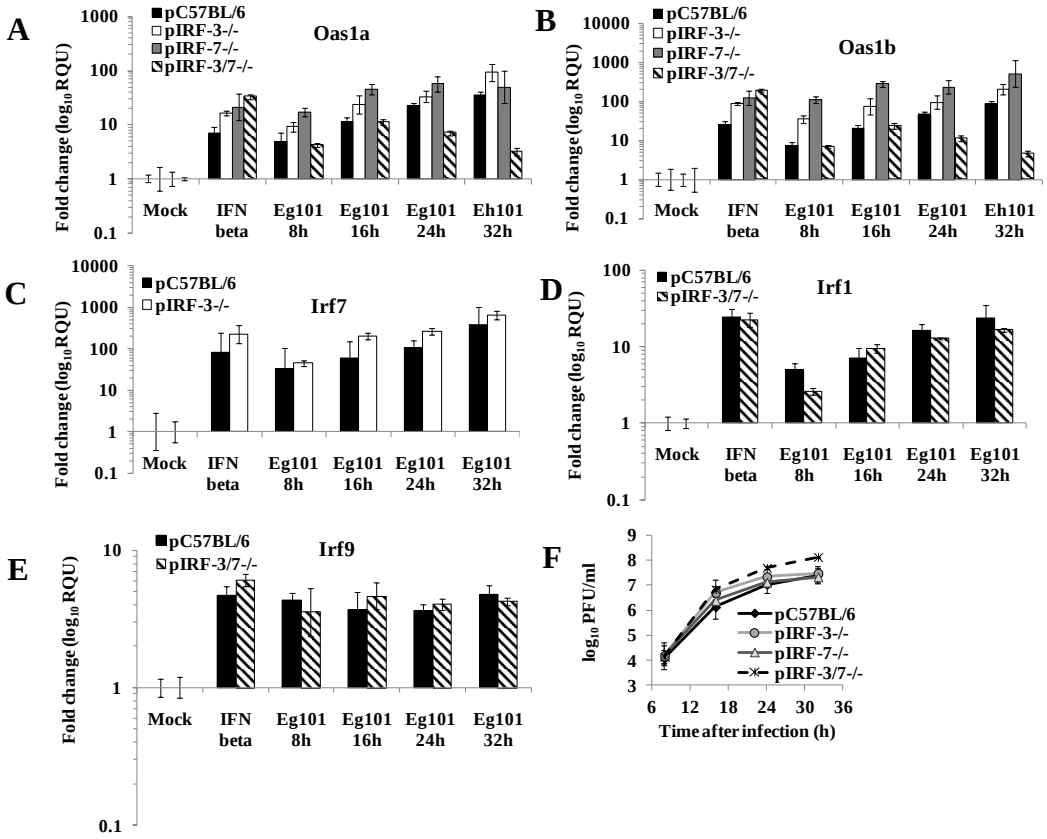


**Figure 3.5. The expression of Oas1a and Oas1b but not Irf1 and Irf9 is reduced in IRF-3/7-/- MEFs.** Fold increase in **(A)** Oas1a, **(B)** Oas1b, **(C)** Irf7 mRNA, **(D)** Irf9 and **(E)** Irf1 expression levels in pC57BL/6, pIRF-3-/-, pIRF-7-/- and pIRF-3/7-/- MEFs was measured by real-time qRT-PCR. Each experiment was repeated at least two times in triplicate. The mRNA level of each gene was normalized to the level of GAPDH mRNA in that sample and is shown as the fold change over the amount of mRNA in mock samples expressed in RQU. The error bars represent the calculated SEM (n = 3) and are based on an $RQ_{Min/Max}$ of the 95% confidence level. **(F)** Culture fluid harvested at the indicated times after infection was titered for infectivity by plaque assay. Each data point is the average of duplicate titrations from at least two experiments. Error bars indicate SDM.

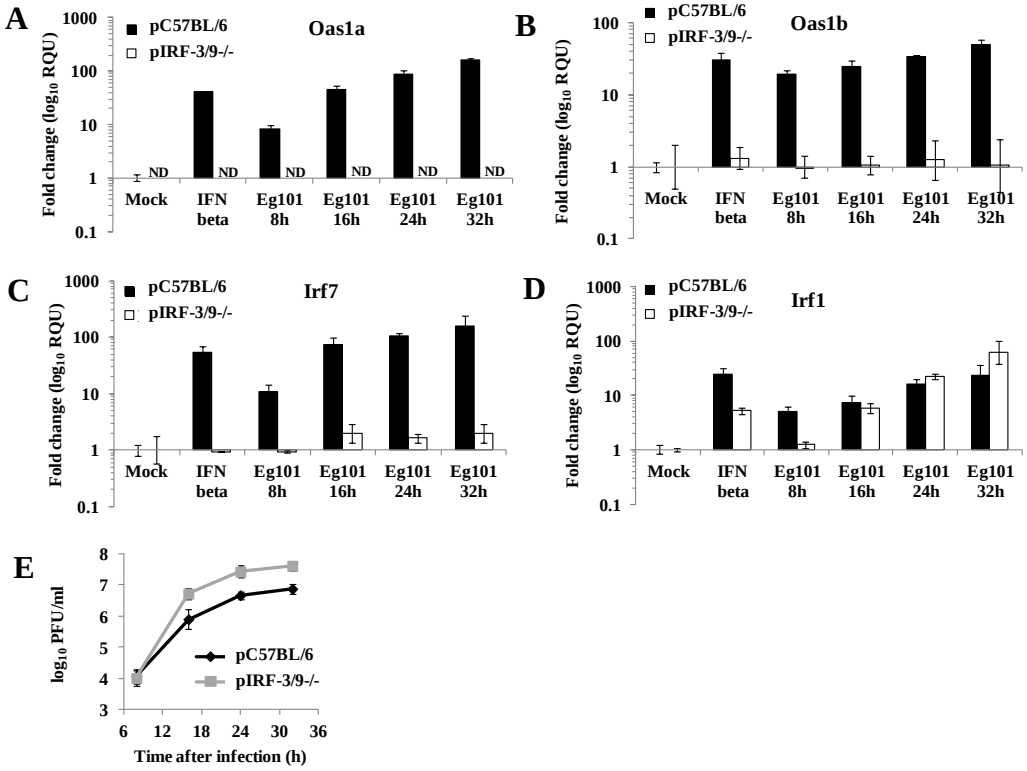


**Figure 3.6. Irf1 but not Oas1a, Oas1b and Irf7, is upregulated in IRF-3/9-/- MEFs infected with WNV Eg101.** Fold increase in **(A)** Oas1a, **(B)** Oas1b, **(C)** Irf7 and **(D)** Irf1 mRNA expression levels in C57BL/6 and IRF-3/9/- MEFs was measured by real-time qRT-PCR. Each experiment was repeated at least two times in triplicate. The mRNA level of each gene was normalized to the level of GAPDH mRNA in that sample and is shown as the fold change over the amount of mRNA in mock samples expressed in RQUs. The error bars represent the calculated SEM (n = 3) and are based on an $RQ_{Min/Max}$ of the 95% confidence level. **(E)** Culture fluid harvested at the indicated times after infection was titered for infectivity by plaque assay. Each data point is the average of duplicate titrations from at least two experiments. Error bars indicate SDM.

efficiently in pIRF-3-/- and pIRF-7-/- MEFs as in wild type cells but the pIRF-3/7-/- MEFs produced higher yields of virus (Fig. 3.5F).

The induction of Irf7, Irf1 and Oas1a gene expression by poly(I:C) was previously shown to be blocked in IRF-3/9-/- MEFs (DeWitte-Orr et al., 2009). To test whether the expression of these ISGs is induced by WNV Eg101 infection in the absence of IRF-3 and IRF-9, pIRF-3/9-/- MEFs were infected with WNV Eg101 (MOI 5) for 8, 16, 24 or 32 h and Oas1a, Oas1b, Irf7 and Irf1 mRNA levels were measured by real time qRT-PCR. No significant upregulation of Oas1a, Oas1b or Irf7 expression was observed in these knockout cells (Fig. 3.6A, B and C). Since IRF-3 was shown not to be required for ISG upregulation in WNV infected MEFs, the data obtained with the pIRF-3/9-/- MEFs suggested that IRF-9 was required. Irf1 expression was upregulated in pIRF-3/-9-/- MEFs to the same or higher levels than in control MEFs (Fig. 3.6D) indicating that this gene is upregulated in infected cells by a different set of TFs than those regulating the Oas1a, Oas1b and Irf7 genes. Analysis of the WNV Eg101 yields produced by control and pIRF-3/9-/- MEFs indicated that virus replication was more efficient in the pIRF-3/9-/- MEFs (Fig. 3.6E).

Previous studies showed that a WNV infection is sensed by the cytoplasmic RNA sensors RIG-I and MDA5 (Fredericksen and Gale, 2006; Fredericksen et al., 2008). Upon recognition of viral RNA RIG-I and MDA5 interact through their caspase activation and recruitment domains (CARDs) with adaptor molecule promoter-stimulating factor (IPS-I) (Kato et al., 2008; Takeuchi and Akira, 2008). A previous study showed that IPS-1 is required for the activation of IRF-3 and the IRF-3 target genes, ISG54 and ISG56, in WNV infected cells (Fredericksen et al., 2008; Suthar et al., 2010). To assess the roles of RIG-I, MDA5 and IPS-1 in the induction of IRF-3 independent ISG upregulation, pRIG-I-/-, pMDA5-/- and pIPS-1-/- MEFs were mock treated,

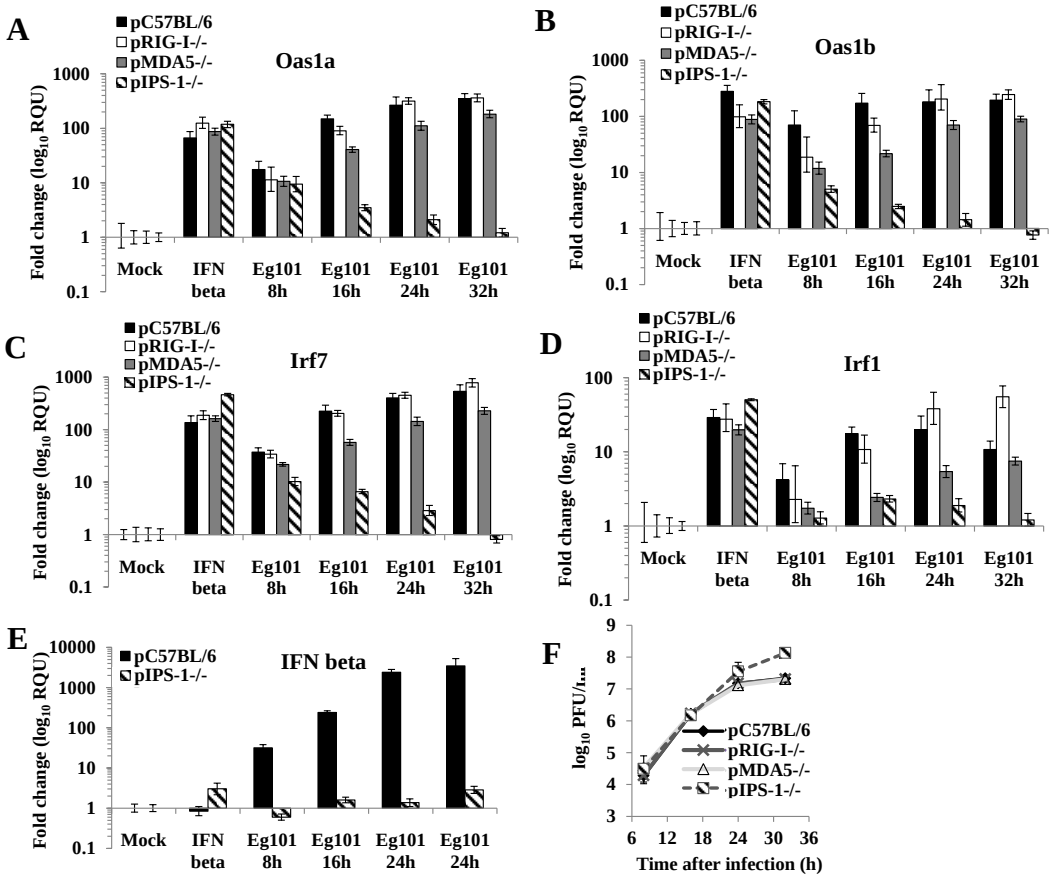


**Figure 3.7. IPS-1 is involved in the upregulation of Oas1a, Oas1b, Irf7 and Irf1 in MEFs infected with WNV Eg101.** Fold increase in **(A)** Oas1a, **(B)** Oas1b, **(C)** Irf7, **(D)** Irf1 and **(E)** IFN beta mRNA expression levels in pC57BL/6, pRIG-I-/-, pMDA5-/- and pIPS-1-/- MEFs was measured by real-time qRT-PCR. Each experiment was repeated at least twice in triplicate. The mRNA level of each gene was normalized to the level of GAPDH mRNA in that sample and is shown as the fold change over the amount of mRNA in mock samples expressed in RQUs. The error bars represent the calculated SEM (n = 3) and are based on an $RQ_{Min/Max}$ of the 95% confidence level. **(F)** Culture fluid harvested at the indicated times after infection was titered for infectivity by plaque assay. Each data point is the average of duplicate titrations from at least two experiments. Error bars indicate SDM.

treated with 1000 U/ml of IFN beta or infected with WNV Eg101 at a MOI of 5 and the Oas1a, Oas1b, Irf7 and Irf1 mRNA levels were measured by real time qRT-PCR (Fig. 3.7A, B, C and D). Although the level of Oas1a, Oas1b, Irf7 and Irf1 upregulation was similar in WNV infected RIG-I-/- and control MEFs, the expression of these ISGs in infected MDA5-/- MEFs was lower suggesting that MDA5 signaling plays a more important role during WNV infection. It was previously reported that RIG-I and MDA5 play different but redundant roles in the activation of IRF-3 and IRF-3 dependent genes in WNV infected cells (Fredericksen et al., 2008; Loo et al., 2008). At 8 h after infection, Oas1a was upregulated to similar levels in control and IPS-1-/- MEFs while the upregulation of Oas1b and Irf7 was lower in infected IPS-1-/- MEFs than in control cells. However, the mRNA levels of all three of these ISGs decreased progressively at later times after infection. No significant upregulation of Irf1 was observed in infected IPS-1-/- MEFs at 8h. A small increase in Irf1 upregulation was observed at 16 h but the mRNA levels decreased at later times. The data indicate that IPS-1 is only partially involved in the initial induction of IRF-3-independent ISGs in WNV infected cells but is required for gene expression at later times after infection. Only minimal upregulation of the IFN beta gene was observed in either IFN beta or WNV infected pIPS-1-/- MEFs (Fig. 3.7E). Higher WNV Eg101 yields were produced by IPS-1-/- MEFs than by RIG-I-/-, MDA5-/- or wild type MEFs (Fig. 3.7F).

**DISCUSSION**

Activation of ISGs by type 1 IFN is mediated by the ISGF3 TF complex composed of STAT1, STAT2 and IRF-9. STAT1 and STAT2 proteins primarily reside in the cytoplasm and the formation and nuclear translocation of the ISGF3 complex depends on IFN-mediated phosphorylation of STAT1 on Tyr701 and STAT2 on Tyr690 (Schindler et al., 1992; Shuai et al., 1992; Qureshi et al., 1996). Most viruses, including flaviviruses, have evolved mechanisms

to suppress the type 1 IFN pathway. The lineage I WNV strains TX02 and NY99 inhibit STAT1 and STAT2 nuclear translocation by blocking phosphorylation of these proteins in primate cells and the WNV NY99 NS5 protein was shown to mediate this suppression (Keller et al., 2006; Laurent-Rolle et al., 2010). In contrast, the attenuated lineage I strain, Kunjin, is a poor suppressor of STAT1 phosphorylation due to a single NS5 mutation, Phe653Ser (Laurent-Rolle et al., 2010). Eg101 and NY99 are closely related lineage I viruses but Eg101 it is less neuroinvasive (Beasley et al., 2002). The WNV Eg101 NS5 has a Phe at position 653 and blocks STAT phosphorylation in primate cells (Scherbik and Brinton, unpublished data). In contrast, WNV Eg101 infections did not block STAT1 phosphorylation at Tyr701 or STAT2 phosphorylation of Tyr690 in MEFs. A decrease in STAT2 phosphorylation was only observed at 48 h. These results indicate host species specific differences in the ability of WNV to suppress STAT phosphorylation. How a WNV Eg101 infection prevents nuclear translocation of phospho-STAT1 and phospho-STAT2 in MEFs is currently under investigation. The dengue virus NS5 protein was previously reported to bind to and target human STAT2 for degradation but was not able to mediate the degradation of murine STAT2 (Ashour et al., 2010). No evidence of either STAT1 or STAT2 degradation was observed in WNV Eg101-infected MEFs.

Activation of the Oas1a, Oas1b, Irf7 and Irf1 genes was previously reported to be IRF-3-independent (Nakaya et al., 2001; Andersen et al., 2008) and the Oas1a and Irf7 genes were reported to be activated only by canonical type I IFN signaling (Nakaya et al., 2001). Data from the present study indicated that upregulation of Oas1a, Oas1b, Irf7 and Irf1 occurred by a STAT1-, STAT2- and type I IFN-independent regulatory mechanism in WNV Eg101-infected MEFs. Although the activation of IRF factors, such as IRF-3 and IRF-7, by viral infections was previously reported to mediate IFN-independent upregulation of subsets of ISGs, the Oas1a,

Oas1b, Irf7 and Irf1genes were efficiently upregulated by WNV Eg101 infection in IRF-3-/- MEFs and the Oas1a, Oas1b, and Irf1 genes were efficiently activated in IRF-7-/- MEFs indicating that neither IRF-3 nor IRF-7 alone was sufficient to induce upregulation of these genes in infected MEFs. A previous study done with WNV NY 2000-infected IRF-3/7 -/- MEFs reported that both IRF-3 and IRF-7 were necessary for production of type I IFN and induction of ISGs such as ISG54, ISG49 and RIG-I (Daffis et al., 2009). We also found only a very low level of IFN beta gene upregulation in WNV Eg101-infected IRF-3/7 -/- MEFs; at 32 h after infection, there was a 27 fold increase in IFN beta mRNA levels compared to an 8000 fold increase in wild type MEFs (data not shown). In contrast, efficient induction of the Oas1a, Oas1b, Irf7 and Irf1 genes was observed in IRF-3/7 -/- MEFs infected for 8 and 16 h with WNV Eg101. However, the absence of both IRF-3 and IRF-7 reduced the levels of Oas1a and Oas1b expression at later times of infection suggesting that at least one of these IRFs is needed to enhance and sustain the upregulation of these two ISGs. No Oas1a and Oas1b upregulation was observed in IRF-3/9-/- MEFs and the expression of Irf7 was also not upregulated in these cells. These observations together with the observation that Irf9 was upregulated in infected IRF-3/7-/- MEFs suggest the possibility that IRF-9 is involved in the initial upregulation of these ISGs in WNV Eg101-infected cells. Since IRF-9 cannot transactivate gene expression alone (Kraus et al., 2003), it must interact with additional partners to active ISG expression in MEFs infected with WNV Eg101. However, it is not currently known whether IRF-9 can form complexes with as yet unidentified TF(s) and whether IRF-9 can interact with IRF-3 and/or IRF-7 to upregulate a subset of ISGs in WNV Eg101-infected MEFs.

IRF-1 was originally described as a TF involved in the induction of the IFN-alpha and IFN-beta genes (Miyamoto et al., 1988). However, it can also upregulate the expression of some ISGs in

an IFN-independent manner (Schoggins et al., 2011). Overexpression of Irf1 was recently shown to inhibit the replication of WNV, dengue virus, yellow fever virus, hepatitis C virus, Chikungunya virus, Venezuelan encephalitis virus and human immunodeficiency virus I (Schoggins et al., 2011). One of the IRF-1 target genes, viperin, (Stirnweiss et al., 2010) was reported to inhibit both WNV and dengue virus infections (Jiang et al., 2010). In a previous study from our lab, the kinetics of upregulation of multiple ISGs in primary C3H/He MEFs infected with WNV Eg101 was analyzed (Scherbik et al., 2007). ISGs such as Oas1a, Oas1b and Irf7 were efficiently upregulated by WNV Eg101 at early times after infection while the upregulation of a subset of ISGS including Irf1 was delayed. The Irf1 gene promoter contains a GAS element instead of an ISRE and upregulation of this gene by type I and type II IFNs is dependent on STAT1 dimers rather than the ISGF3 TF complex (Pine et al., 1994). The murine Irf1 gene was previously reported to be activated in an IRF-3-independent manner (Andersen et al., 2008). However, another study reported that Irf1 upregulation by poly(I:C) was blocked in IRF-3/9-/- MEFs (DeWitte-Orr et al., 2009). The results of the present study indicate that the upregulation of Irf1 gene expression in WNV Eg101-infected MEFs is mediated in an IRF-3-, IRF-9- and IRF-7-independent manner. An Irf1 promoter analysis predicted the presence of NF-kappa B binding sites (Harada et al., 1994; Pine et al., 1994) and Irf1 gene expression was previously reported to be induced by this TF (Pahl, 1999). NF-kappa B is activated by a WNV Eg101-infection in MEFs (Scherbik et al., unpublished results) and the involvement of NF-kappa B components in regulating Irf1 upregulation in infected cells is currently under investigation.

During a WNV infection, viral RNA is recognized by RIG-I and MDA5 cytoplasmic sensors (Fredericksen et al., 2008) which signal through the IPS-1 adaptor molecule to activate IRF-3 leading to the induction of IFN and IRF-3-dependent gene expression (Fredericksen et al., 2008;

Daffis et al., 2009; Suthar et al., 2010). The results of the present study showed that lack of MDA5 but not of of RIG-I resulted in reduction in the upregulation of Oas1a, Oas1b, Irf7 and Irf1 suggesting that MDA5 may be functionally more important for the upregulation of these genes. In addition, the results of this study showed that the initial upregulation of Oas1a, Oas1b and Irf7 but not of Irf1 in WNV Eg101infected MEFs is only partially dependent on IPS-1 since the mRNA levels of these genes were upregulated in IPS-1 deficient cells at 8 h after infection. The lack of induction of IFN beta gene expression at 8 h after infection in IPS-1-/- MEFs confirmed that the upregulation of these genes was independent of IFN-beta. The mechanism by which the initial IFN- and IPS-1-independent upregulation of a subset of ISGs occurs is currently not known. Early induction of ISGs may be due to activation of signaling pathways activated by WNV entry. The existence of such a response to virus particle entry was previously reported and shown to be IFN-, TLR- and RIG-I independent (Paladino et al., 2006). The interaction of the fusion peptides of enveloped viruses with cellular membranes were also shown to activate several cell transduction pathways leading to early activation of ISGs by AP-1 and NF-kappa B (Vitiello et al., 2010). However, IPS-1 is required for ISG expression at later times of infection.

The higher viral loads in tissues and increased mortality observed with WNV NY99-infected IFN alpha/beta R-/- and IFN beta-/- mice indicate the importance of the type I IFN response for host protection (Samuel and Diamond, 2005; Lazear et al., 2011). Type I IFN secreted by infected cells induces an antiviral state in uninfected cells through the induction of ISGs and this reduces viral spread. The upregulation of ISGs by IFN-independent mechanisms in infected cells would be expected to reduce virus yields even though canonical IFN signaling was blocked by the infection in these cells. It was previously shown that IRF-3-dependent ISGs could be

upregulated in WNV-infected cells and experiments in IRF-3-/- mice indicated that IRF-3 protected mice by both IFN-dependent and IFN-independent mechanisms (Fredericksen et al., 2004; Daffis et al., 2007). IRF-7 was shown to protect mice primarily through the induction of IFN alpha (Daffis et al., 2008). The data obtained in the present study indicate that there are additional mechanisms of IFN-independent ISG upregulation for subsets of ISGs in infected MEFs and that IFN-independent ISG upregulation is more complex than previously appreciated. The data also suggest that IRF-9 may also be involved in both IFN-dependent as well as IFN-independent activation complexes for some ISGs.

## MATERIALS AND METHODS

### 3.7 Cells and viruses.

SV40-T antigen transformed C3H/He (tC3H/He) MEFs were grown in minimal essential medium (MEM) supplemented with 5% fetal bovine serum (FBS) and 10 µg/ml gentamicin. Primary C3H/He MEFs (pC3H/He), pIRF-3-/-, pIRF-7-/- and pC57BL/6 MEFs (provided by Michael Diamond, Washington University School of Medicine, ST. Louis, Missouri) were grown in DMEM supplemented with 10% FBS and 10 µg/ml gentamicin. pIRF-3/7-/- MEFs (provided by Michael Diamond, Washington University School of Medicine, ST. Louis, Missouri) were grown DMEM supplemented with 15% FBS and 1% PenStrep (Gibco). t129/SvEv, tSTAT1-/- and tSTAT2-/- MEF lines (provided by Christian Schindler, Columbia University, New York, NY) were grown in MEM supplemented with 10% FBS and 1% PenStrep. p129 MEFs and pIFN alpha/beta R -/- MEFs (provided by Herbert Virgin, Washington University School of Medicine, St. Louis, MO) were grown in DMEM supplemented with 10% FBS and 1% PenStrep. IRF-3/9-/- MEFs (provided by Karen Mossman, McMaster University,

Hamilton, Ontario, Canada) were grown in MEM alpha supplemented with 10% FBS and 1% PenStrep. All cell cultures were grown at 37°C in a 5% $CO_2$ atmosphere.

A stock of lineage I WNV strain Eg101 was prepared by infecting BHK cells (Vaheri et al., 1965) grown in MEM supplemented with 5% FBS and 10 µg/ml gentamicin at a MOI of 0.1 and harvesting culture fluid 32 h after infection, a time when the infected cell monolayer was still intact. Clarified culture fluid was aliquoted and stored at –80°C. The titer of the stock virus was ~ 1 x $10^8$ PFU/ml.

### 3.8 ELISA.

Cell culture fluid was collected at various times after WNV Eg101 infection and the levels of secreted IFN beta protein in these samples were measured by a capture ELISA according to the manufacturer's instructions (PBL Biomedical Laboratories, NJ) using a standard curve prepared by titrating a known concentration of recombinant murine IFN beta.

### 3.9 ChIP.

Confluent tC3H/He monolayers were mock-infected, infected with WNV Eg101 at a MOI 5 for 7, 16 or 24 h or treated with 1000 U/ml of murine IFN beta for 3 h. The ChIP assay was done as previously described (Pulit-Penaloza et al., 2012). Isolated DNA was analyzed by real-time PCR using probes and primers designed to span the proximal Oas1a and Oas1b promoters. The sequences of the primers were: Oas1a forward primer 5'-GGATCCTAAGAAAGCTCAGACTTCA-3', Oas1a reverse primer 5'-CCCGGCAGCCAATGG-3', Oas1b forward primer 5'- GAAGCCCTAACGCCATTGG-3', Oas1b reverse primer 5'-AGGGCGCGGATATGCA-3', Irf7 forward primer 5'-

CCTGCCTTGTCCCAATGTG-3' and Irf7 reverse primer 5'-ACACCCGACCCTTACTCAGATC-3' and Irf1 forward primer 5'-CCTTCGCCGCTTAGCTCTAC-3' and Irf1 reverse primer 5'-CCCACTCGGCCTCATCATT-3'. The sequence of the FAM-MGB Oas1a probe was 5'-TGGAAGTGTGGGAAAGGTCTTT-3', that of the Oas1b probe was 5'-CGGGCCTGGATGAT-3' and that of the Irf7 probe was 5'-TTTCCTGAAGAGGTCCTG-3' and that of Irf-1 probe was 5'-ACAGCCTGATTTCC-3'. To obtain standard curves, known amounts of Oas1a, Oas1b and Irf7 and Irf1 promoter DNA cloned into a TOPO-XL vector (Invitrogen) were titrated and assayed by real-time quantitative PCR (qPCR) using a FastStart Universal Probe Master (ROX) kit (Roche Applied Science) according to the manufacturer's protocol. To quantify the immunoprecipitated DNA, standard curves were independently generated at the same time as the immunoprecipitated DNA samples by qPCR and the value of the fold change over the value obtained with a mock-infected sample was calculated. The average values from at least two independent experiments were plotted. Error bars represent SDM.

### 3.10 Quantification of mRNA levels.

Real-time quantitative reverse transcription-PCR (qRT-PCR) analyses of mouse Oas1a and Oas1b gene expression were performed using a 50 µl reaction mixture containing 500 ng of total cellular RNA, the primer pair (1 µM), and the probe (0.2 µM) and an Applied Biosystems 7500 Sequence Detection System. Applied Biosystems Assays-on-Demand 20x primer and fluorogenic TaqMan FAM/MGB probe mixes Mn00836412_m1 for Oas1a, Mn00449297_m1 for Oas1b, Mn00516788_m1 for Ifr7 and Mn01288580_m1 for Irf1 were used. Glyceraldehyde-3-phosphate dehydrogenase (GAPDH) mRNA was used as an endogenous control for each sample and was detected using TaqMan mouse GAPDH primers and probe (Applied Biosystems). One-step RT-

PCR was performed for each target gene and for the endogenous control in a singleplex format using 200 ng of RNA and the TaqMan One-Step RT-PCR Master Mix Reagent Kit (Applied Biosystems). The cycling parameters were as follows: reverse transcription at 48°C for 30 m, AmpliTaq activation at 95°C for 10 m, denaturation at 95°C for 15 s, and annealing/extension at 60°C for 1 m (cycle repeated 40 times). Each experiment was repeated at least two times in triplicate. Triplicate Ct values were analyzed with Microsoft Excel using the comparative Ct (ΔΔCt) method of the SDS Applied Biosystems software which also applied statistical analysis to the data (TINV test in Microsoft Excel). The values were normalized to those for GAPDH and presented as the relative fold change compared to the uninfected calibrator sample in relative quantification (RQ) units. Error bars represent the standard error of the mean (SEM) and indicate the calculated minimum ($RQ_{Min}$) and maximum ($RQ_{Max}$) of the mRNA expression levels based on a $RQ_{Min/Max}$ of the 95% confidence level. The expression levels between two samples were considered statistically different (P value of $<0.05$) when the error bars did not overlap.

### 3.11 Confocal immunofluorescence microscopy.

tC3H/He MEFs grown to 50% confluency on 15-mm glass coverslips in 12-well plates were infected with WNV Eg101 at a MOI of 5. The cells were fixed with 4% paraformaldehyde in PBS for 10 min at RT and then permeabilized with 0.1% Triton X-100 in PBS for 10 min. Coverslips were washed with PBS, blocked overnight in 5% heat-inactivated horse serum (Invitrogen) in PBS, and then incubated with mouse anti-dsRNA antibody (English and Scientific Consulting Bt, Hungary) diluted 1:500 in the blocking buffer or with rabbit anti-STAT2 antibody (generously provided by Christian Schindler, Columbia University, New York, NY) diluted 1:200 for 1h at room temperature. The coverslips were washed three times with PBS and incubated with donkey anti-mouse Alexa Fluor 594 or donkey anti-rabbit Alexa Fluor 488

secondary antibodies (Invitrogen) diluted 1:400 in blocking buffer containing 0.5 μg/ml of Hoescht 33342 dye (Invitrogen). The coverslips were washed with PBS and mounted on glass slides with Prolong Gold Antifade reagent (Invitrogen). Cells were visualized with a 40x oil-immersion objective on a LSM 700 laser confocal microscope (Zeiss, Oberkochen, Germany) using LSM 5 (version 4.2) software (Carl Zeiss Inc.). All of the images compared were obtained using the same instrument settings.

### 3.12 Western blotting.

Whole tC3H/He cell extracts were prepared using radioimmunoprecipitation assay buffer [1x PBS, 1% Nonidet P-40, 0.5% sodium deoxycholate, and 0.1% SDS containing Halt Protease and Phosphatase Inhibitor Single-Use Cocktail (Thermo Scientific). t129 MEF and STAT2-/- MEF nuclear and cytoplasmic extracts were prepared using Nuclear Extract kit (Active Motif) according to the manufacturer's protocol. Following separation by SDS-polyacrylamide gel electrophoresis (PAGE), the proteins were electrophoretically transferred to a nitrocellulose membrane. The membrane was blocked with Tris-buffered saline pH 8, containing 5% dry milk (5% bovine serum albumin was substituted for milk when phosphorylated proteins were detected) and 0.1% Tween-20 for 1 h at 22°C and then incubated with a polyclonal primary antibody specific for: STAT1 (Cell Signaling), phospho-STAT1 (Tyr701) (Cell Signaling), STAT2 (generously provided by Christian Schindler, Columbia University, New York, NY), phospho-STAT2 (Tyr 690) (Abcam), IRF-9 (Santa Cruz Biotechnology), WNV NS3 (R&D Systems) or beta-actin (Abcam) overnight at 4°C in the presence of blocking buffer. The blots were then incubated with anti-rabbit antibody conjugated with horseradish peroxidase (Santa Cruz Biotechnology) or anti-mouse antibody conjugated with horseradish peroxidase (Cell

Signaling) for 1 h at 22°C and processed for enhanced chemiluminescence using a Super-Signal West Pico detection kit (Thermo Scientific) according to the manufacturer's instructions.

**ADDITIONAL DATA**

The results of this study showed that ISGs including Oas1a, Oas1b, Irf7 and Irf1 are upregulated in a type I IFN-independent manner by WNV Eg101 infection. A previous analysis of the induction of ISGs in pC3H/He MEFs infected with WNV Eg101 showed that one subset of genes including Oas1a, Oas1b and Irf7 was efficiently upregulated by WNV Eg101 at early times after infection while the upregulation of a second subset of ISGS including Irf1 was delayed (Scherbik et al., 2007) suggesting differential regulation of these two subsets of ISGs. Consistent with this hypothesis, the results of this study confirmed that the two ISG subsets are regulated by different sets of TFs in WNV Eg101-infected MEFs. The expression of Oas1a, Oas1b and Irf7 was shown to depend on IRF-9 TF and additional as yet unknown transactivating factors. Either IRF-3 or IRF-7 enhanced the upregulation of these genes at later times after infection. However, Irf1 was shown not to be regulated by any of these transcription factors in WNV-infected cells.

As a means of determining which TFs might be involved in the activation of Irf1 in WNV Eg101-infected MEFs, the involvement of the mitogen activated protein kinase (MAPK) pathways that are involved in numerous signaling events were first analyzed. There are three major MAPK signaling pathways: c-Jun N-terminal kinase (JNK), extracellular signal-regulated kinase (ERK) and p38 (Chang and Karin, 2001) (Fig. 3.8A). Both the ERK (Scherbik and Brinton, 2010) and JNK (Scherbik, Courtney and Brinton, unpublished data) pathways are activated in cells infected with WNV Eg101. The involvement of the JNK and ERK signaling pathways in the upregulation of ISG mRNA production in WNV Eg101-infected MEFs was analyzed using pathway specific inhibitors. The JNK II inhibitor (anthra[1,9-*cd*]pyrazol-6(2*H*)-one, 1,9-pyrazoloanthrone) (Calbiochem) is a specific inhibitor of JNK while U0126 (1,4-

diamino-2,3-dicyano-1,4-bis[2-aminophenylthio] butadiene) (Cell Signaling) is a highly selective inhibitor of the ERK kinases MEK 1 and MEK 2. Cells that were mock-treated or infected with WNV Eg101 at a MOI 5 were incubated with the JNK or ERK inhibitor at concentration of 50μM or with DMSO (vehicle control) for 24h. Prior to collecting total RNA, replicate mock-treated cells were incubated with 1000 U/ml of IFN beta for 3h. Total RNA was extracted and the upregulation of Oas1a, Oas1b and Irf1 mRNA was analyzed by real time qRT-PCR. No reduction in the expression of Oas1a, Oas1b or Irf1 was observed in cells incubated with either the ERK or JNK inhibitor compared to cells treated with DMSO (Fig. 3.8B, C and D) indicating that these pathways are not required for the induction of Oas1a, Oas1b or Irf1 by IFN beta or WNV Eg101 infection.

Although it was reported that p38 can be activated by dsRNA or encephalomyocarditis virus (ECMV) infection in a PKR- and RNase L- independent manner (Iordanov et al., 2000), the activation of the p38 MAPK pathway during WNV Eg101 infection was not previously tested. The p38 kinase is activated by the MAPK kinases, MKK3, MKK4 and MKK6, through dual phosphorylation of p38 on Thr180 and Tyr182 (Bellon et al., 1999; Davis, 2000; Chang and Karin, 2001). To determine whether p38 was activated during WNV Eg101 infection of tC3H/He cells, Western blotting of cell extracts using antibodies against p38 phosphorylated at Thr180 andTyr182 was done at different times after infection (Fig. 3.9A). A decrease in both total and phospho-p38 was observed at 8h after WNV Eg101 infection compared to control samples. However, a robust increase in phospho-p38 was observed in cells infected with WNV Eg101 for 24 or 32 h indicating that p38 was activated at these times after infection. To determine whether the p38 pathway is involved in the upregulation of Oas1a, Oas1b and Irf1 in WNV Eg101-infected MEFs, the mRNA levels of these genes were measured in mock-treated, IFN beta

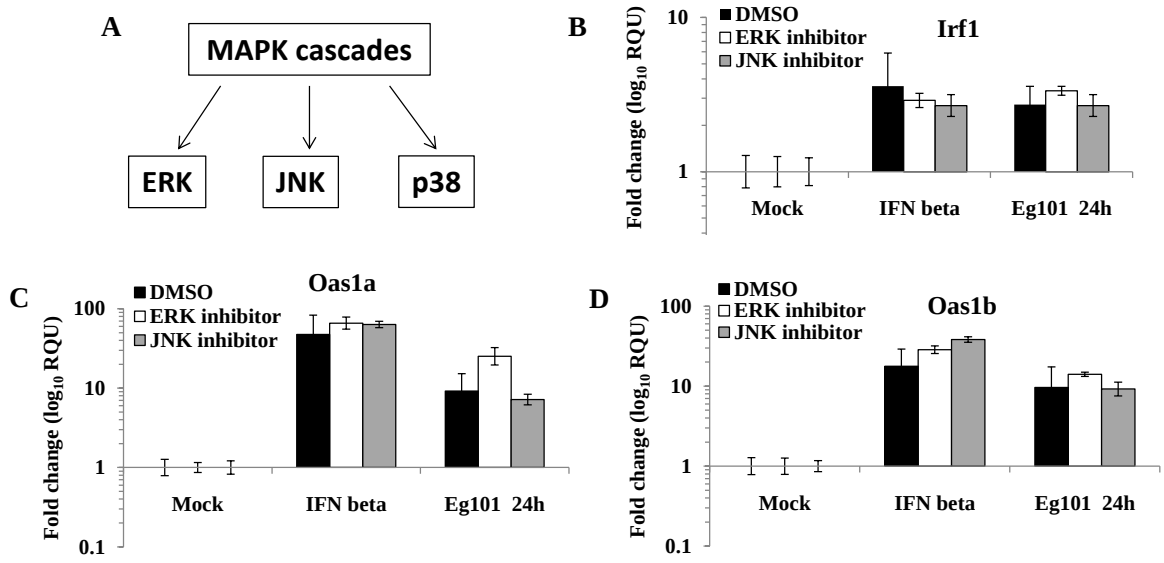


**Figure 3.8. Analysis of the involvement of the ERK and JNK MAPK pathways in the upregulation of ISG mRNAs in WNV Eg101-infected MEFs. (A)** MAPK cascades. tC3H/He cells that were mock- or WNV Eg101-infected (MOI of 5) **for 24 h** were incubated with ERK inhibitor or JNK inhibitor at a final concentration of 50 µM or with DMSO. Prior to collecting total RNA, replicate cultures of mock-treated cells was incubated with 1000 U/ml of IFN beta for 3h. **(B)** Irf1, **(C)** Oas1a and **(D)** Oas1b mRNA levels were analyzed by real time qRT-PCR. The mRNA level of each gene was normalized to the level of GAPDH mRNA in the same sample and is shown as the fold change over the amount of mRNA in mock samples expressed in relative quantification units (RQU). Error bars represent the SE ($n$ = 3) and are based on an $RQ_{Min/Max}$ of the 95% confidence level.

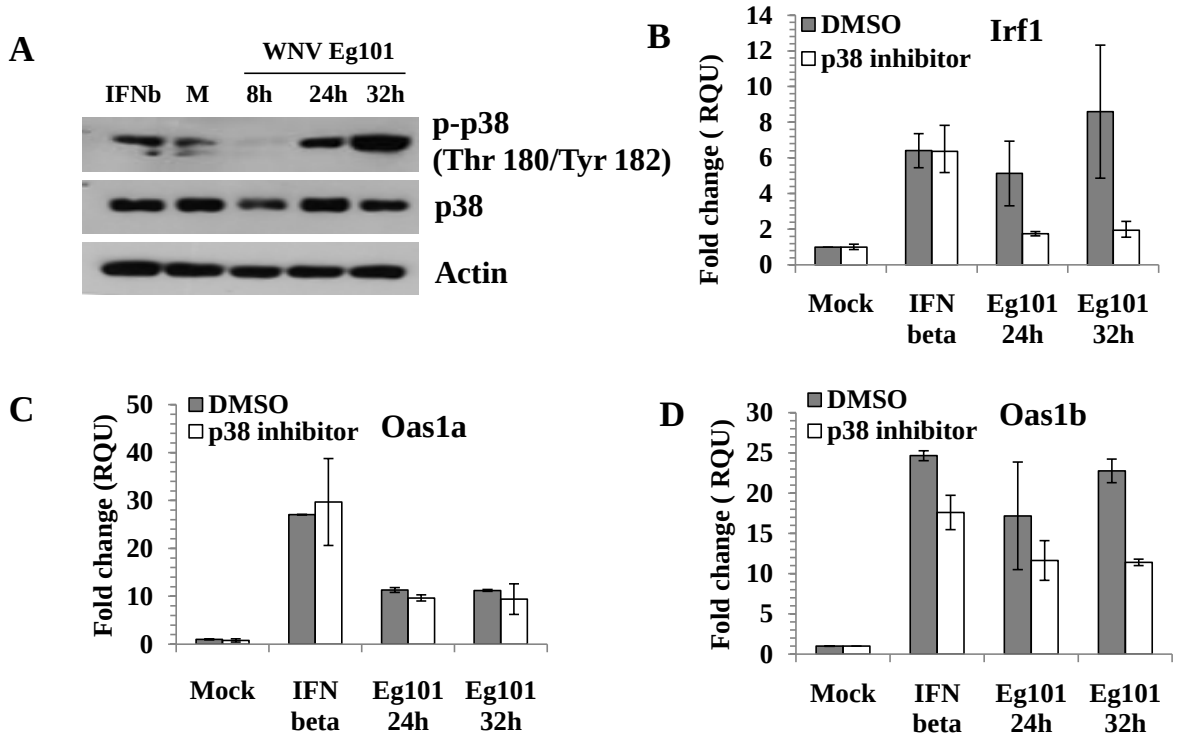


**Figure 3.9. Analysis of the activation and involvement of the p38 MAPK pathway in the upregulation of ISG mRNAs in WNV Eg101-infected MEFs. (A)** tC3H/He MEFs were mock- or WNV Eg101-infected (MOI of 5) for 24 or 32 h or treated with 1000 U/ml of IFN beta. Cell lysates were analyzed by Western blotting using antibodies against p38 (Cell Signaling), p38 phosphorylated at Thr 180 and Tyr 182 (Cell Signaling) or beta actin (loading control) (Abcam). tC3H/He MEFs mock- or WNV Eg101-infected (MOI of 5) were incubated with 20 µM of p38 inhibitor or with DMSO. Prior to collecting total RNA, replicate mock-treated cultures were incubated with 1000 U/ml of IFN beta for 3h. **(B)** Irf1, **(C)** Oas1a and **(D)** Oas1b mRNA levels were analyzed by real time qRT-PCR. The mRNA level of each gene was normalized to the level of GAPDH mRNA in that sample and is shown as the fold change over the amount of mRNA in mock samples expressed in RQU. Error bars represent the SE ($n$ = 3) and are based on an $RQ_{Min/Max}$ of the 95% confidence level.

treated and infected cells incubated in the presence of 20 µM of the p38 inhibitor SB202190 (Calbiochem) or DMSO. The expression of Oas1a in cells treated with IFN beta or infected with WNV Eg101 was not affected by the inhibitor (Fig. 3.9C). However, inhibitor treatment of cells infected for 24 or 32 h reduced the expression of Irf1 by 70% or more (Fig. 3.9B) indicating that the p38 pathway is important for the upregulation of Irf1 in WNV Eg101-infected MEFs. In contrast, no reduction in Irf1 mRNA levels was observed in IFN-treated cells in the presence of the inhibitor. However, the expression of Oas1b was decreased by about 30% in cells treated with IFN and by about 50% in cells infected for 32 h (Fig. 3.9D) suggesting that p38 might play a partial role in the upregulation of Oas1b by IFN and during WNV Eg101 infection.

A TFBS analysis of the Irf1 promoter sequence predicted the presence of NF-kappa B binding sites (Harada et al., 1994; Pine et al., 1994) and consistent with this prediction a previous study showed that Irf1 gene expression was induced by this TF (Pahl, 1999). Also, NF-kappa B was shown to be activated in WNV Eg101-infected MEFs (Scherbik, Pulit-Penaloza and Brinton, unpublished data). The involvement of NF-kappa B components in upregulating Irf1 in infected cells was tested using the NF-kappa B activation inhibitor 6-amino-4-(4-phenoxyphenylethylamino)quinazoline. tC3H/He MEFs were mock-treated, infected with WNV Eg101 at a MOI of 5 for 24 h or treated with 1000 U/ml of IFN beta for 3 h and then incubated with media containing the NF-kappa B inhibitor at concentrations of 5, 30 or 60 nM or with DMSO for 24 h prior to harvesting RNA from cells. Real time qRT- PCR was done to determine the levels of Oas1a, Oas1b and Irf1 mRNA in each sample. The results showed that inhibition of NF-kappa B did not affect the upregulation of Oas1a (Fig. 3.10A) suggesting that the upregulation of Oas1a in MEFs infected with WNV Eg101 is not mediated by NF-kappa B. However, a dose dependent decrease in the expression of Oas1b was observed in inhibitor

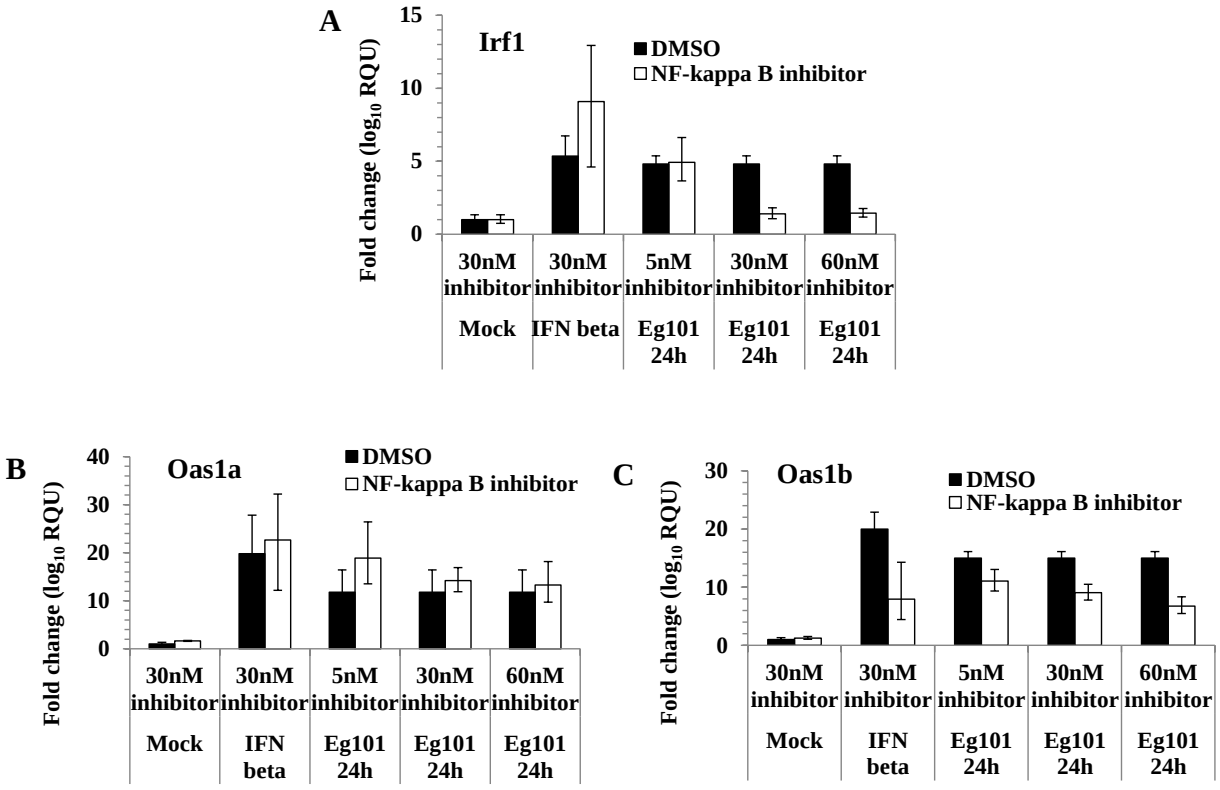


**Figure 3.10. Analysis of the involvement of NF-kappa B in the upregulation of ISG mRNAs in WNV Eg101-infected MEFs.** tC3H/He MEFs mock or WNV Eg101infected (MOI of 5) for 24 or 32 h were incubated with NF-kappa B inhibitor at a final concentration of 5, 30 or 60 nM or with DMSO. Prior to collecting total RNA, replicate mock-treated cultures were incubated with 1000 U/ml of IFN beta for 3h. **(A)** Irf1, **(B)** Oas1a and **(C)** Oas1b mRNA levels were analyzed by real time qRT-PCR. The mRNA level of each gene was normalized to the level of GAPDH mRNA in the same sample and is shown as the fold change over the amount of mRNA in mock samples expressed in RQU. Error bars represent the SE ($n$ = 3) and are based on an $RQ_{Min/Max}$ of the 95% confidence level.

treated cells also treated with IFN as well as in infected cells (Fig. 3.10B) suggesting that NF-kappa B plays a partial role in the upregulation of this gene by IFN beta and WNV Eg101 infection. Oas1b contains an NF-kappa B site located just downstream of the ISRE, while Oas1a does not. Although this site was shown not to be involved in the activation of the Oas1b promoter by IFN beta, it could play a role in the upregulation of Oas1b in an IFN-independent manner in WNV Eg101-infected MEFs. Analysis of the Oas1b promoter by GENOMATIX predicted three additional NF-kappa B binding sites upstream of the ISRE which might also play a role in regulating Oas1b expression induced by IFN beta and/or WNV Eg101 infection. In contrast, the NF-kappa B inhibitor did not affect Irf1 expression in cells treated with IFN beta but reduced the expression of Irf1 in WNV Eg101-infected cells to the levels observed in mock at both 30 and 60 nM concentrations (Fig. 3.10C).

The mammalian NF-kappa B family consists of RelA (p65), NF-kappa B1 (p50/p105), NF-kappa B2 (p52/p100), c-Rel, RelB. RelA, RelB and c-Rel. Each subunit has a carboxy-terminal activation domain and is involved in transcriptional activation of promoters that contain NF-kappa B sites. p50 and p52 lack a transactivation domain but can still bind NF-kappa B sites and repress gene expression. Each member of the NF-kappa B family can form heterodimers and/or homodimers with one another. The most common form of NF-Kappa B is the p65/p50 heterodimer (Li and Verma, 2002; Pomerantz and Baltimore, 2002). To further investigate the involvement of NF-kappa B in the upregulation of Irf1 in WNV Eg101-infected MEFs, Irf1 mRNA levels as well as those of Oas1a and Oas1b mRNAs were analyzed in cells with either the p65 or p50 subunit of NF-kappa B knocked out. As expected based on the results with the NF-kappa B inhibitor, the upregulation of Oas1a by WNV Eg101 infection was not affected in either cell line (Fig. 3.11B and E). Oas1b mRNA levels were reduced in p65-/- MEFs treated with IFN

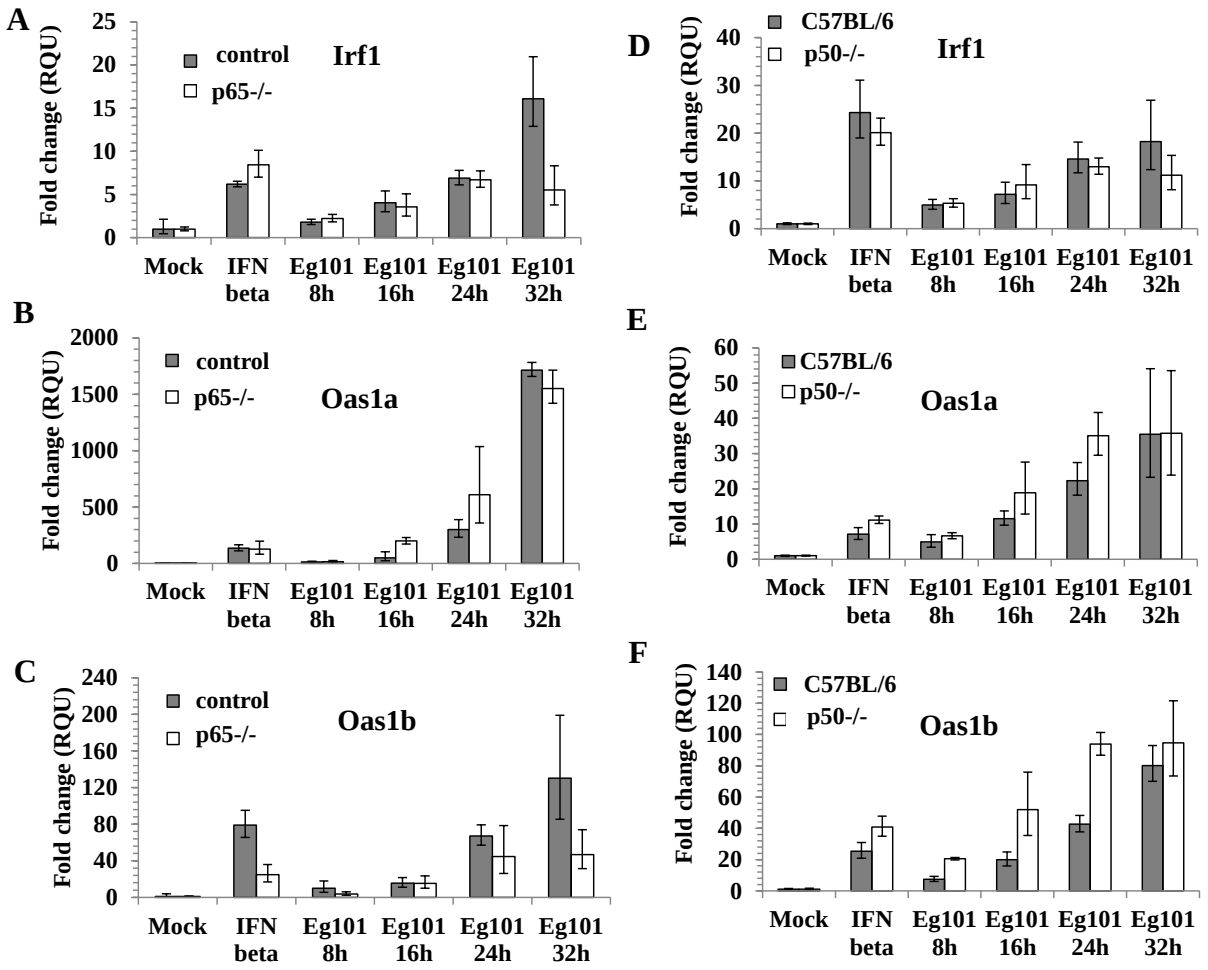


**Figure 3.11. Analysis of the involvement of the p65 and p50 NF-kappa B subunits in the upregulation of ISG mRNAs in WNV Eg101-infected MEFs. (A-C)** p65-/- MEFs or p65-/- MEFs stably transfected with a p65 expression vector (control), **(D-E)** C57BL/6 (wild type) MEFs or p50-/- MEFs. Cells were mock- or WNV Eg101-infected (MOI of 5) for the indicated times or treated with 1000 U/ml of IFN beta. Total RNA was collected and the Oas1a, Oas1b and Irf1 mRNA levels were analyzed by real time qRT-PCR. The mRNA level of each gene was normalized to the level of GAPDH mRNA in the same sample and is shown as the fold change over the amount of mRNA in mock samples expressed in RQU. Error bars represent the SE ($n$ = 3) and are based on an $RQ_{Min/Max}$ of the 95% confidence level

beta (Fig. 3.11C). However, the expression of Oas1b and Irf1 in WNV Eg101-infected p65-/- MEFs was reduced but only at late times after infection (32 h) with a maximum reduction of about a three-fold (Fig. 3.11A and C). These data suggest a partial role for p65 in regulating the expression of Oas1b and Irf1 in infected cells. A slight but not a significant reduction in the Irf1 mRNA at 32 h was observed in WNV Eg101-infected p50-/- MEFs (Fig. 3.11E) suggesting that the p50 subunit of NF-kappa B is not required for the upregulation of Irf1. In contrast, a significant increase in Oas1b mRNA levels at 8, 16 and 24 h after infection was observed in WNV Eg101-infected p50-/- MEFs (Fig 3.11 F) suggesting that p50 subunit of NF-kappa B may play a role in downregulating Oas1b in infected cells. The p50/p50 homodimer is known to be a transcriptional repressor (Li and Verma, 2002; Pomerantz and Baltimore, 2002).

The data indicate that both the p38 and NF-kappa B pathways are involved in Irf-1 and Oas1b gene regulation in WNV Eg101-infected MEFs. It is possible that NF-kappa B may be activated by p38 in infected cells since the involvement of p38 in the activation of NF-kappa B was previously reported (Maulik et al., 1998; Vanden Berghe et al., 1998; Liang and Gardner, 1999; Saha et al., 2007).

# CHAPTER 4

## 4 AIM 3. Translational suppression of IRF-1 expression in WNV Eg101-infected cells.

### INTRODUCTION

IRF-1 is a transcription factor that induces the expression of various antiviral genes including IFN-alpha and IFN-beta, MHC class I and some ISGs (Miyamoto et al., 1988; Taniguchi et al., 2001; Schoggins et al., 2011). Recent studies demonstrated the importance of IRF-1 in inhibiting the replication of many viruses including WNV (Jiang et al., 2010; Schoggins et al., 2011). In addition, studies using IRF-1 knockout mice showed that IRF-1 mediates a broad spectrum of antiviral processes in response to IFN gamma. Mice lacking IRF-1 showed defects in maturation and development of various types of immune cells (Paun and Pitha, 2007).

In contrast to other ISGs such as Irf7, Oas1a and Oas1b which are induced at 12 h after WNV Eg101 infection of tC3H/He MEFs, the induction of Irf1 is delayed until 24 h after infection (Scherbik et al., 2007). Although the levels of Irf1 mRNA in MEFs infected with WNV Eg101 for 24 h and MEFs treated with IFN beta for 3 h are similar, only a small increase in IRF-1 protein levels is observed in infected cells in contrast to the high IRF-1 levels in type I IFN-treated MEFs suggesting translational repression of IRF-1 in WNV Eg101-infected cells (Scherbik et al., 2007).

Protein expression can be regulated post-transcriptionally at the level of mRNA synthesis, mRNA turnover, translation or protein turnover. Since induction of IFN is the initial host cell response against viral infection, many viruses have developed strategies to circumvent either the upregulation of IFN genes or the induction of IFN signaling in order to block the upregulation of

the genes encoding antiviral proteins (Randall and Goodbourn, 2008). Induction of increased cellular mRNA decay was previously reported to be mediated by Kaposi's sarcoma virus, EBV and herpes simplex virus (HSV) infections (Glaunsinger and Ganem, 2004; Feng et al., 2005; Lee and Glaunsinger, 2009; Clyde and Glaunsinger, 2010). Adenovirus, influenza virus and VSV infections have been shown to interfere with mRNA trafficking by blocking the export of cellular mRNAs from the nucleus (Faria et al., 2005; Satterly et al., 2007; Yatherajam et al., 2011). Cell protein levels are most commonly blocked by viruses at the level of translation. A variety of viruses have been reported to inhibit global translation through targeting either initiation factors, including 4EBP1, eIF4E, eIF4G, eIF4A, eIF5B, eIF3 and eIF2 or elongation factors, including eEF1A and eEF1B, or release factor eRF1, or PABP or ribosomes (reviewed in (Walsh and Mohr, 2011)). However, none of these mechanisms are limited to only a subset of genes.

Transcript specific translation regulation can be achieved by the binding of cell proteins to *cis*-acting elements, such as AU rich elements (ARE), in the 3'UTRs of target mRNAs (Zhang et al., 2002; Abaza and Gebauer, 2008) or by the binding of specific miRNAs to target mRNAs (Eulalio et al., 2008; Hutvagner and Simard, 2008). The binding of proteins to AREs can lead to destabilization or stabilization of a mRNA or cause translational suppression (silencing) (Zhang et al., 2002). miRNAs can also specifically regulate the stability or translation of target mRNAs. Some viruses encode miRNAs while others induce or repress the expression of particular host miRNAs. For example, expression of EBV latent membrane protein 1 was shown to induce the expression of cellular miR-146a that plays a role in the antiviral response (Motsch et al., 2007; Cameron et al., 2008). An enterovirus infection was reported to induce host miR-141 miRNA which specifically targets eIF4E mRNA leading to inhibition of cap-dependent initiation of protein translation (Ho et al., 2011). HIV infection was shown to repress a polycistroninc cluster

of cell miRNAs and this allows more efficient replication (Triboulet et al., 2007). Herpesviruses encoded miRNAs were shown to target viral lytic genes as well as host genes involved in the induction of the innate antiviral immune response and apoptosis (Skalsky and Cullen, 2010).

## RESULTS

### 4.1 Analysis of the expression of IRF-1 in WNV Eg101-infected tC3H/He MEFs.

A previous analysis of ISG expression in primary C3H/He MEFs showed that both Irf1 mRNA and protein levels were upregulated in cells treated with IFN beta for 3 h. However, although Irf1 transcript levels were upregulated to similar levels at 24 h after infection with WNV Eg101 and 3 h after treatment with IFN beta, IRF-1 protein levels increased only slightly over those in control cells (Scherbik et al., 2007). To determine whether IRF-1 translational suppression also occurs in transformed C3H/He (tC3H/He) MEFs, the cells were mock- or WNV Eg101-infected (MOI of 5) or IFN beta-treated and total RNA and cellular lystates were collected and analyzed by real time qRT-PCR or Western blotting. Similar to the results of the previous study (Scherbik et al., 2007), mRNA levels of Irf1 were significantly upregulated (Fig. 4.1A) but only a small increase in IRF-1 protein levels was observed in the WNV Eg101-infected transformed MEFs (Fig. 4.1B). In contrast, STAT1 protein levels, were significantly upregulated at 24 and 32 h after WNV Eg101 infection and at 3 h after IFN treatment. As an additional means of confirming the translational suppression of IRF-1 in WNV Eg101-infected cells, tC3H/He cells were infected with WNV Eg101 at a MOI of 5 and 3 h before cell harvest, cells were treated with 1000 U/ml of IFN beta or left untreated. As expected mRNA levels in WNV Eg101-infected increased at 19 and 27 h after infection (Fig. 4.1C). Similar high levels of Irf1 mRNA were observed in samples from mock-treated or infected cells treated with IFN beta prior to harvesting (Fig. 4.1C). Increased IRF-1 protein levels were observed in mock-treated and 5 h WNV infected cells

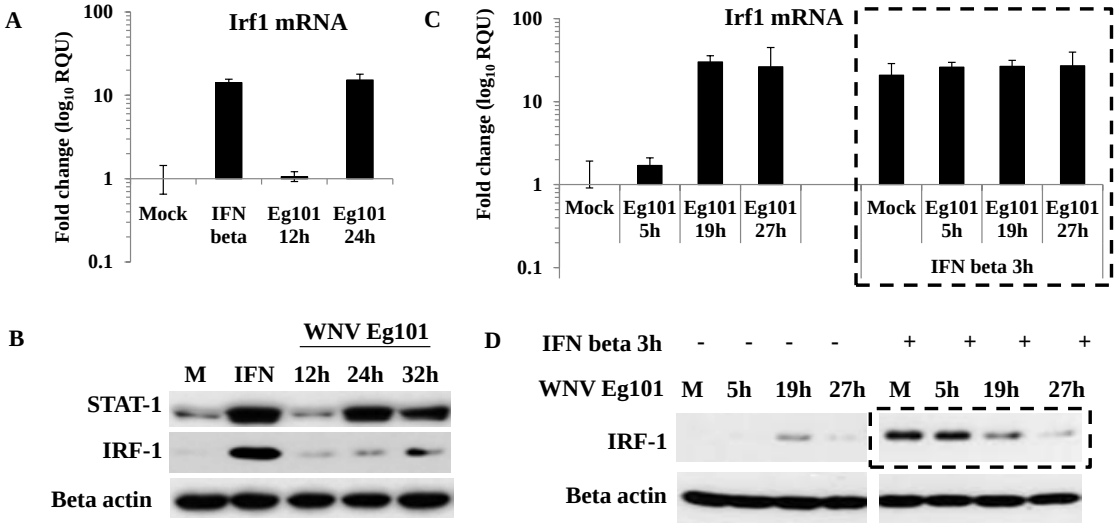


**Figure 4.1. Expression of IRF-1 in WNV Eg101-infected tC3H/He MEFs.** tC3H/He MEFs were mock-infected or infected with WNV Eg101 at a MOI of 5 for the indicated times or treated with 1000 U/ml of murine IFN beta for 3 h. **(A)** Total RNA from tC3H/He MEFs was extracted and Irf1 mRNA levels were measured by real-time qRT-PCR. **(B)** tC3H/He cell lysates were analyzed by Western blotting using antibodies specific for the indicated proteins. **(C, D)** tC3H/He MEFs were mock-infected or infected with WNV Eg101 at a MOI of 5 for the indicated times. Three h before collecting total RNA or cell lysates, the cells were either treated with 1000 U/ml of murine IFN beta for 3 h or left untreated. **(C)** Irf1 mRNA levels were measured by real-time qRT-PCR. **(D)** IRF-1 protein expression in cell lysates was analyzed by Western blotting using specific antibodies. In each real time qRT-PCR experiment, the mRNA level of each gene was normalized to the level of GAPDH mRNA in the same sample and shown as the fold change over the amount of mRNA in mock samples expressed in relative quantification units (RQU). Error bars represent the SE ($n$ = 3) and are based on an $RQ_{Min/Max}$ of the 95% confidence level. Actin was used as a loading control in each Western blot experiment. The blots shown are representative of the results obtained from at least two independent experiments.

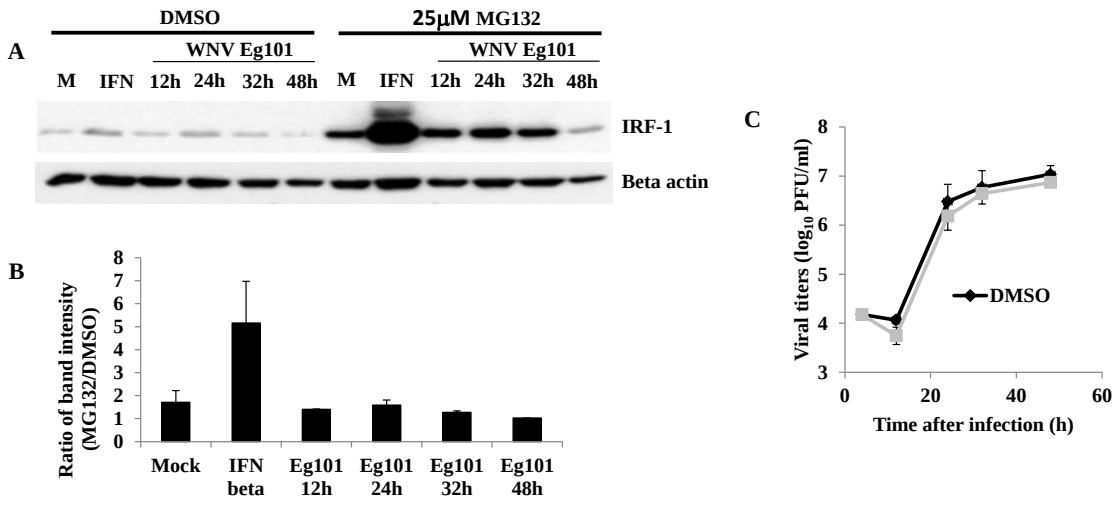


**Figure 4.2. The effect of the proteasomal inhibitor MG132 or IRF-1 protein levels in tC3H/He MEFs. Fig. 4.2.** tC3H/He MEFs were mock-infected, infected with WNV Eg101 at a MOI of 5 for the indicated times or treated with 1000 U/ml of murine IFN beta. Six hours before collecting cell lysates, the cells were treated with MG132 (25 μM) or DMSO. **(A)** IRF-1 protein levels in cell lysates were analyzed by Western blotting. Actin was used as a loading control. **(B)** Results obtained from three independent Western blot experiments were quantified by densitometry using ImageJ software. The average results were summarized graphically as the ratio of band intensity DMSO/MG132. Error bars indicate SDM (*n*=3). **(C)** Culture fluid from samples harvested at the indicated times after infection were titered for infectivity by plaque assay. Each data point is the average of duplicate titrations from at least two experiments. Error bars indicate SDM (*n*=3).

treated with IFN but the protein levels in the IFN-treated infected cells decreased with increasing time after infection (Fig. 4.1D).

## 4.2 The effect of a proteasomal inhibitor on IRF-1 protein levels in MEFs infected with WNV Eg101.

Since decreased protein levels could be due to increased proteasomal degradation, the extent of protein turnover was analyzed using the proteasome inhibitor MG132. tC3H/He MEFs were mock-infected, infected with WNV Eg101 at a MOI of 5 for the indicated times or treated with 1000 U/ml of murine IFN beta for 3 h. Six hours before collecting cell lysates, the cells were treated with MG132 (Calbiochem) (25 μM) or DMSO (vehicle control). Protein expression in cell lysates was analyzed by Western blotting using antibodies specific for IRF-1 (Fig. 4.2A and B). IRF-1 has a 30 m half-life (Watanabe et al., 1991) and in the presence of the proteasomal inhibitor, high levels of IRF-1 accumulated in cells treated with IFN consistent with increased synthesis of IRF-1 in these cells. In contrast, the levels of IRF-1 in mock-treated cells and infected cells treated with the inhibitor were similar suggesting that only low basal IRF-1 levels are produced and no enhancement of IRF-1 translation occurs in infected cells. These results suggest that the low IRF-1 protein levels in infected cells are not due to enhanced proteasomal degradation of IRF-1 but to a lack of increased IRF-1 translation. MG132 treatment had no effect on viral replication (Fig. 4.2C).

## 4.3 WNV infection does not lead to production of alternatively spliced variants of Irf1 mRNAs.

One mechanism of altering gene expression is by inducing alternative splicing of a mRNA species. Exon skipping can result in the loss of the initiation codon preventing translation initiation (Harada et al., 1994; Maratheftis et al., 2006). To test whether the IRF-1 translational

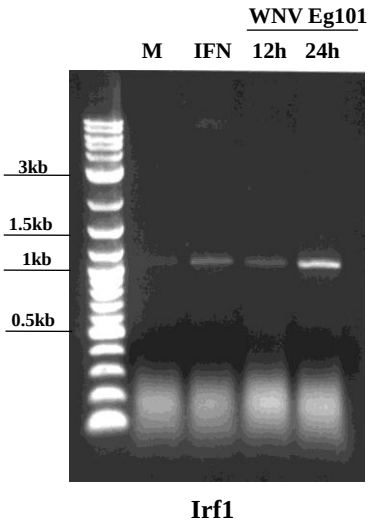


**Figure 4.3. Comparison of the sizes of Irf1 mRNA transcripts in mock- or WNV Eg101-infected or IFN beta-treated MEFs.** tC3H/He cells were mock-infected, infected with WNV Eg101 (MOI of 5) for 12 or 24 h or treated with 1000 U/ml IFN beta for 3 h. Total RNA was extracted and used for RT-PCR with primers specific for Irf1. Amplified cDNA was resolved on a 1% agarose gel.

suppression is due to production of alternatively spliced isoforms of Irf1 in WNV Eg101-infected cells, total RNA was isolated from cells that were mock-treated, infected with WNV Eg101 at MOI 5 or treated with 1000 U/ml of IFN beta for 3 h and analyzed by RT PCR. Only a single size Irf1 transcript band was detected in cells from the three conditions (Fig. 4.3) indicating that the IRF1 translational suppression is not due to alternative splicing of Irf1 mRNA.

### 4.4 The effect of the Irf1 3'UTR on luciferase reporter expression in WNV infected cells.

To determine whether the 3'UTR of Irf1 mRNAs contains elements required for translation suppression in WNV infected cells, a firefly luciferase reporter gene with the Irf1 3'UTR under the control of eIF1 alpha promoter was cloned into the pGL3 vector (Promega) (Fig. 4.4A). The expression vector containing Irf1 3'UTR or the control vector (luciferase reporter gene with the firefly luciferase 3'UTR under the control of eIF1 alpha promoter) were co-transfected with the pGL4.74 *Renilla* luciferase reporter construct into tC3H/He MEFs. At 24 h after transfection, the cells were either mock- or WNV Eg101-infected at a MOI of 5 for 24 h. Firefly luciferase activity produced by the reporter vector containing the Irf1 3'UTR was normalized to the luciferase activity produced by a control luciferase reporter vector. The eIF1 alpha promoter provides constitutive expression of the firefly luciferase gene. Lower luciferase activity was expected in cells that were infected compared to mock-treated cells. However, no significant difference in the luciferase activity was observed in infected and uninfected cells suggesting that the presence of Irf1 3'UTR downstream of the firefly luciferase gene does not negatively regulate the expression of firefly luciferase in infected cells (Fig.4.4B).

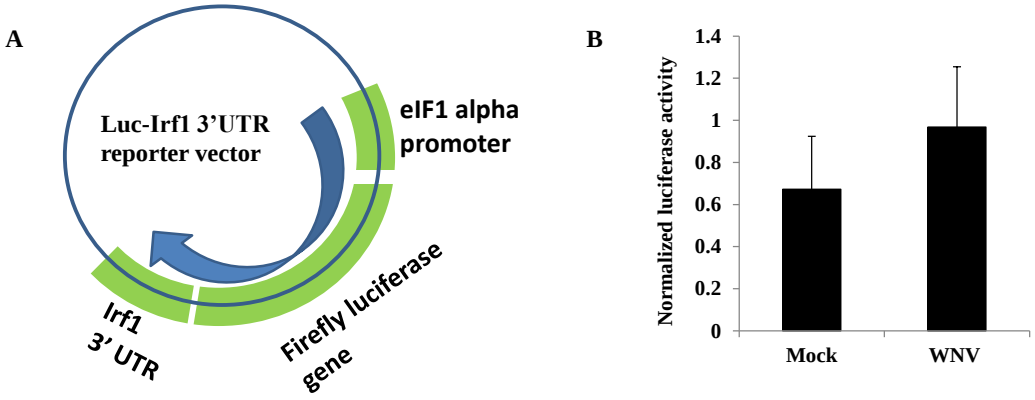


**Figure 4.4. Analysis of the effect of the Irf1 3'UTR on firefly luciferase reporter gene expression.** **(A)** The Irf1 3'UTR DNA fragment was cloned immediately downstream of the firefly luciferase reporter gene. **(B)** The Luc-Irf1 3'UTR or a control Luc vector were co-transfected with the pGL4.74 *Renilla* luciferase reporter construct into tC3H/He MEFs. Twenty four hours after transfection, cell lysates were collected and luciferase activity was measured using a luminometer. Firefly luciferase activity measured in triplicate was normalized to *Renilla* luciferase activity and the activity of the firefly luciferase control vector. The error bars represent SDM ($n$=3).

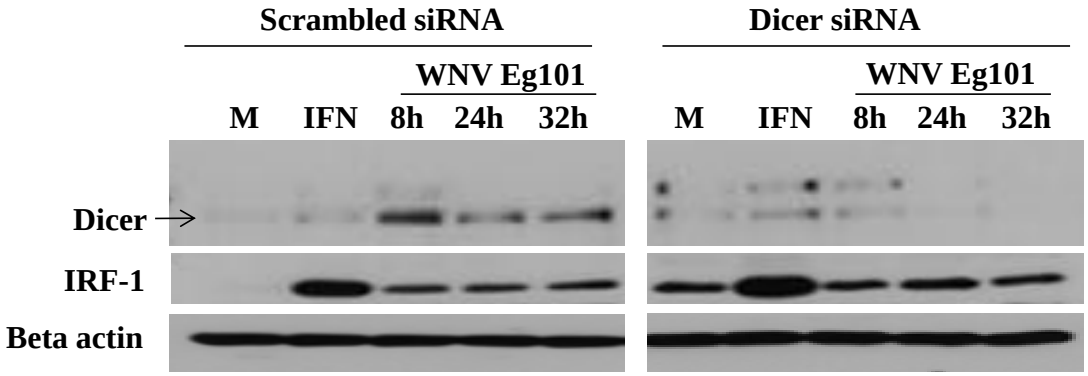


**Figure 4.5. Effect of dicer knock-down on the protein levels of IRF-1 in cells infected with WNV Eg101.** tC3H/He cells were transfected with dicer siRNA (20nM) or scrambled control siRNA (20nM) for 24 h and then infected with WNV Eg101 (MOI of 5) or treated with 1000 U/ml of IFN beta for 3 h. Cell lysates were collected and Western blotting was done using antibodies to the the indicated proteins. Actin was used as a loading control. The results shown are representative of two independent experiments.

### 4.5 Analysis of the effect of dicer knock-down on IRF-1 protein levels in WNV Eg101-infected.

Transcription specific suppression of translation can be mediated by the binding of miRNAs to the 3'UTRs of target mRNAs (Eulalio et al., 2008). As one means of investigating whether the suppression of IRF-1 translation during WNV infection is mediated by miRNAs, tC3H/He MEFs were transfected with nonspecific or dicer-specific siRNAs and 24 h later, the cells were infected with WNV Eg101 at a MOI of 5. In cells transfected with scrambled siRNA, dicer protein levels were almost undetectable in mock-treated cells (Fig. 4.5). An increase in dicer levels was observed in cells infected for 8 h. Although the levels remained above those in mock-infected cells throughout the infection, they decreased by 24 h after infection. In cells transfected with dicer specific siRNAs, efficient knock down of dicer was observed in infected cells. Analysis of IRF-1 protein levels in cells transfected with nonspecific siRNAs showed efficient IRF-1 protein production upon IFN stimulation and less efficient IRF-1 production in WNV infected cells. A small increase in IRF-1 protein levels in infected cells transfected with specific siRNAs was observed suggesting that miRNAs might be involved in regulating IRF-1 translational suppression. Interestingly, higher IRF-1 protein levels were observed in mock-infected cells that were transfected with dicer-specific siRNAs than in mock-treated cells that were transfected with nonspecific siRNAs. This result suggests that basal expression of IRF-1 in unstimulated cells may be regulated by miRNAs.

## DISCUSSION

Viruses depend entirely on the host translational machinery for synthesis of the viral proteins required for viral replication and the assembly of viral particles. Many viruses have evolved

mechanisms to control host protein synthesis in order to suppress the production of antiviral proteins. Since IRF-1 has demonstrated antiviral activity against WNV (Schoggins et al., 2011), it would be beneficial for the virus to suppress IRF-1 production. In this study analysis of the production of IRF-1 protein in transformed C3H/He cells confirmed the previously published observation that IRF-1 levels in WNV Eg101-infected primary C3H/He cells remained similar to those in mock-treated cells even though the Irf1 mRNA levels increased significantly in the infected cells. Since IRF-1 has a short half-life (about 30 m) (Watanabe et al., 1991), the levels of this protein would be expected to increase in the presence of the proteasomal inhibitor MG132. The levels of IRF-1 in cells treated with IFN beta and MG132 increased indicating that IFN beta induced increased translation of IRF-1. However, the levels of IRF-1 in mock-treated or WNV Eg101-infected cells increased only slightly after treatment with the inhibitor indicating that IRF-1 is constantly translated at a low basal level in control cells and that this does not change with infection.

Transcript specific suppression of translation can occur due to the binding of proteins to *cis*-acting elements in the 3'UTRs of target mRNAs (Kuersten and Goodwin, 2003; Mazumder et al., 2003; Abaza and Gebauer, 2008). In many instances, translational control is mediated by AREs located in the 3'UTR of mRNAs (Chen and Shyu, 1995). Analysis of the Irf1 3'UTR sequence with the ARE database program showed the presence of AREs and suggested the possibility that 3'UTR mediated regulation may be occurring in WNV Eg101-infected cells. Transcript specific translational inhibition can also be mediated by binding of miRNAs to regions of the 3'UTR of a target mRNA (Lytle et al., 2007). However, the Irf1 3'UTR did not suppress the translation of a reporter gene. The insertion of the Irf1 3'UTR downstream of a heterologous gene could have

altered mRNA folding which prevented protein binding to Irf1 3'UTR. Alternatively, the endogenous factors (proteins and/or miRNAs) may not be expressed at sufficient levels to suppress the translation of the overexpressed 3'UTRs. Additional experiments need to be done before the involvement of the Irf1 3'UTR in translational suppression can be ruled out.

Analysis of ISG mRNAs by real time qRT-PCR showed that the basal Irf1 mRNA levels in untreated cells are more than 100 fold higher than the mRNA levels of other ISGs including Oas1a, Oas1b and Irf7 (data not shown). The observation that relatively high basal levels of Irf1 mRNA are induced in untreated cells but protein levels are very low suggests the presence of a mechanism that tightly controls the amount of IRF-1 protein produced at basal levels. In contrast, when the cells are stimulated with type I IFN, Irf1 mRNA levels increase by tenfold or more and the translational suppression mechanism is overcome resulting in high IRF-1 protein levels. However, in the case of a WNV Eg101 infection, a similar increase in Irf1 mRNA levels does not result in relief of the translational suppression and low IRF-1 protein levels are observed. It appears that the WNV infection induces an increased suppression of IRF-1 translation to accommodate the increased Irf1 mRNA levels. One possibility is that Irf1 mRNA may be sequestered in P-bodies. It was previously shown that mRNAs with miRNAs bound to them are sequestered in P-bodies (Parker and Sheth, 2007). The preliminary results suggest that IRF-1 protein levels might be regulated by miRNAs. The observations that Irf1 mRNA levels in untreated cells are higher than those of other ISGs and that knock-down of dicer resulted in an increase in IRF-1 protein levels in mock-treated cells suggested that miRNAs might be involved in maintaining low basal levels of IRF-1. Since the use of siRNAs does not result in a complete

knock-down of expression, the experiments need to be repeated in cells that have dicer depleted through homologous recombination (Tan et al., 2009).

Although, it was previously reported that translation initiation can be also blocked through the binding of RNA binding proteins to cis-elements in the 5'UTR of a target message (Garfinkel and Katze, 1993; Damgaard and Lykke-Andersen, 2011), the required sites for this type of regulation were not predicted in the 5'UTR of Irf1. It is also unlikely that the translational suppression is mediated by miRNAs binding to the Irf1 5'UTR or ORF. Binding of miRNAs to these sites were shown to produce less effective silencing of translation (Lytle et al., 2007).

## MATERIALS AND METHODS

### 4.6 Cells and viruses.

SV40-transformed tC3H/He (tC3H/He) MEFs were grown in minimal essential medium (MEM) supplemented with 5% fetal bovine serum (FCS) and 10 μg/ml gentamicin. The cells were grown at 37°C in a 5% $CO_2$ atmosphere.

To prepare a lineage I WNV strain Eg101 stock, BHK cells were infected at a MOI of 0.1 and culture fluid was collected 32 h after infection. The virus was titered by plaque assay. The titer of the stock virus was ~ 1 x $10^8$ PFU/ml.

### 4.7 Cloning of the Irf1 3'UTR.

The Irf1 3'UTR was amplified by PCR using primers designed based on the GenBank sequence NM_008390.2. The sequence of the Irf1 forward primer was 5' ATCTAGATTTGGGTCTCTGACCCGTTCTTGCCCTCC 3', and that of the Irf1 reverse primer was 5' ATCTAGAGTAAACAACTTAAATTTTTATAAAAAGAC 3'. Each PCR reaction consisted of 100 ng of tC3H/He MEF genomic DNA, 200 μM dNTP mix, 0.2 μM of the specific

forward and reverse primers, 1X BD Advantage 2 Polymerase Mix and 1X BD Advantage 2 PCR Buffer (BD Biosciences Clontech). The amplified Irf1 3'UTR was cloned into the Topo-XL vector and the sequence was verified by sequencing. The DNA fragment was then subcloned into a modified pGL3 basic firefly luciferase reporter vector (Promega) containing the eIF1 alpha promoter using XbaI cloning sites to construct the Luc-Irf1 3'UTR construct.

### 4.8 Luciferase assay.

Luc-Irf1 3'UTR firefly luciferase reporter plasmid DNA or control firefly luciferase reporter plasmid (1μg) and pGL4.74 *Renilla* luciferase reporter construct DNA (20 ng) (Promega) were added to a solution containing 3 μl of FuGENE 6 (Roche Applied Science) and 97 μl of serum free media. Cells at about 70% confluency were transfected and then incubated at 37°C for 24 h. Next, the cells were infected with WNV Eg101 at a MOI of 5 for 24 h and then harvested according to the Dual Luciferase Reporter Assay System (Promega) protocol. Firefly and *Renilla* luciferase activities were separately measured using a luminometer (LMax $II^{384}$, Molecular Devices). The firefly luciferase activity obtained for each sample was divided by the *Renilla* luciferase activity and the results were then normalized to the results obtained with a control construct without an Irf1 3'UTR.

### 4.9 Quantification of mRNA levels.

Real-time qRT-PCR analyses of mouse Irf1 gene expression were performed using an Applied Biosystems 7500 Sequence Detection System with Applied Biosystems Assays-on-Demand primer and fluorogenic TaqMan FAM/MGB probe mix Mn01288580_m1 Ifr1 and a One-Step RT-PCR Master Mix Reagent Kit (Applied Biosystems) according to the manufacturers' protocol. The reaction was set up as followes: reverse transcription at 48°C for 30 m, activation at 95°C for 10 m, denaturation at 95°C for 15 s, and annealing/extension at 60°C for 1 m (cycle

repeated 40 times). Each value was normalized to that of GAPDH detected using TaqMan primers and probe (Applied Biosystems). The values are shown as the relative fold change compared to the mock-infected calibrator sample in RQUs..

### 4.10 RT-PCR analysis of Irf1 mRNA splice variants.

Analysis of Irf1 splice variants was done using the SuperScript III One-Step RT-PCR system with a Platinum Ta2 DNA polymerase kit (Invitrogen). Total RNA was extracted from tC3H/He MEFs that were mock- or WNV Eg101-infected (MOI of 5) for 12 or 24 h or treated with 1000 U/ml of murine IFN beta. Each reaction was set up according to the manufacturer's protocol and contained 0.5 μg of RNA per 50 μl of reaction volume. The Irf1 forward primer: 5' AATCTTTCGCTTCGTGCGCGCATCGCG 3' and reverse primer: 5' TGATGGAGTCCATATTCTTCATCTCCG 3' were complementary to the terminal sequences of the IRF1 mRNA and were designed based on the GenBank sequence NM_008390. These primers amplified the entire mRNA. The PCR products were resolved on a 1% agarose gel.

### 4.11 Western blotting.

tC3H/He cell monolayers were washed with ice-cold PBS and then scraped into radioimmunoprecipitation assay buffer [1x PBS, 1% Nonidet P-40, 0.5% sodium deoxycholate, and 0.1% SDS containing Halt Protease and Phosphatase Inhibitor Single-Use Cocktail (100X) (Thermo Scientific)]. The proteins were separated by 7.5% or 10% SDS-polyacrylamide gel electrophoresis (PAGE) and then electrophoretically transferred to a nitrocellulose membrane. The membrane was blocked with 1x Tris-buffered saline pH 8 containing 5% dry milk and 0.1% Tween-20 for 1 h at 22°C and then incubated with a rabbit polyclonal primary antibody specific for IRF-1 or dicer (Santa Cruz Biotechnology) or beta-actin (Abcam) overnight at 4°C in the

presence of blocking buffer. The blots were then incubated with anti-rabbit secondary antibody conjugated with horseradish peroxidase (Santa Cruz Biotechnology) or anti-mouse secondary antibody conjugated with horseradish peroxidase (Cell Signaling) for 1 h at 22°C. The proteins were detected using a Super-Signal West Pico detection kit (Thermo Scientific) according to the manufacturer's instructions.

### 4.12 Dicer knock-down using RNAi.

tC3H/He cells at about 70% confluency were transfected with dicer siRNA (20 nM) or scrambled siRNA (20 nM) (Santa Cruz Biotechnology) using HiPerFect transfection reagent (Qiagen) according to the manufacturer's protocol. Twenty four hours after transfection, the cells were mock- or, WNV Eg101-infected (MOI of 5) for the indicated times or treated with 1000 U/ml of IFN beta for 3 h. Cell lysates were collected for Western blot analysis.

# CHAPTER 5

## 5 CONCLUSIONS AND FUTURE DIRECTIONS

The majority of WNV infections in humans are asymptomatic. However, in about 1 in 150 infected humans, the infection can induce severe disease (Petersen et al., 2003). Since no antiviral therapies or vaccines have been developed so far to treat or prevent infections it is important to gain a better understanding of WNV-host interactions to facilitate future development of effective treatments. In this study, we analyzed the the strategies utilized by the host cell to counteract virus-mediated blockage of the the type 1 IFN signaling pathway though upregulation of ISGs via alternative mechanisms as well as strategies used by WNV Eg101 to block the expression of an antiviral protein.

### 5.1 Type I IFN mediated induction of a subset of ISGs in a STAT1 independent manner.

Although ISGs are classically induced by type I IFN through the STAT1/STAT2/IRF-9 trimetric complex (Pestka et al., 2004), the results of this and other studies suggest that alternative TF complexes can also activate the expression of some ISGs in IFN-treated cells (Ousman et al., 2005; Sarkis et al., 2006; George et al., 2008). The observation that the antiviral ISG Oas1b can be induced by IFN in a STAT1-independent manner indicates that alternative regulatory complexes can be utilized by the cell to mount an antiviral immune response. The importance of a STAT2-dependent but STAT-1-independent response to viral infection was previously reported (Hahm et al., 2005; Perry et al., 2011). However, the components of the complex in the STAT1-independent activation of gene expression by IFN is currently not known. IRF-9 was previously shown to be unable to activate gene expression by binding to the ISRE alone while either an IRF-9/STAT2 fusion protein or an IRF-9/STAT2 protein complex efficiently activated ISRE-

driven transcription (Kraus et al., 2003; Lou et al., 2009). However, it is currently not known whether additional factors are also involved in the STAT1-independent upregulation of ISGs by type I IFN. To determine whether the STAT2/IRF-9 complex interacts with additional proteins to induce STAT1 independent transcription, immunoprecipitation experiments in STAT1-/- MEFs treated with IFN beta could be done. Proteins immunoprecipitated with STAT2 antibody could be identified by mass spectrometry. It is expected that IRF-9 would be immunoprecipitated with STAT2 in cells treated with type I IFN. If IRF-9 is the only protein immunoprecipitated with STAT2 from WNV infected cells, this would suggest that the STAT2/IRF-9 complex is sufficient for the induction of STAT1-independent upregulation of some ISGs by type I IFN. If additional factors are identified, it would be interesting to determine the exact DNA motifs required for the binding of the alternative complex. This could be achieved by EMSA using nuclear extracts from STAT1-/- MEFs and DNA probes consisting of labeled wild type or mutated promoter fragments.

## 5.2 WNV Eg101 mediated blockage of STAT1 and STAT2 translocation to the nucleus of infected MEFs.

Since the IFN pathway plays a critical role in the induction of innate immune response to infection it is an attractive target of many viruses. The results of this and other studies showed that flaviviruses have evolved several mechanisms to effectively block the type I IFN signaling pathway (Munoz-Jordan et al., 2003; Lin et al., 2004; Best et al., 2005; Guo et al., 2005; Ho et al., 2005; Jones et al., 2005; Liu et al., 2005; Munoz-Jordan et al., 2005; Keller et al., 2006; Mackenzie et al., 2007; Mazzon et al., 2009; Laurent-Rolle et al., 2010). The results of this study showed that the infection of MEFs with lineage 1 WNV strains Eg101 and NY99 induces phosphorylation of STAT1 and STAT2 but blocks the translocation of these TFs to the nucleus.

In contrast, lineage I WNV strain TX02 infection of human cells (Keller et al., 2006) and WNV Eg101 and NY99 infection of human or monkey cells (Scherbik, Pulit-Penaloza and Brinton, unpublished data) were shown to block the phosphorylation of STAT1 and STAT2. These results indicate that nuclear translocation of STAT1 and STAT2 in primate cells infected by WNV is blocked by suppression of STAT phosphorylation required for nuclear translocation while in murine cells, the blockage occurs at the level of transport of phosphorylated STAT proteins to the nucleus. Since the murine model is commonly used to study WNV-host interaction, it is important to understand the differences in the response to viral infection between murine and human cells. Species specific mechanisms of suppression of STAT signaling have been previously reported for dengue virus. The dengue virus NS5 protein was shown to bind and target for degradation human but not murine STAT2 (Ashour et al., 2010). Mice are not a natural host for dengue virus infections.

The mechanism by which WNV Eg101 blocks STAT1 and STAT 2 translocation to the nucleus in MEFs is currently not known. One possibility is that the blockage might be due to interference with the ISGF3 complex-importin interaction. ISGF3 binds importin alpha 5 (also known an karyopherin alpha 1) which recruits importin beta 1 (karyopherin beta 1). This allows the passage of the ISGF3 complex through the nuclear pore (McBride et al., 2002; Reich, 2007). Suppression of STAT1 translocation to the nucleus though blockage of the interaction with importins was previously reported for Ebola (Reid et al., 2006) and SARS (Frieman et al., 2007) viruses. Immunoprecipitation experiments could be done to pull down STAT1 or STAT2 proteins and assay for the binding of importin alpha 5. It is expected that this interaction would be observed in cells treated with IFN beta but not in cells infected with WNV Eg101. Alternatively, pull down experiments could be done to determine whether STAT1, STAT2 and

IRF-9 interact to form the trimetric ISGF3 complex in WNV Eg101-infected MEFs. It is possible that the lack of nuclear translocation is due to inhibition of the assembly of the ISGF3 complex in infected cells.. If this is the case, STAT1, STAT2 and IRF-9 would immunoprecipitate in samples from cells treated with IFN beta but not in samples from WNV Eg101-infected cells.

### 5.3 IFN-independent upregulation of ISGs in MEFs infected with WNV Eg101.

Despite the fact that neither phospho-STAT1 nor phopsho-STAT2 could translocate to the nucleus in MEFs infected with WNV Eg101, efficient induction of ISGs was observed (Scherbik et al., 2007) suggesting that the host cell can utilize alternative mechanism(s) to activate ISG expression. IFN-independent upregulation of some ISGs such as ISG15 and ISG54 can be mediated by the activation of IRF-3 (Nakaya et al., 2001; Grandvaux et al., 2002; Andersen et al., 2008). However it is still not clear how IRF-3 independent ISGs such as Oas1a, Oas1b, Irf7 and Irf1 are upregulated during infection. Although Oas1a and Irf7 were previously classified as ISGs that could only be induced by type I IFN and ISGF3 complex (Nakaya et al., 2001), the results of our study clearly show that these genes, as well as Oas1b and Irf1, are regulated in a type I-IFN- and IRF-3- independent manner in WNV Eg101-infected MEFs. Either IRF-3 or IRF-7 are needed to maintain the upregulation of these genes in infected cells but are not needed for the initial upreguation. Although the upregulation of Oas1a, Oas1b and Irf7 is independent of STAT1 and STAT2, the results of this study suggest that IRF-9 is required for upregulation in WNV infected cells. To confirm that IRF-9 is the key regulatory factor, IRF-3/9-/- MEFS could reconstituted with IRF-9 and/or IRF-3 TFs and the effect on the expression in Oas1a, Oas1b and Irf7 after WNV infection could be analyzed. Since these genes are efficiently expressed in IRF-3-/- MEFs, it would be expected that similar results are observed in IRF-3/9-/- MEFs overexpressing IRF-9. If IRF-9 is the key regulator of Oas1a, Oas1b and Irf7 expression in

MEFS infected with WNV Eg101, then no or low levels of expression of Oas1a, Oas1b and Irf7 should be observed in IRF-3/9-/- MEFs overexpressing IRF-3. A possible problem with this experiment could be that the expression of IRF-3 or IRF-9 from the expression vector would be regulated by a heterologous promoter resulting in inadequate levels of protein expression. The best means of testing the importance of IRF-9 in upregulation of these ISGs would be by using IRF-9-/- MEFs.

If IRF-9 is confirmed to be the key regulator of IFN- and IRF-3-independent ISG expression in WNV Eg101-infected cells, the factors that interact with IRF-9 could be analyzed next. Although our preliminary data showed that IRF-9 is abundant in the nucleus in WNV Eg101-infected MEFs (data not shown), it cannot transactivate ISG expression by binding alone to an ISRE (Kraus et al., 2003). To identify the protein(s) that interact with IRF-9 in the absence of STAT1 and STAT2 in WNV Eg101-infected cells, proteins immunoprecipitated with IRF-9 from infected IFN alpha/beta R-/- and/or STAT2-/- cells could be analyzed by mass spectrometry. The relevance of identified candidate TF(s) for the upregulation of ISGs in infected cells could be then tested by RNAi knockdown or in MEFs from TF knockout mice, if available. ChIP assays could be done to confirm that an identified TF(s) binds to ISG promoters in WNV Eg101-infected IFN alpha/beta R -/- MEFs and/or STAT2-/- MEFs.

Interestingly, the upregulation of Irf1 by WNV Eg101 infection was shown not to depend on any of the IRFs tested. In contrast, the preliminary results suggested that the p38 MAPK signaling pathway and NF-kappa B may be involved in the regulation of Irf1 expression in infected cells. To confirm these results the expression of Irf1 could be analyzed in infected cells stably transfected with a p38 dominant negative construct or in p38 alpha -/- and p38 beta -/- MEFs,

which are available. Since p38 and NF-kappa B drugs had similar effects on the upregulation of the Oas1b and Irf1 genes by WNV Eg101 infection, it is possible that NF-kappa B is activated by p38 in infected cells. The involvement of p38 in the activation of NF-kappa B was previously reported (Maulik et al., 1998; Vanden Berghe et al., 1998; Liang and Gardner, 1999; Saha et al., 2007). Unpublished data from our lab showed that NF-kappa B is activated in WNV Eg101-infected MEFs. Whether WNV Eg101 infection activates NF-kappa B in p38 alpha -/- and p38 beta -/- MEFs could be tested. To directly determine whether NF-kappa B is involved in regulation of Irf1 in cells infected with WNV Eg101, gene expression could be analyzed in mock and WNV-infected IKK alpha-/- and IKKbeta-/- MEFs to determine whether the non-canonical or classical NF-kappaB pathway, respectively, is involved (Massa et al., 2005). If Irf-1gene expression is reduced when the classical pathway is knocked out, the activation of Irf1 could next be tested in c-Rel-/- MEFs to determine whether this NF-kappa B subunit is involved.

### 5.4 WNV Eg101-mediated translational suppression of a subset of ISGs

Another means by which viruses can suppress the induction of the antiviral state is through blockage of the expression of antiviral proteins. The results of this and a previous study (Scherbik et al., 2007) showed that although the transcription of a subset of antiviral genes, including Irf1, caspase 4 and caspase 12, is efficiently upregulated at 24 and 32 h after WNV Eg101 infection, the translation of these transcripts is suppressed. The results of this study show that low IRF-1 protein levels are not due to a virus infection induced increase in proteasomal degradation and also are not due to alternative splicing. Similar results were also observed for caspase 4 and and caspase 12 (data not shown). However, preliminary results in cells with dicer knocked down by transient transfection of specific siRNAs suggested that IRF-1 translation may be regulated to some extent by miRNAs. However, since complete knock down of a protein

cannot be achieved with RNAi, additional studies are needed. To confirm the results, dicer(+/Lox-P) and dicer(Lox-P/Lox-P) cells will be treated with 50 nM 4-hydroxytamoxifen (4-OHT) to induce recombination and deplete dicer (Tan et al., 2009). Preliminary microarray analyses done by our lab showed that miR-483 and miR-1895 expression was downregulated in IFN beta-treated cells but upregulated WNV-infected MEFs (data not shown) suggesting that these miRNAs could potentially be involved in the regulation of IRF-1 protein expression. However, according to the miRDB.org database, neither of these miRNAs target Irf1 or caspase 4 or caspase 11. The miRNA microarray data and the bioinformatics predictions suggest that if miRNAs are involved in transaltional suppression of these ISGs, they are involved indirectly through targeting proteins involved in regulating IRF-1 translation.

Analysis of the Irf1 3'UTR with the ARE database search program revealed the presence of AREs and supported the possibility that this type of regulation occurs in WNV Eg101-infected cells. Cell proteins binding to ARE containing regions of the Irf1 3'UTR could be analyzed by EMSA and UV-induced crosslinking assays done with cytoplasmic extracts from WNV Eg101 IFN alpha/beta R-/- MEFs. If no binding is observed with the ARE regions, other regions of the 3'UTRs could be subsequently tested. An RNA affinity column could be used to enrich for proteins interacting with labeled RNA. The eluted proteins could be separated by SDS-PAGE and identified by mass spectrometry. Candidate proteins could be then analyzed for functional relevance by RNAi.

**SIGNIFICANCE**

Overall the results of this study add to the understanding of virus-host cell interactions. Analysis of the strategies utilized by host cells to overcome virus-induced suppression of antiviral protein expression furthers the general understanding of WNV-host interactions and provides evidence

about alternative signaling pathways. This study also increases general knowledge about the diverse strategies that viruses have evolved to evade host cell antiviral responses. Further study of these mechanisms will provide more detailed insights about the alternative mechanisms that regulate gene transcription in infected cells and facilitate establishment of an effective antiviral state. The importance of this study is based on the fact that many flaviviruses, such as JEV, TBEV and dengue virus cause significant human morbidity and mortality in many geographic regions of the world. Because there are no effective antiviral therapies, the cost of medical care provided for individuals that develop severe disease is high. The information gained from this study is expected to ultimately aid in the development of antiviral strategies that target WNV and possibly other flaviviruses.

**REFERENCES**

Abaza, I.Gebauer, F., 2008. Trading translation with RNA-binding proteins. Rna. 14, 404-409.

Akira, S., 2009. Pathogen recognition by innate immunity and its signaling. Proc Jpn Acad Ser B Phys Biol Sci. 85, 143-156.

Alexopoulou, L., Holt, A. C., Medzhitov, R.Flavell, R. A., 2001. Recognition of double-stranded RNA and activation of NF-kappaB by Toll-like receptor 3. Nature. 413, 732-738.

Anandalakshmi, R., Pruss, G. J., Ge, X., Marathe, R., Mallory, A. C., Smith, T. H.Vance, V. B., 1998. A viral suppressor of gene silencing in plants. Proc Natl Acad Sci U S A. 95, 13079-13084.

Andersen, J., VanScoy, S., Cheng, T. F., Gomez, D.Reich, N. C., 2008. IRF-3-dependent and augmented target genes during viral infection. Genes Immun. 9, 168-175.

Ashour, J., Morrison, J., Laurent-Rolle, M., Belicha-Villanueva, A., Plumlee, C. R., Bernal-Rubio, D., Williams, K. L., Harris, E., Fernandez-Sesma, A., Schindler, C.Garcia-Sastre, A., 2010. Mouse STAT2 restricts early dengue virus replication. Cell Host Microbe. 8, 410-421.

Barnes, B. J., Moore, P. A.Pitha, P. M., 2001. Virus-specific activation of a novel interferon regulatory factor, IRF-5, results in the induction of distinct interferon alpha genes. J Biol Chem. 276, 23382-23390.

Barnes, B. J., Richards, J., Mancl, M., Hanash, S., Beretta, L.Pitha, P. M., 2004. Global and distinct targets of IRF-5 and IRF-7 during innate response to viral infection. J Biol Chem. 279, 45194-45207.

Barral, P. M., Sarkar, D., Su, Z. Z., Barber, G. N., DeSalle, R., Racaniello, V. R.Fisher, P. B., 2009. Functions of the cytoplasmic RNA sensors RIG-I and MDA-5: key regulators of innate immunity. Pharmacol Ther. 124, 219-234.

Bartee, E.McFadden, G., 2009. Human cancer cells have specifically lost the ability to induce the synergistic state caused by tumor necrosis factor plus interferon-beta. Cytokine. 47, 199-205.

Basagoudanavar, S. H., Thapa, R. J., Nogusa, S., Wang, J., Beg, A. A.Balachandran, S., 2011. Distinct roles for the NF-kappa B RelA subunit during antiviral innate immune responses. J Virol. 85, 2599-2610.

Beasley, D. W., Li, L., Suderman, M. T.Barrett, A. D., 2002. Mouse neuroinvasive phenotype of West Nile virus strains varies depending upon virus genotype. Virology. 296, 17-23.

Bellon, S., Fitzgibbon, M. J., Fox, T., Hsiao, H. M.Wilson, K. P., 1999. The structure of phosphorylated p38gamma is monomeric and reveals a conserved activation-loop conformation. Structure. 7, 1057-1065.

Bentwich, I., 2005. Prediction and validation of microRNAs and their targets. FEBS Lett. 579, 5904-5910.

Best, S. M., Morris, K. L., Shannon, J. G., Robertson, S. J., Mitzel, D. N., Park, G. S., Boer, E., Wolfinbarger, J. B.Bloom, M. E., 2005. Inhibition of interferon-stimulated JAK-STAT signaling by a tick-borne flavivirus and identification of NS5 as an interferon antagonist. J Virol. 79, 12828-12839.

Black, B. L., Lu, J.Olson, E. N., 1997. The MEF2A 3' untranslated region functions as a cis-acting translational repressor. Mol Cell Biol. 17, 2756-2763.

Bluyssen, H. A.Levy, D. E., 1997. Stat2 is a transcriptional activator that requires sequence-specific contacts provided by stat1 and p48 for stable interaction with DNA. J Biol Chem. 272, 4600-4605.

Bluyssen, H. A., Muzaffar, R., Vlieststra, R. J., van der Made, A. C., Leung, S., Stark, G. R., Kerr, I. M., Trapman, J.Levy, D. E., 1995. Combinatorial association and abundance of components of interferon-stimulated gene factor 3 dictate the selectivity of interferon responses. Proc Natl Acad Sci U S A. 92, 5645-5649.

Bonnevie-Nielsen, V., Field, L. L., Lu, S., Zheng, D. J., Li, M., Martensen, P. M., Nielsen, T. B., Beck-Nielsen, H., Lau, Y. L.Pociot, F., 2005. Variation in antiviral 2',5'-oligoadenylate synthetase (2'5'AS) enzyme activity is controlled by a single-nucleotide polymorphism at a splice-acceptor site in the OAS1 gene. Am J Hum Genet. 76, 623-633.

Brandes, C., Plautz, J. D., Stanewsky, R., Jamison, C. F., Straume, M., Wood, K. V., Kay, S. A.Hall, J. C., 1996. Novel features of drosophila period Transcription revealed by real-time luciferase reporting. Neuron. 16, 687-692.

Brigneti, G., Voinnet, O., Li, W. X., Ji, L. H., Ding, S. W.Baulcombe, D. C., 1998. Viral pathogenicity determinants are suppressors of transgene silencing in Nicotiana benthamiana. EMBO J. 17, 6739-6746.

Brinton, M. A., 2002. The molecular biology of West Nile Virus: a new invader of the western hemisphere. Annu Rev Microbiol. 56, 371-402.

Cameron, J. E., Yin, Q., Fewell, C., Lacey, M., McBride, J., Wang, X., Lin, Z., Schaefer, B. C.Flemington, E. K., 2008. Epstein-Barr virus latent membrane protein 1 induces cellular MicroRNA miR-146a, a modulator of lymphocyte signaling pathways. J Virol. 82, 1946-1958.

Chang, L.Karin, M., 2001. Mammalian MAP kinase signalling cascades. Nature. 410, 37-40.

Chang, T. H., Liao, C. L.Lin, Y. L., 2006. Flavivirus induces interferon-beta gene expression through a pathway involving RIG-I-dependent IRF-3 and PI3K-dependent NF-kappaB activation. Microbes Infect. 8, 157-171.

Chen, C. Y.Shyu, A. B., 1995. AU-rich elements: characterization and importance in mRNA degradation. Trends Biochem Sci. 20, 465-470.

Chen, P. J., Wei, C. C., Wang, C., Chen, F. W., Hsu, Y. H.Chang, M. S., 2006. Promoter analysis of interleukin 19. Biochem Biophys Res Commun. 344, 713-720.

Chu, J. J.Ng, M. L., 2004. Infectious entry of West Nile virus occurs through a clathrin-mediated endocytic pathway. J Virol. 78, 10543-10555.

Chu, P. W.Westaway, E. G., 1985. Replication strategy of Kunjin virus: evidence for recycling role of replicative form RNA as template in semiconservative and asymmetric replication. Virology. 140, 68-79.

Clyde, K.Glaunsinger, B. A., 2010. Getting the message direct manipulation of host mRNA accumulation during gammaherpesvirus lytic infection. Adv Virus Res. 78, 1-42.

Currie, R. A., 1998. NF-Y is associated with the histone acetyltransferases GCN5 and P/CAF. J Biol Chem. 273, 1430-1434.

Daffis, S., Samuel, M. A., Keller, B. C., Gale, M., Jr.Diamond, M. S., 2007. Cell-specific IRF-3 responses protect against West Nile virus infection by interferon-dependent and -independent mechanisms. PLoS Pathog. 3, e106.

Daffis, S., Samuel, M. A., Suthar, M. S., Gale, M., Jr.Diamond, M. S., 2008. Toll-like receptor 3 has a protective role against West Nile virus infection. J Virol. 82, 10349-10358.

Daffis, S., Samuel, M. A., Suthar, M. S., Keller, B. C., Gale, M., Jr.Diamond, M. S., 2008. Interferon regulatory factor IRF-7 induces the antiviral alpha interferon response and protects against lethal West Nile virus infection. J Virol. 82, 8465-8475.

Daffis, S., Suthar, M. S., Szretter, K. J., Gale, M., Jr.Diamond, M. S., 2009. Induction of IFN-beta and the innate antiviral response in myeloid cells occurs through an IPS-1-dependent signal that does not require IRF-3 and IRF-7. PLoS Pathog. 5, e1000607.

Damgaard, C. K.Lykke-Andersen, J., 2011. Translational coregulation of 5'TOP mRNAs by TIA-1 and TIAR. Genes Dev. 25, 2057-2068.

Darnell, J. E., Jr., 1997. STATs and gene regulation. Science. 277, 1630-1635.

Darnell, J. E., Jr., Kerr, I. M.Stark, G. R., 1994. Jak-STAT pathways and transcriptional activation in response to IFNs and other extracellular signaling proteins. Science. 264, 1415-1421.

Davis, R. J., 2000. Signal transduction by the JNK group of MAP kinases. Cell. 103, 239-252.

de Weerd, N. A., Samarajiwa, S. A.Hertzog, P. J., 2007. Type I interferon receptors: biochemistry and biological functions. J Biol Chem. 282, 20053-20057.

Decker, T., Kovarik, P.Meinke, A., 1997. GAS elements: a few nucleotides with a major impact on cytokine-induced gene expression. J Interferon Cytokine Res. 17, 121-134.

Decker, T., Lew, D. J., Mirkovitch, J.Darnell, J. E., Jr., 1991. Cytoplasmic activation of GAF, an IFN-gamma-regulated DNA-binding factor. EMBO J. 10, 927-932.

DeWitte-Orr, S. J., Mehta, D. R., Collins, S. E., Suthar, M. S., Gale, M., Jr.Mossman, K. L., 2009. Long double-stranded RNA induces an antiviral response independent of IFN regulatory factor 3, IFN-beta promoter stimulator 1, and IFN. J Immunol. 183, 6545-6553.

Diamond, M. S., 2009. Mechanisms of evasion of the type I interferon antiviral response by flaviviruses. J Interferon Cytokine Res. 29, 521-530.

Diebold, S. S., Kaisho, T., Hemmi, H., Akira, S.Reis e Sousa, C., 2004. Innate antiviral responses by means of TLR7-mediated recognition of single-stranded RNA. Science. 303, 1529-1531.

Dolfini, D., Zambelli, F., Pavesi, G.Mantovani, R., 2009. A perspective of promoter architecture from the CCAAT box. Cell Cycle. 8, 4127-4137.

Ehret, G. B., Reichenbach, P., Schindler, U., Horvath, C. M., Fritz, S., Nabholz, M.Bucher, P., 2001. DNA binding specificity of different STAT proteins. Comparison of in vitro specificity with natural target sites. J Biol Chem. 276, 6675-6688.

Elbahesh, H., Jha, B. K., Silverman, R. H., Scherbik, S. V.Brinton, M. A., 2011. The Flvr-encoded murine oligoadenylate synthetase 1b (Oas1b) suppresses 2-5A synthesis in intact cells. Virology. 409, 262-270.

Elbahesh, H., Scherbik, S. V.Brinton, M. A., 2011. West Nile virus infection does not induce PKR activation in rodent cells. Virology. 421, 51-60.

Elco, C. P., Guenther, J. M., Williams, B. R.Sen, G. C., 2005. Analysis of genes induced by Sendai virus infection of mutant cell lines reveals essential roles of interferon regulatory factor 3, NF-kappaB, and interferon but not toll-like receptor 3. J Virol. 79, 3920-3929.

Eskildsen, S., Hartmann, R., Kjeldgaard, N. O.Justesen, J., 2002. Gene structure of the murine 2'-5'-oligoadenylate synthetase family. Cell Mol Life Sci. 59, 1212-1222.

Eskildsen, S., Justesen, J., Schierup, M. H.Hartmann, R., 2003. Characterization of the 2'-5'-oligoadenylate synthetase ubiquitin-like family. Nucleic Acids Res. 31, 3166-3173.

Eulalio, A., Huntzinger, E.Izaurralde, E., 2008. Getting to the root of miRNA-mediated gene silencing. Cell. 132, 9-14.

Evans, J. D., Crown, R. A., Sohn, J. A.Seeger, C., 2011. West Nile virus infection induces depletion of IFNAR1 protein levels. Viral Immunol. 24, 253-263.

Faria, P. A., Chakraborty, P., Levay, A., Barber, G. N., Ezelle, H. J., Enninga, J., Arana, C., van Deursen, J.Fontoura, B. M., 2005. VSV disrupts the Rae1/mrnp41 mRNA nuclear export pathway. Mol Cell. 17, 93-102.

Feng, P., Everly, D. N., Jr.Read, G. S., 2005. mRNA decay during herpes simplex virus (HSV) infections: protein-protein interactions involving the HSV virion host shutoff protein and translation factors eIF4H and eIF4A. J Virol. 79, 9651-9664.

Fensterl, V.Sen, G. C., 2009. Interferons and viral infections. Biofactors. 35, 14-20.

Fitzgerald, K. A., McWhirter, S. M., Faia, K. L., Rowe, D. C., Latz, E., Golenbock, D. T., Coyle, A. J., Liao, S. M.Maniatis, T., 2003. IKKepsilon and TBK1 are essential components of the IRF3 signaling pathway. Nat Immunol. 4, 491-496.

Floyd-Smith, G., Wang, Q.Sen, G. C., 1999. Transcriptional induction of the p69 isoform of 2',5'-oligoadenylate synthetase by interferon-beta and interferon-gamma involves three regulatory elements and interferon-stimulated gene factor 3. Exp Cell Res. 246, 138-147.

Fredericksen, B. L.Gale, M., Jr., 2006. West Nile virus evades activation of interferon regulatory factor 3 through RIG-I-dependent and -independent pathways without antagonizing host defense signaling. J Virol. 80, 2913-2923.

Fredericksen, B. L., Keller, B. C., Fornek, J., Katze, M. G.Gale, M., Jr., 2008. Establishment and maintenance of the innate antiviral response to West Nile Virus involves both RIG-I and MDA5 signaling through IPS-1. J Virol. 82, 609-616.

Fredericksen, B. L., Smith, M., Katze, M. G., Shi, P. Y.Gale, M., Jr., 2004. The host response to West Nile Virus infection limits viral spread through the activation of the interferon regulatory factor 3 pathway. J Virol. 78, 7737-7747.

Frieman, M., Yount, B., Heise, M., Kopecky-Bromberg, S. A., Palese, P.Baric, R. S., 2007. Severe acute respiratory syndrome coronavirus ORF6 antagonizes STAT1 function by sequestering nuclear import factors on the rough endoplasmic reticulum/Golgi membrane. J Virol. 81, 9812-9824.

Fu, L.Benchimol, S., 1997. Participation of the human p53 3'UTR in translational repression and activation following gamma-irradiation. Embo J. 16, 4117-4125.

Garban, H. J.Bonavida, B., 2001. Nitric oxide inhibits the transcription repressor Yin-Yang 1 binding activity at the silencer region of the Fas promoter: a pivotal role for nitric oxide in the up-regulation of Fas gene expression in human tumor cells. J Immunol. 167, 75-81.

Garfinkel, M. S.Katze, M. G., 1993. Translational control by influenza virus. Selective translation is mediated by sequences within the viral mRNA 5'-untranslated region. J Biol Chem. 268, 22223-22226.

George, C. X., Das, S.Samuel, C. E., 2008. Organization of the mouse RNA-specific adenosine deaminase Adar1 gene 5'-region and demonstration of STAT1-independent, STAT2-dependent transcriptional activation by interferon. Virology. 380, 338-343.

Gillespie, L. K., Hoenen, A., Morgan, G.Mackenzie, J. M., 2010. The endoplasmic reticulum provides the membrane platform for biogenesis of the flavivirus replication complex. J Virol. 84, 10438-10447.

Glaunsinger, B.Ganem, D., 2004. Lytic KSHV infection inhibits host gene expression by accelerating global mRNA turnover. Mol Cell. 13, 713-723.

Gottwein, E.Cullen, B. R., 2008. Viral and cellular microRNAs as determinants of viral pathogenesis and immunity. Cell Host Microbe. 3, 375-387.

Grandvaux, N., Servant, M. J., tenOever, B., Sen, G. C., Balachandran, S., Barber, G. N., Lin, R.Hiscott, J., 2002. Transcriptional profiling of interferon regulatory factor 3 target genes: direct involvement in the regulation of interferon-stimulated genes. J Virol. 76, 5532-5539.

Gray, N. K.Hentze, M. W., 1994. Iron regulatory protein prevents binding of the 43S translation pre-initiation complex to ferritin and eALAS mRNAs. Embo J. 13, 3882-3891.

Grilli, M., Chiu, J. J.Lenardo, M. J., 1993. NF-kappa B and Rel: participants in a multiform transcriptional regulatory system. Int Rev Cytol. 143, 1-62.

Grundhoff, A.Sullivan, C. S., 2011. Virus-encoded microRNAs. Virology. 411, 325-343.

Guo, J. T., Hayashi, J.Seeger, C., 2005. West Nile virus inhibits the signal transduction pathway of alpha interferon. J Virol. 79, 1343-1350.

Guo, Z., Garg, S., Hill, K. M., Jayashankar, L., Mooney, M. R., Hoelscher, M., Katz, J. M., Boss, J. M.Sambhara, S., 2005. A distal regulatory region is required for constitutive and IFN-beta-induced expression of murine TLR9 gene. J Immunol. 175, 7407-7418.

Hahm, B., Trifilo, M. J., Zuniga, E. I.Oldstone, M. B., 2005. Viruses evade the immune system through type I interferon-mediated STAT2-dependent, but STAT1-independent, signaling. Immunity. 22, 247-257.

Hamilton, A. J.Baulcombe, D. C., 1999. A species of small antisense RNA in posttranscriptional gene silencing in plants. Science. 286, 950-952.

Harada, H., Fujita, T., Miyamoto, M., Kimura, Y., Maruyama, M., Furia, A., Miyata, T.Taniguchi, T., 1989. Structurally similar but functionally distinct factors, IRF-1 and IRF-2, bind to the same regulatory elements of IFN and IFN-inducible genes. Cell. 58, 729-739.

Harada, H., Kondo, T., Ogawa, S., Tamura, T., Kitagawa, M., Tanaka, N., Lamphier, M. S., Hirai, H.Taniguchi, T., 1994. Accelerated exon skipping of IRF-1 mRNA in human myelodysplasia/leukemia; a possible mechanism of tumor suppressor inactivation. Oncogene. 9, 3313-3320.

Harada, H., Takahashi, E., Itoh, S., Harada, K., Hori, T. A.Taniguchi, T., 1994. Structure and regulation of the human interferon regulatory factor 1 (IRF-1) and IRF-2 genes: implications for a gene network in the interferon system. Mol Cell Biol. 14, 1500-1509.

Harada, H., Willison, K., Sakakibara, J., Miyamoto, M., Fujita, T.Taniguchi, T., 1990. Absence of the type I IFN system in EC cells: transcriptional activator (IRF-1) and repressor (IRF-2) genes are developmentally regulated. Cell. 63, 303-312.

Hartmann, R., Olsen, H. S., Widder, S., Jorgensen, R.Justesen, J., 1998. p59OASL, a 2'-5' oligoadenylate synthetase like protein: a novel human gene related to the 2'-5' oligoadenylate synthetase family. Nucleic Acids Res. 26, 4121-4128.

Heil, F., Hemmi, H., Hochrein, H., Ampenberger, F., Kirschning, C., Akira, S., Lipford, G., Wagner, H.Bauer, S., 2004. Species-specific recognition of single-stranded RNA via toll-like receptor 7 and 8. Science. 303, 1526-1529.

Hida, S., Ogasawara, K., Sato, K., Abe, M., Takayanagi, H., Yokochi, T., Sato, T., Hirose, S., Shirai, T., Taki, S.Taniguchi, T., 2000. CD8(+) T cell-mediated skin disease in mice lacking IRF-2, the transcriptional attenuator of interferon-alpha/beta signaling. Immunity. 13, 643-655.

Higai, K., Miyazaki, N., Azuma, Y.Matsumoto, K., 2008. Transcriptional regulation of the fucosyltransferase VI gene in hepatocellular carcinoma cells. Glycoconj J. 25, 225-235.

Ho, B. C., Yu, S. L., Chen, J. J., Chang, S. Y., Yan, B. S., Hong, Q. S., Singh, S., Kao, C. L., Chen, H. Y., Su, K. Y., Li, K. C., Cheng, C. L., Cheng, H. W., Lee, J. Y., Lee, C. N.Yang, P. C., 2011. Enterovirus-induced miR-141 contributes to shutoff of host protein translation by targeting the translation initiation factor eIF4E. Cell Host Microbe. 9, 58-69.

Ho, L. J., Hung, L. F., Weng, C. Y., Wu, W. L., Chou, P., Lin, Y. L., Chang, D. M., Tai, T. Y.Lai, J. H., 2005. Dengue virus type 2 antagonizes IFN-alpha but not IFN-gamma antiviral effect via down-regulating Tyk2-STAT signaling in the human dendritic cell. J Immunol. 174, 8163-8172.

Honda, K.Taniguchi, T., 2006. IRFs: master regulators of signalling by Toll-like receptors and cytosolic pattern-recognition receptors. Nat Rev Immunol. 6, 644-658.

Hornung, V., Ellegast, J., Kim, S., Brzozka, K., Jung, A., Kato, H., Poeck, H., Akira, S., Conzelmann, K. K., Schlee, M., Endres, S.Hartmann, G., 2006. 5'-Triphosphate RNA is the ligand for RIG-I. Science. 314, 994-997.

Hovnanian, A., Rebouillat, D., Levy, E. R., Mattei, M. G.Hovanessian, A. G., 1999. The human 2',5'-oligoadenylate synthetase-like gene (OASL) encoding the interferon-induced 56-kDa protein maps to chromosome 12q24.2 in the proximity of the 2',5'-OAS locus. Genomics. 56, 362-363.

Hovnanian, A., Rebouillat, D., Mattei, M. G., Levy, E. R., Marie, I., Monaco, A. P.Hovanessian, A. G., 1998. The human 2',5'-oligoadenylate synthetase locus is composed of three distinct genes clustered on chromosome 12q24.2 encoding the 100-, 69-, and 40-kDa forms. Genomics. 52, 267-277.

Hussain, M., Torres, S., Schnettler, E., Funk, A., Grundhoff, A., Pijlman, G. P., Khromykh, A. A.Asgari, S., 2011. West Nile virus encodes a microRNA-like small RNA in the 3' untranslated region which up-regulates GATA4 mRNA and facilitates virus replication in mosquito cells. Nucleic Acids Res.

Hutvagner, G.Simard, M. J., 2008. Argonaute proteins: key players in RNA silencing. Nat Rev Mol Cell Biol. 9, 22-32.

Iordanov, M. S., Paranjape, J. M., Zhou, A., Wong, J., Williams, B. R., Meurs, E. F., Silverman, R. H.Magun, B. E., 2000. Activation of p38 mitogen-activated protein kinase and c-Jun NH(2)-terminal kinase by double-stranded RNA and encephalomyocarditis virus: involvement of RNase L, protein kinase R, and alternative pathways. Mol Cell Biol. 20, 617-627.

Isaacs, A.Lindenmann, J., 1957. Virus interference. I. The interferon. Proc R Soc Lond B Biol Sci. 147, 258-267.

Jackson, S. M., Ericsson, J., Mantovani, R.Edwards, P. A., 1998. Synergistic activation of transcription by nuclear factor Y and sterol regulatory element binding protein. J Lipid Res. 39, 767-776.

Jesse, T. L., LaChance, R., Iademarco, M. F.Dean, D. C., 1998. Interferon regulatory factor-2 is a transcriptional activator in muscle where It regulates expression of vascular cell adhesion molecule-1. J Cell Biol. 140, 1265-1276.

Jiang, D., Weidner, J. M., Qing, M., Pan, X. B., Guo, H., Xu, C., Zhang, X., Birk, A., Chang, J., Shi, P. Y., Block, T. M.Guo, J. T., 2010. Identification of five interferon-induced cellular proteins that inhibit west nile virus and dengue virus infections. J Virol. 84, 8332-8341.

Jin, S.Scotto, K. W., 1998. Transcriptional regulation of the MDR1 gene by histone acetyltransferase and deacetylase is mediated by NF-Y. Mol Cell Biol. 18, 4377-4384.

Jones, M., Davidson, A., Hibbert, L., Gruenwald, P., Schlaak, J., Ball, S., Foster, G. R.Jacobs, M., 2005. Dengue virus inhibits alpha interferon signaling by reducing STAT2 expression. J Virol. 79, 5414-5420.

Justesen, J., Hartmann, R.Kjeldgaard, N. O., 2000. Gene structure and function of the 2'-5'-oligoadenylate synthetase family. Cell Mol Life Sci. 57, 1593-1612.

Kabe, Y., Yamada, J., Uga, H., Yamaguchi, Y., Wada, T.Handa, H., 2005. NF-Y is essential for the recruitment of RNA polymerase II and inducible transcription of several CCAAT box-containing genes. Mol Cell Biol. 25, 512-522.

Kakuta, S., Shibata, S.Iwakura, Y., 2002. Genomic structure of the mouse 2',5'-oligoadenylate synthetase gene family. J Interferon Cytokine Res. 22, 981-993.

Kasschau, K. D.Carrington, J. C., 1998. A counterdefensive strategy of plant viruses: suppression of posttranscriptional gene silencing. Cell. 95, 461-470.

Kato, H., Takeuchi, O., Mikamo-Satoh, E., Hirai, R., Kawai, T., Matsushita, K., Hiiragi, A., Dermody, T. S., Fujita, T.Akira, S., 2008. Length-dependent recognition of double-stranded ribonucleic acids by retinoic acid-inducible gene-I and melanoma differentiation-associated gene 5. J Exp Med. 205, 1601-1610.

Katsoulidis, E., Li, Y., Mears, H.Platanias, L. C., 2005. The p38 mitogen-activated protein kinase pathway in interferon signal transduction. J Interferon Cytokine Res. 25, 749-756.

Kaur, S., Uddin, S.Platanias, L. C., 2005. The PI3' kinase pathway in interferon signaling. J Interferon Cytokine Res. 25, 780-787.

Keller, B. C., Fredericksen, B. L., Samuel, M. A., Mock, R. E., Mason, P. W., Diamond, M. S.Gale, M., Jr., 2006. Resistance to alpha/beta interferon is a determinant of West Nile virus replication fitness and virulence. J Virol. 80, 9424-9434.

Kessler, D. S., Levy, D. E.Darnell, J. E., Jr., 1988. Two interferon-induced nuclear factors bind a single promoter element in interferon-stimulated genes. Proc Natl Acad Sci U S A. 85, 8521-8525.

Kessler, D. S., Veals, S. A., Fu, X. Y.Levy, D. E., 1990. Interferon-alpha regulates nuclear translocation and DNA-binding affinity of ISGF3, a multimeric transcriptional activator. Genes Dev. 4, 1753-1765.

Kotenko, S. V., Gallagher, G., Baurin, V. V., Lewis-Antes, A., Shen, M., Shah, N. K., Langer, J. A., Sheikh, F., Dickensheets, H.Donnelly, R. P., 2003. IFN-lambdas mediate antiviral protection through a distinct class II cytokine receptor complex. Nat Immunol. 4, 69-77.

Kowenz-Leutz, E.Leutz, A., 1999. A C/EBP beta isoform recruits the SWI/SNF complex to activate myeloid genes. Mol Cell. 4, 735-743.

Kraus, T. A., Lau, J. F., Parisien, J. P.Horvath, C. M., 2003. A hybrid IRF9-STAT2 protein recapitulates interferon-stimulated gene expression and antiviral response. J Biol Chem. 278, 13033-13038.

Kuersten, S.Goodwin, E. B., 2003. The power of the 3' UTR: translational control and development. Nat Rev Genet. 4, 626-637.

Laurent-Rolle, M., Boer, E. F., Lubick, K. J., Wolfinbarger, J. B., Carmody, A. B., Rockx, B., Liu, W., Ashour, J., Shupert, W. L., Holbrook, M. R., Barrett, A. D., Mason, P. W., Bloom, M. E., Garcia-Sastre, A., Khromykh, A. A.Best, S. M., The NS5 protein of the virulent West Nile virus NY99 strain is a potent antagonist of type I interferon-mediated JAK-STAT signaling. J Virol. 84, 3503-3515.

Laurent-Rolle, M., Boer, E. F., Lubick, K. J., Wolfinbarger, J. B., Carmody, A. B., Rockx, B., Liu, W., Ashour, J., Shupert, W. L., Holbrook, M. R., Barrett, A. D., Mason, P. W., Bloom, M. E., Garcia-Sastre, A., Khromykh, A. A.Best, S. M., 2010. The NS5 protein of the virulent West Nile virus NY99 strain is a potent antagonist of type I interferon-mediated JAK-STAT signaling. J Virol. 84, 3503-3515.

Lazear, H. M., Pinto, A. K., Vogt, M. R., Gale, M., Jr.Diamond, M. S., 2011. Beta interferon controls west nile virus infection and pathogenesis in mice. J Virol. 85, 7186-7194.

Lee, Y. J.Glaunsinger, B. A., 2009. Aberrant herpesvirus-induced polyadenylation correlates with cellular messenger RNA destruction. PLoS Biol. 7, e1000107.

Levy, D. E., Kessler, D. S., Pine, R., Reich, N.Darnell, J. E., Jr., 1988. Interferon-induced nuclear factors that bind a shared promoter element correlate with positive and negative transcriptional control. Genes Dev. 2, 383-393.

Lew, D. J., Decker, T., Strehlow, I.Darnell, J. E., 1991. Overlapping elements in the guanylate-binding protein gene promoter mediate transcriptional induction by alpha and gamma interferons. Mol Cell Biol. 11, 182-191.

Li, M., Liu, X., Zhou, Y.Su, S. B., 2009. Interferon-lambdas: the modulators of antivirus, antitumor, and immune responses. J Leukoc Biol. 86, 23-32.

Li, Q., Herrler, M., Landsberger, N., Kaludov, N., Ogryzko, V. V., Nakatani, Y.Wolffe, A. P., 1998. Xenopus NF-Y pre-sets chromatin to potentiate p300 and acetylation-responsive transcription from the Xenopus hsp70 promoter in vivo. EMBO J. 17, 6300-6315.

Li, Q.Verma, I. M., 2002. NF-kappaB regulation in the immune system. Nat Rev Immunol. 2, 725-734.

Liang, F.Gardner, D. G., 1999. Mechanical strain activates BNP gene transcription through a p38/NF-kappaB-dependent mechanism. J Clin Invest. 104, 1603-1612.

Lin, R., Genin, P., Mamane, Y.Hiscott, J., 2000. Selective DNA binding and association with the CREB binding protein coactivator contribute to differential activation of alpha/beta interferon genes by interferon regulatory factors 3 and 7. Mol Cell Biol. 20, 6342-6353.

Lin, R. J., Liao, C. L., Lin, E.Lin, Y. L., 2004. Blocking of the alpha interferon-induced Jak-Stat signaling pathway by Japanese encephalitis virus infection. J Virol. 78, 9285-9294.

Lindas, A. C.Tomkinson, B., 2007. Characterization of the promoter of the gene encoding human tripeptidyl-peptidase II and identification of upstream silencer elements. Gene. 393, 62-69.

Lindbo, J. A., Silva-Rosales, L., Proebsting, W. M.Dougherty, W. G., 1993. Induction of a Highly Specific Antiviral State in Transgenic Plants: Implications for Regulation of Gene Expression and Virus Resistance. Plant Cell. 5, 1749-1759.

Lindenbach, B. D., Thiel, H-J. and Rice, C. M., 2007. Flaviviridae: The viruses and their replication. In: Fields, Knipe, D. M., Howley, P. N., Griffin, D. E., Lamb, R. A., Martin,

M. A., Roizman, B. and Straus, S. E. (Editors), Fields Virology, 5th ed., Lippincott Williams and Wilkins, Philadelphia, Pennsylvania, pp, 1102-52.

Lindenbach, B. D., Thiel, H. J, and Rice, C. M. (2007). Flaviviridae: The Viruses and Their Replication. Fields Virology. D. M. Knipe, and Howley, P. M. Philadelphia, Lippincott Williams and Wilkins**:** 1101-1152.

Liu, W. J., Chen, H. B., Wang, X. J., Huang, H.Khromykh, A. A., 2004. Analysis of adaptive mutations in Kunjin virus replicon RNA reveals a novel role for the flavivirus nonstructural protein NS2A in inhibition of beta interferon promoter-driven transcription. J Virol. 78, 12225-12235.

Liu, W. J., Wang, X. J., Clark, D. C., Lobigs, M., Hall, R. A.Khromykh, A. A., 2006. A single amino acid substitution in the West Nile virus nonstructural protein NS2A disables its ability to inhibit alpha/beta interferon induction and attenuates virus virulence in mice. J Virol. 80, 2396-2404.

Liu, W. J., Wang, X. J., Mokhonov, V. V., Shi, P. Y., Randall, R.Khromykh, A. A., 2005. Inhibition of interferon signaling by the New York 99 strain and Kunjin subtype of West Nile virus involves blockage of STAT1 and STAT2 activation by nonstructural proteins. J Virol. 79, 1934-1942.

Loo, Y. M., Fornek, J., Crochet, N., Bajwa, G., Perwitasari, O., Martinez-Sobrido, L., Akira, S., Gill, M. A., Garcia-Sastre, A., Katze, M. G.Gale, M., Jr., 2008. Distinct RIG-I and MDA5 signaling by RNA viruses in innate immunity. J Virol. 82, 335-345.

Lopez-Lastra, M., Ramdohr, P., Letelier, A., Vallejos, M., Vera-Otarola, J.Valiente-Echeverria, F., 2010. Translation initiation of viral mRNAs. Rev Med Virol. 20, 177-195.

Lou, Y. J., Pan, X. R., Jia, P. M., Li, D., Xiao, S., Zhang, Z. L., Chen, S. J., Chen, Z.Tong, J. H., 2009. IRF-9/STAT2 functional interaction drives retinoic acid-induced gene G expression independently of STAT1. Cancer Res. 69, 3673-3680.

Lytle, J. R., Yario, T. A.Steitz, J. A., 2007. Target mRNAs are repressed as efficiently by microRNA-binding sites in the 5' UTR as in the 3' UTR. Proc Natl Acad Sci U S A. 104, 9667-9672.

Mackenzie, J., 2005. Wrapping things up about virus RNA replication. Traffic. 6, 967-977.

Mackenzie, J. M., Khromykh, A. A.Parton, R. G., 2007. Cholesterol manipulation by West Nile virus perturbs the cellular immune response. Cell Host Microbe. 2, 229-239.

Mackenzie, J. M.Westaway, E. G., 2001. Assembly and maturation of the flavivirus Kunjin virus appear to occur in the rough endoplasmic reticulum and along the secretory pathway, respectively. J Virol. 75, 10787-10799.

Mantovani, R., 1999. The molecular biology of the CCAAT-binding factor NF-Y. Gene. 239, 15-27.

Maratheftis, C. I., Bolaraki, P. E., Giannouli, S., Kapsogeorgou, E. K., Moutsopoulos, H. M.Voulgarelis, M., 2006. Aberrant alternative splicing of interferon regulatory factor-1 (IRF-1) in myelodysplastic hematopoietic progenitor cells. Leuk Res. 30, 1177-1186.

Marie, I., Durbin, J. E.Levy, D. E., 1998. Differential viral induction of distinct interferon-alpha genes by positive feedback through interferon regulatory factor-7. EMBO J. 17, 6660-6669.

Marques, J. T., Devosse, T., Wang, D., Zamanian-Daryoush, M., Serbinowski, P., Hartmann, R., Fujita, T., Behlke, M. A.Williams, B. R., 2006. A structural basis for discriminating between self and nonself double-stranded RNAs in mammalian cells. Nat Biotechnol. 24, 559-565.

Mashimo, T., Glaser, P., Lucas, M., Simon-Chazottes, D., Ceccaldi, P. E., Montagutelli, X., Despres, P.Guenet, J. L., 2003. Structural and functional genomics and evolutionary relationships in the cluster of genes encoding murine 2',5'-oligoadenylate synthetases. Genomics. 82, 537-552.

Massa, P. E., Li, X., Hanidu, A., Siamas, J., Pariali, M., Pareja, J., Savitt, A. G., Catron, K. M., Li, J.Marcu, K. B., 2005. Gene expression profiling in conjunction with physiological rescues of IKKalpha-null cells with wild type or mutant IKKalpha reveals distinct classes of IKKalpha/NF-kappaB-dependent genes. J Biol Chem. 280, 14057-14069.

Matsumoto, M., Funami, K., Tanabe, M., Oshiumi, H., Shingai, M., Seto, Y., Yamamoto, A.Seya, T., 2003. Subcellular localization of Toll-like receptor 3 in human dendritic cells. J Immunol. 171, 3154-3162.

Maulik, N., Sato, M., Price, B. D.Das, D. K., 1998. An essential role of NFkappaB in tyrosine kinase signaling of p38 MAP kinase regulation of myocardial adaptation to ischemia. FEBS Lett. 429, 365-369.

Mazumder, B., Seshadri, V.Fox, P. L., 2003. Translational control by the 3'-UTR: the ends specify the means. Trends Biochem Sci. 28, 91-98.

Mazzon, M., Jones, M., Davidson, A., Chain, B.Jacobs, M., 2009. Dengue virus NS5 inhibits interferon-alpha signaling by blocking signal transducer and activator of transcription 2 phosphorylation. J Infect Dis. 200, 1261-1270.

McBride, K. M., Banninger, G., McDonald, C.Reich, N. C., 2002. Regulated nuclear import of the STAT1 transcription factor by direct binding of importin-alpha. EMBO J. 21, 1754-1763.

Merika, M.Thanos, D., 2001. Enhanceosomes. Curr Opin Genet Dev. 11, 205-208.

Miyamoto, M., Fujita, T., Kimura, Y., Maruyama, M., Harada, H., Sudo, Y., Miyata, T.Taniguchi, T., 1988. Regulated expression of a gene encoding a nuclear factor, IRF-1, that specifically binds to IFN-beta gene regulatory elements. Cell. 54, 903-913.

Morin, P., Braganca, J., Bandu, M. T., Lin, R., Hiscott, J., Doly, J.Civas, A., 2002. Preferential binding sites for interferon regulatory factors 3 and 7 involved in interferon-A gene transcription. J Mol Biol. 316, 1009-1022.

Motsch, N., Pfuhl, T., Mrazek, J., Barth, S.Grasser, F. A., 2007. Epstein-Barr Virus-Encoded Latent Membrane Protein 1 (LMP1) Induces the Expression of the Cellular MicroRNA miR-146a. RNA Biol. 4,

Munoz-Jordan, J. L., Laurent-Rolle, M., Ashour, J., Martinez-Sobrido, L., Ashok, M., Lipkin, W. I.Garcia-Sastre, A., 2005. Inhibition of alpha/beta interferon signaling by the NS4B protein of flaviviruses. J Virol. 79, 8004-8013.

Munoz-Jordan, J. L., Sanchez-Burgos, G. G., Laurent-Rolle, M.Garcia-Sastre, A., 2003. Inhibition of interferon signaling by dengue virus. Proc Natl Acad Sci U S A. 100, 14333-14338.

Murchison, E. P.Hannon, G. J., 2004. miRNAs on the move: miRNA biogenesis and the RNAi machinery. Curr Opin Cell Biol. 16, 223-229.

Nakaya, T., Sato, M., Hata, N., Asagiri, M., Suemori, H., Noguchi, S., Tanaka, N.Taniguchi, T., 2001. Gene induction pathways mediated by distinct IRFs during viral infection. Biochem Biophys Res Commun. 283, 1150-1156.

Ning, S., Huye, L. E.Pagano, J. S., 2005. Regulation of the transcriptional activity of the IRF7 promoter by a pathway independent of interferon signaling. J Biol Chem. 280, 12262-12270.

Ostareck, D. H., Ostareck-Lederer, A., Wilm, M., Thiele, B. J., Mann, M.Hentze, M. W., 1997. mRNA silencing in erythroid differentiation: hnRNP K and hnRNP E1 regulate 15-lipoxygenase translation from the 3' end. Cell. 89, 597-606.

Ousman, S. S., Wang, J.Campbell, I. L., 2005. Differential regulation of interferon regulatory factor (IRF)-7 and IRF-9 gene expression in the central nervous system during viral infection. J Virol. 79, 7514-7527.

Ozato, K., Tailor, P.Kubota, T., 2007. The interferon regulatory factor family in host defense: mechanism of action. J Biol Chem. 282, 20065-20069.

Pahl, H. L., 1999. Activators and target genes of Rel/NF-kappaB transcription factors. Oncogene. 18, 6853-6866.

Paladino, P., Cummings, D. T., Noyce, R. S.Mossman, K. L., 2006. The IFN-independent response to virus particle entry provides a first line of antiviral defense that is independent of TLRs and retinoic acid-inducible gene I. J Immunol. 177, 8008-8016.

Park, J., Kim, K., Lee, E. J., Seo, Y. J., Lim, S. N., Park, K., Rho, S. B., Lee, S. H.Lee, J. H., 2007. Elevated level of SUMOylated IRF-1 in tumor cells interferes with IRF-1-mediated apoptosis. Proc Natl Acad Sci U S A. 104, 17028-17033.

Parker, R.Sheth, U., 2007. P bodies and the control of mRNA translation and degradation. Mol Cell. 25, 635-646.

Paun, A.Pitha, P. M., 2007. The innate antiviral response: new insights into a continuing story. Adv Virus Res. 69, 1-66.

Paun, A., Reinert, J. T., Jiang, Z., Medin, C., Balkhi, M. Y., Fitzgerald, K. A.Pitha, P. M., 2008. Functional characterization of murine interferon regulatory factor 5 (IRF-5) and its role in the innate antiviral response. J Biol Chem. 283, 14295-14308.

Perelygin, A. A., Scherbik, S. V., Zhulin, I. B., Stockman, B. M., Li, Y.Brinton, M. A., 2002. Positional cloning of the murine flavivirus resistance gene. Proc Natl Acad Sci U S A. 99, 9322-9327.

Perelygin, A. A., Zharkikh, A. A., Scherbik, S. V.Brinton, M. A., 2006. The mammalian 2'-5' oligoadenylate synthetase gene family: evidence for concerted evolution of paralogous Oas1 genes in Rodentia and Artiodactyla. J Mol Evol. 63, 562-576.

Perry, S. T., Buck, M. D., Lada, S. M., Schindler, C.Shresta, S., 2011. STAT2 mediates innate immunity to Dengue virus in the absence of STAT1 via the type I interferon receptor. PLoS Pathog. 7, e1001297.

Pestka, S., Krause, C. D.Walter, M. R., 2004. Interferons, interferon-like cytokines, and their receptors. Immunol Rev. 202, 8-32.

Peters, K. L., Smith, H. L., Stark, G. R.Sen, G. C., 2002. IRF-3-dependent, NFkappa B- and JNK-independent activation of the 561 and IFN-beta genes in response to double-stranded RNA. Proc Natl Acad Sci U S A. 99, 6322-6327.

Petersen, L. R., Marfin, A. A.Gubler, D. J., 2003. West Nile virus. JAMA. 290, 524-528.

Pijlman, G. P., Funk, A., Kondratieva, N., Leung, J., Torres, S., van der Aa, L., Liu, W. J., Palmenberg, A. C., Shi, P. Y., Hall, R. A.Khromykh, A. A., 2008. A highly structured, nuclease-resistant, noncoding RNA produced by flaviviruses is required for pathogenicity. Cell Host Microbe. 4, 579-591.

Pine, R., Canova, A.Schindler, C., 1994. Tyrosine phosphorylated p91 binds to a single element in the ISGF2/IRF-1 promoter to mediate induction by IFN alpha and IFN gamma, and is likely to autoregulate the p91 gene. EMBO J. 13, 158-167.

Pomerantz, J. L.Baltimore, D., 2002. Two pathways to NF-kappaB. Mol Cell. 10, 693-695.

Pulit-Penaloza, J. A., Scherbik, S. V.Brinton, M. A., 2012. Activation of Oas1a gene expression by type I IFN requires both STAT1 and STAT2 while only STAT2 is required for Oas1b activation.

Qureshi, S. A., Leung, S., Kerr, I. M., Stark, G. R.Darnell, J. E., Jr., 1996. Function of Stat2 protein in transcriptional activation by alpha interferon. Mol Cell Biol. 16, 288-293.

Qureshi, S. A., Salditt-Georgieff, M.Darnell, J. E., Jr., 1995. Tyrosine-phosphorylated Stat1 and Stat2 plus a 48-kDa protein all contact DNA in forming interferon-stimulated-gene factor 3. Proc Natl Acad Sci U S A. 92, 3829-3833.

Randall, R. E.Goodbourn, S., 2008. Interferons and viruses: an interplay between induction, signalling, antiviral responses and virus countermeasures. J Gen Virol. 89, 1-47.

Ratcliff, F., Harrison, B. D.Baulcombe, D. C., 1997. A similarity between viral defense and gene silencing in plants. Science. 276, 1558-1560.

Rebouillat, D., Hovnanian, A., David, G., Hovanessian, A. G.Williams, B. R., 2000. Characterization of the gene encoding the 100-kDa form of human 2',5' oligoadenylate synthetase. Genomics. 70, 232-240.

Rebouillat, D., Marie, I.Hovanessian, A. G., 1998. Molecular cloning and characterization of two related and interferon-induced 56-kDa and 30-kDa proteins highly similar to 2'-5' oligoadenylate synthetase. Eur J Biochem. 257, 319-330.

Reich, N. C., 2007. STAT dynamics. Cytokine Growth Factor Rev. 18, 511-518.

Reid, S. P., Leung, L. W., Hartman, A. L., Martinez, O., Shaw, M. L., Carbonnelle, C., Volchkov, V. E., Nichol, S. T.Basler, C. F., 2006. Ebola virus VP24 binds karyopherin alpha1 and blocks STAT1 nuclear accumulation. J Virol. 80, 5156-5167.

Reith, W., Siegrist, C. A., Durand, B., Barras, E.Mach, B., 1994. Function of major histocompatibility complex class II promoters requires cooperative binding between factors RFX and NF-Y. Proc Natl Acad Sci U S A. 91, 554-558.

Rouha, H., Thurner, C.Mandl, C. W., 2010. Functional microRNA generated from a cytoplasmic RNA virus. Nucleic Acids Res. 38, 8328-8337.

Rutherford, M. N., Kumar, A., Nissim, A., Chebath, J.Williams, B. R., 1991. The murine 2-5A synthetase locus: three distinct transcripts from two linked genes. Nucleic Acids Res. 19, 1917-1924.

Saha, R. N., Jana, M.Pahan, K., 2007. MAPK p38 regulates transcriptional activity of NF-kappaB in primary human astrocytes via acetylation of p65. J Immunol. 179, 7101-7109.

Saito, T.Gale, M., Jr., 2007. Principles of intracellular viral recognition. Curr Opin Immunol. 19, 17-23.

Saito, T., Owen, D. M., Jiang, F., Marcotrigiano, J.Gale, M., Jr., 2008. Innate immunity induced by composition-dependent RIG-I recognition of hepatitis C virus RNA. Nature. 454, 523-527.

Salsi, V., Caretti, G., Wasner, M., Reinhard, W., Haugwitz, U., Engeland, K.Mantovani, R., 2003. Interactions between p300 and multiple NF-Y trimers govern cyclin B2 promoter function. J Biol Chem. 278, 6642-6650.

Samuel, C. E., 2001. Antiviral actions of interferons. Clin Microbiol Rev. 14, 778-809, table of contents.

Samuel, M. A.Diamond, M. S., 2005. Alpha/beta interferon protects against lethal West Nile virus infection by restricting cellular tropism and enhancing neuronal survival. J Virol. 79, 13350-13361.

Sarkis, P. T., Ying, S., Xu, R.Yu, X. F., 2006. STAT1-independent cell type-specific regulation of antiviral APOBEC3G by IFN-alpha. J Immunol. 177, 4530-4540.

Sato, M., Hata, N., Asagiri, M., Nakaya, T., Taniguchi, T.Tanaka, N., 1998. Positive feedback regulation of type I IFN genes by the IFN-inducible transcription factor IRF-7. FEBS Lett. 441, 106-110.

Sato, M., Suemori, H., Hata, N., Asagiri, M., Ogasawara, K., Nakao, K., Nakaya, T., Katsuki, M., Noguchi, S., Tanaka, N.Taniguchi, T., 2000. Distinct and essential roles of transcription factors IRF-3 and IRF-7 in response to viruses for IFN-alpha/beta gene induction. Immunity. 13, 539-548.

Satterly, N., Tsai, P. L., van Deursen, J., Nussenzveig, D. R., Wang, Y., Faria, P. A., Levay, A., Levy, D. E.Fontoura, B. M., 2007. Influenza virus targets the mRNA export machinery and the nuclear pore complex. Proc Natl Acad Sci U S A. 104, 1853-1858.

Scherbik, S. V.Brinton, M. A., 2010. Virus-induced Ca2+ influx extends survival of west nile virus-infected cells. J Virol. 84, 8721-8731.

Scherbik, S. V., Paranjape, J. M., Stockman, B. M., Silverman, R. H.Brinton, M. A., 2006. RNase L plays a role in the antiviral response to West Nile virus. J Virol. 80, 2987-2999.

Scherbik, S. V., Stockman, B. M.Brinton, M. A., 2007. Differential expression of interferon (IFN) regulatory factors and IFN-stimulated genes at early times after West Nile virus infection of mouse embryo fibroblasts. J Virol. 81, 12005-12018.

Schindler, C., Shuai, K., Prezioso, V. R.Darnell, J. E., Jr., 1992. Interferon-dependent tyrosine phosphorylation of a latent cytoplasmic transcription factor. Science. 257, 809-813.

Schmid, S., Mordstein, M., Kochs, G., Garcia-Sastre, A.Tenoever, B. R., 2010. Transcription factor redundancy ensures induction of the antiviral state. J Biol Chem. 285, 42013-42022.

Schoenborn, J. R.Wilson, C. B., 2007. Regulation of interferon-gamma during innate and adaptive immune responses. Adv Immunol. 96, 41-101.

Schoenemeyer, A., Barnes, B. J., Mancl, M. E., Latz, E., Goutagny, N., Pitha, P. M., Fitzgerald, K. A.Golenbock, D. T., 2005. The interferon regulatory factor, IRF5, is a central mediator of toll-like receptor 7 signaling. J Biol Chem. 280, 17005-17012.

Schoggins, J. W., Wilson, S. J., Panis, M., Murphy, M. Y., Jones, C. T., Bieniasz, P.Rice, C. M., 2011. A diverse range of gene products are effectors of the type I interferon antiviral response. Nature. 472, 481-485.

Sharma, S., tenOever, B. R., Grandvaux, N., Zhou, G. P., Lin, R.Hiscott, J., 2003. Triggering the interferon antiviral response through an IKK-related pathway. Science. 300, 1148-1151.

Shibata, S., Kakuta, S., Hamada, K., Sokawa, Y.Iwakura, Y., 2001. Cloning of a novel 2',5'-oligoadenylate synthetase-like molecule, Oasl5 in mice. Gene. 271, 261-271.

Shuai, K., Schindler, C., Prezioso, V. R.Darnell, J. E., Jr., 1992. Activation of transcription by IFN-gamma: tyrosine phosphorylation of a 91-kD DNA binding protein. Science. 258, 1808-1812.

Skalsky, R. L.Cullen, B. R., 2010. Viruses, microRNAs, and host interactions. Annu Rev Microbiol. 64, 123-141.

Smale, S. T., 1997. Transcription initiation from TATA-less promoters within eukaryotic protein-coding genes. Biochim Biophys Acta. 1351, 73-88.

Smale, S. T.Baltimore, D., 1989. The "initiator" as a transcription control element. Cell. 57, 103-113.

Stadler, K., Allison, S. L., Schalich, J.Heinz, F. X., 1997. Proteolytic activation of tick-borne encephalitis virus by furin. J Virol. 71, 8475-8481.

Stark, G. R., Kerr, I. M., Williams, B. R., Silverman, R. H.Schreiber, R. D., 1998. How cells respond to interferons. Annu Rev Biochem. 67, 227-264.

Stirnweiss, A., Ksienzyk, A., Klages, K., Rand, U., Grashoff, M., Hauser, H.Kroger, A., 2010. IFN regulatory factor-1 bypasses IFN-mediated antiviral effects through viperin gene induction. J Immunol. 184, 5179-5185.

Su, Z. Z., Sarkar, D., Emdad, L., Barral, P. M.Fisher, P. B., 2007. Central role of interferon regulatory factor-1 (IRF-1) in controlling retinoic acid inducible gene-I (RIG-I) expression. J Cell Physiol. 213, 502-510.

Suhara, W., Yoneyama, M., Kitabayashi, I.Fujita, T., 2002. Direct involvement of CREB-binding protein/p300 in sequence-specific DNA binding of virus-activated interferon regulatory factor-3 holocomplex. J Biol Chem. 277, 22304-22313.

Suthar, M. S., Ma, D. Y., Thomas, S., Lund, J. M., Zhang, N., Daffis, S., Rudensky, A. Y., Bevan, M. J., Clark, E. A., Kaja, M. K., Diamond, M. S.Gale, M., Jr., 2010. IPS-1 is essential for the control of West Nile virus infection and immunity. PLoS Pathog. 6, e1000757.

Takahasi, K., Yoneyama, M., Nishihori, T., Hirai, R., Kumeta, H., Narita, R., Gale, M., Jr., Inagaki, F.Fujita, T., 2008. Nonself RNA-sensing mechanism of RIG-I helicase and activation of antiviral immune responses. Mol Cell. 29, 428-440.

Takaoka, A.Yanai, H., 2006. Interferon signalling network in innate defence. Cell Microbiol. 8, 907-922.

Takaoka, A., Yanai, H., Kondo, S., Duncan, G., Negishi, H., Mizutani, T., Kano, S., Honda, K., Ohba, Y., Mak, T. W.Taniguchi, T., 2005. Integral role of IRF-5 in the gene induction programme activated by Toll-like receptors. Nature. 434, 243-249.

Takeuchi, O.Akira, S., 2008. MDA5/RIG-I and virus recognition. Curr Opin Immunol. 20, 17-22.

Tan, G. S., Garchow, B. G., Liu, X., Yeung, J., Morris, J. P. t., Cuellar, T. L., McManus, M. T.Kiriakidou, M., 2009. Expanded RNA-binding activities of mammalian Argonaute 2. Nucleic Acids Res. 37, 7533-7545.

Tanaka, N., Ishihara, M., Lamphier, M. S., Nozawa, H., Matsuyama, T., Mak, T. W., Aizawa, S., Tokino, T., Oren, M.Taniguchi, T., 1996. Cooperation of the tumour suppressors IRF-1 and p53 in response to DNA damage. Nature. 382, 816-818.

Taniguchi, T., Lamphier, M. S.Tanaka, N., 1997. IRF-1: the transcription factor linking the interferon response and oncogenesis. Biochim Biophys Acta. 1333, M9-17.

Taniguchi, T., Ogasawara, K., Takaoka, A.Tanaka, N., 2001. IRF family of transcription factors as regulators of host defense. Annu Rev Immunol. 19, 623-655.

Taniguchi, T.Takaoka, A., 2001. A weak signal for strong responses: interferon-alpha/beta revisited. Nat Rev Mol Cell Biol. 2, 378-386.

Tenoever, B. R., Ng, S. L., Chua, M. A., McWhirter, S. M., Garcia-Sastre, A.Maniatis, T., 2007. Multiple functions of the IKK-related kinase IKKepsilon in interferon-mediated antiviral immunity. Science. 315, 1274-1278.

Thompson, J. F., Hayes, L. S.Lloyd, D. B., 1991. Modulation of firefly luciferase stability and impact on studies of gene regulation. Gene. 103, 171-177.

Town, T., Bai, F., Wang, T., Kaplan, A. T., Qian, F., Montgomery, R. R., Anderson, J. F., Flavell, R. A.Fikrig, E., 2009. Toll-like receptor 7 mitigates lethal West Nile encephalitis via interleukin 23-dependent immune cell infiltration and homing. Immunity. 30, 242-253.

Triantafilou, K., Vakakis, E., Orthopoulos, G., Ahmed, M. A., Schumann, C., Lepper, P. M.Triantafilou, M., 2005. TLR8 and TLR7 are involved in the host's immune response to human parechovirus 1. Eur J Immunol. 35, 2416-2423.

Triboulet, R., Mari, B., Lin, Y. L., Chable-Bessia, C., Bennasser, Y., Lebrigand, K., Cardinaud, B., Maurin, T., Barbry, P., Baillat, V., Reynes, J., Corbeau, P., Jeang, K. T.Benkirane,

M., 2007. Suppression of microRNA-silencing pathway by HIV-1 during virus replication. Science. 315, 1579-1582.

Vaheri, A., Sedwick, W. D., Plotkin, S. A.Maes, R., 1965. Cytopathic effect of rubella virus in RHK21 cells and growth to high titers in suspension culture. Virology. 27, 239-241.

Vanden Berghe, W., Plaisance, S., Boone, E., De Bosscher, K., Schmitz, M. L., Fiers, W.Haegeman, G., 1998. p38 and extracellular signal-regulated kinase mitogen-activated protein kinase pathways are required for nuclear factor-kappaB p65 transactivation mediated by tumor necrosis factor. J Biol Chem. 273, 3285-3290.

Vaughan, P. S., Aziz, F., van Wijnen, A. J., Wu, S., Harada, H., Taniguchi, T., Soprano, K. J., Stein, J. L.Stein, G. S., 1995. Activation of a cell-cycle-regulated histone gene by the oncogenic transcription factor IRF-2. Nature. 377, 362-365.

Vitiello, M., Finamore, E., Falanga, A., Raieta, K., Cantisani, M., Galdiero, F., Pedone, C., Galdiero, M.Galdiero, S., 2010. Viral fusion peptides induce several signal transduction pathway activations that are essential for interleukin-10 and beta-interferon production. Intervirology. 53, 381-389.

Walsh, D.Mohr, I., 2011. Viral subversion of the host protein synthesis machinery. Nat Rev Microbiol.

Wang, Q.Floyd-Smith, G., 1997. The p69/71 2-5A synthetase promoter contains multiple regulatory elements required for interferon-alpha-induced expression. DNA Cell Biol. 16, 1385-1394.

Wang, T., Town, T., Alexopoulou, L., Anderson, J. F., Fikrig, E.Flavell, R. A., 2004. Toll-like receptor 3 mediates West Nile virus entry into the brain causing lethal encephalitis. Nat Med. 10, 1366-1373.

Watanabe, N., Sakakibara, J., Hovanessian, A. G., Taniguchi, T.Fujita, T., 1991. Activation of IFN-beta element by IRF-1 requires a posttranslational event in addition to IRF-1 synthesis. Nucleic Acids Res. 19, 4421-4428.

Wathelet, M. G., Lin, C. H., Parekh, B. S., Ronco, L. V., Howley, P. M.Maniatis, T., 1998. Virus infection induces the assembly of coordinately activated transcription factors on the IFN-beta enhancer in vivo. Mol Cell. 1, 507-518.

Weaver, B. K., Kumar, K. P.Reich, N. C., 1998. Interferon regulatory factor 3 and CREB-binding protein/p300 are subunits of double-stranded RNA-activated transcription factor DRAF1. Mol Cell Biol. 18, 1359-1368.

Welsch, S., Miller, S., Romero-Brey, I., Merz, A., Bleck, C. K., Walther, P., Fuller, S. D., Antony, C., Krijnse-Locker, J.Bartenschlager, R., 2009. Composition and three-dimensional architecture of the dengue virus replication and assembly sites. Cell Host Microbe. 5, 365-375.

Welte, T., Reagan, K., Fang, H., Machain-Williams, C., Zheng, X., Mendell, N., Chang, G. J., Wu, P., Blair, C. D.Wang, T., 2009. Toll-like receptor 7-induced immune response to cutaneous West Nile virus infection. J Gen Virol. 90, 2660-2668.

Whiteside, S. T.Israel, A., 1997. I kappa B proteins: structure, function and regulation. Semin Cancer Biol. 8, 75-82.

Williams, B. R., 1991. Transcriptional regulation of interferon-stimulated genes. Eur J Biochem. 200, 1-11.

Wright, K. L., Moore, T. L., Vilen, B. J., Brown, A. M.Ting, J. P., 1995. Major histocompatibility complex class II-associated invariant chain gene expression is up-regulated by cooperative interactions of Sp1 and NF-Y. J Biol Chem. 270, 20978-20986.

Yan, W., Ma, L., Stein, P., Pangas, S. A., Burns, K. H., Bai, Y., Schultz, R. M.Matzuk, M. M., 2005. Mice deficient in oocyte-specific oligoadenylate synthetase-like protein OAS1D display reduced fertility. Mol Cell Biol. 25, 4615-4624.

Yatherajam, G., Huang, W.Flint, S. J., 2011. Export of adenoviral late mRNA from the nucleus requires the Nxf1/Tap export receptor. J Virol. 85, 1429-1438.

Yoneyama, M., Suhara, W., Fukuhara, Y., Fukuda, M., Nishida, E.Fujita, T., 1998. Direct triggering of the type I interferon system by virus infection: activation of a transcription factor complex containing IRF-3 and CBP/p300. EMBO J. 17, 1087-1095.

Yu, F., Wang, Q.Floyd-Smith, G., 1999. Transcriptional induction of p69 2'-5'-oligoadenylate synthetase by interferon-alpha is stimulated by 12-O-tetradecanoyl phorbol-13-acetate through IRF/ISRE binding motifs. Gene. 237, 177-184.

Zhang, T., Kruys, V., Huez, G.Gueydan, C., 2002. AU-rich element-mediated translational control: complexity and multiple activities of trans-activating factors. Biochem Soc Trans. 30, 952-958.